

**Investigations on the 2-fluorobenzoin
and 2-fluoro-3', 5'-dimethoxybenzoin photochemistry**

INAUGURALDISSERTATION

zur

Erlangung der Würde eines Doktors der Philosophie

vorgelegt der

Philosophisch-Naturwissenschaftlichen Fakultät

der

Universität Basel

von

HASSEN BOUDEBOUS

aus Belfort, Frankreich

Basel, 2006

Genehmigt von der Philosophisch-Naturwissenschaftlichen Fakultät auf Antrag von Prof. Dr.
J.Wirz and Prof. Dr. H.Huber.

Basel, den 23.02.2006

Prof. Dr. J.Wirz

Dekan

Acknowledgements

I would like to thank Prof. Dr. Jakob Wirz for giving me the opportunity to join his research group, for guiding and supporting my work.

I thank Prof. Dr. Hanspeter Huber for agreeing to act as co-referee.

I thank Prof. Dr. Martin Jungen for agreeing to act as chairman of the thesis committee.

A special thanks for the members of the Wirz group:

Anna Paola Pellicioli, Martin Gaplovsky, Markus Ramseier, Bruno Hellrung, Gaby Persy, Yavor Kamdzhilov, Dragana Zivkovic, Jürgen Wintner, Anna Wisla, Pavel Müller, Bogdan Tokarczyk, Dominik Heger.

I would like to thank also Prof. Dr. Bernd Giese, Meike Cordes, Matthias Napp, Olivier Jacques, Christian Jasper for the very fruitful collaboration.

I am also grateful to Dr. Berta Košmrlj, Prof. Dr. Boris Šket for the very fruitful collaboration.

I thank my family, friends and Amar Boudebous for their constant encouragement.

I would like also to thank the Swiss National Science Foundation and the University of Basel for their financial support.

Table of Contents

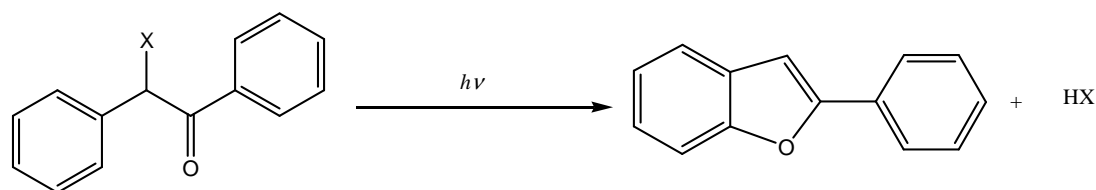
Introduction.....	1
1. Photochemistry of benzoin compounds.....	2
1.1 The deoxybenzoin case.....	8
1.2. The unsubstituted benzoin.....	10
1.3. The dimethoxybenzoin.....	15
2. Investigations on the mechanism of 2-fluorobenzoin photolysis.....	23
2.1. Preparative photolysis.....	23
2.2. Nanosecond LFP of 2-fluorobenzoin.....	24
2.2.1. In MeCN and in water.....	24
2.2.2. In ethanol at low temperature.....	26
2.2.3. In hexane.....	28
2.3. Nanosecond LFP of diethyl phosphate benzoin in hexane.....	29
2.4. Nanosecond LFP of deoxybenzoin.....	32
2.4.1 In hexane	34
2.4.2 In MeCN	36
2.5. Quantum yield determination of 2-fluorobenzoin and diethyl phosphate benzoin photolysis in hexane.....	39
2.6. 2-Fluorobenzoin triplet lifetime determination.....	41
2.7. Diradical trapping experiments.....	44
2.8. Femtosecond LFP of 2-fluorobenzoin in MeCN and in trifluoroethanol	46
2.9. Discussion.....	60
3. Investigations on the mechanism of 2-fluoro-3',5'-dimethoxybenzoin.....	62
3.1. Preparative photolysis.....	62
3.2. Nanosecond LFP of 2-fluoro-3',5'-dimethoxybenzoin in MeCN and in water.....	63
3.3. Femtosecond LFP of 2-fluoro-3',5'-dimethoxybenzoin in MeCN and in trifluoroethanol.....	68
3.4. Discussion.....	77
4. Conclusion.....	80
5. Experimental.....	81
6. References.....	82
7. Summary.....	84

8. Curriculum Vitae.....85

9. Appendix.....87

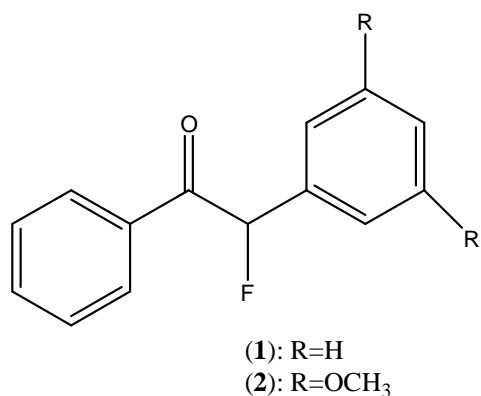
Introduction

Benzoin derivatives are important representatives of “caged compounds”, which are inert in the dark but, upon exposure to light, are converted to active species that are able to participate in a chemical or biochemical process. Benzoin derivatives are an attractive alternative to the widely used 2-nitrobenzyl caging groups for a number of reasons. First of all, the syntheses of benzoin caged derivatives are accomplished in good yield by easy procedures. Benzoin properties fulfill most of the criteria required for the design of a good photoremovable protecting group. The main advantages of benzoin derivatives are the high quantum yields and rates of release. The photochemical by-product accompanying the released reagent is an inert benzofuran (scheme 1), which is an advantage for biological applications. It's also easy to follow the photochemical reaction, because of the strong absorption of the benzofuran by-product centred at 300 nm and its strong fluorescence. These two advantages could, however, also be drawbacks for spectroscopic investigations.



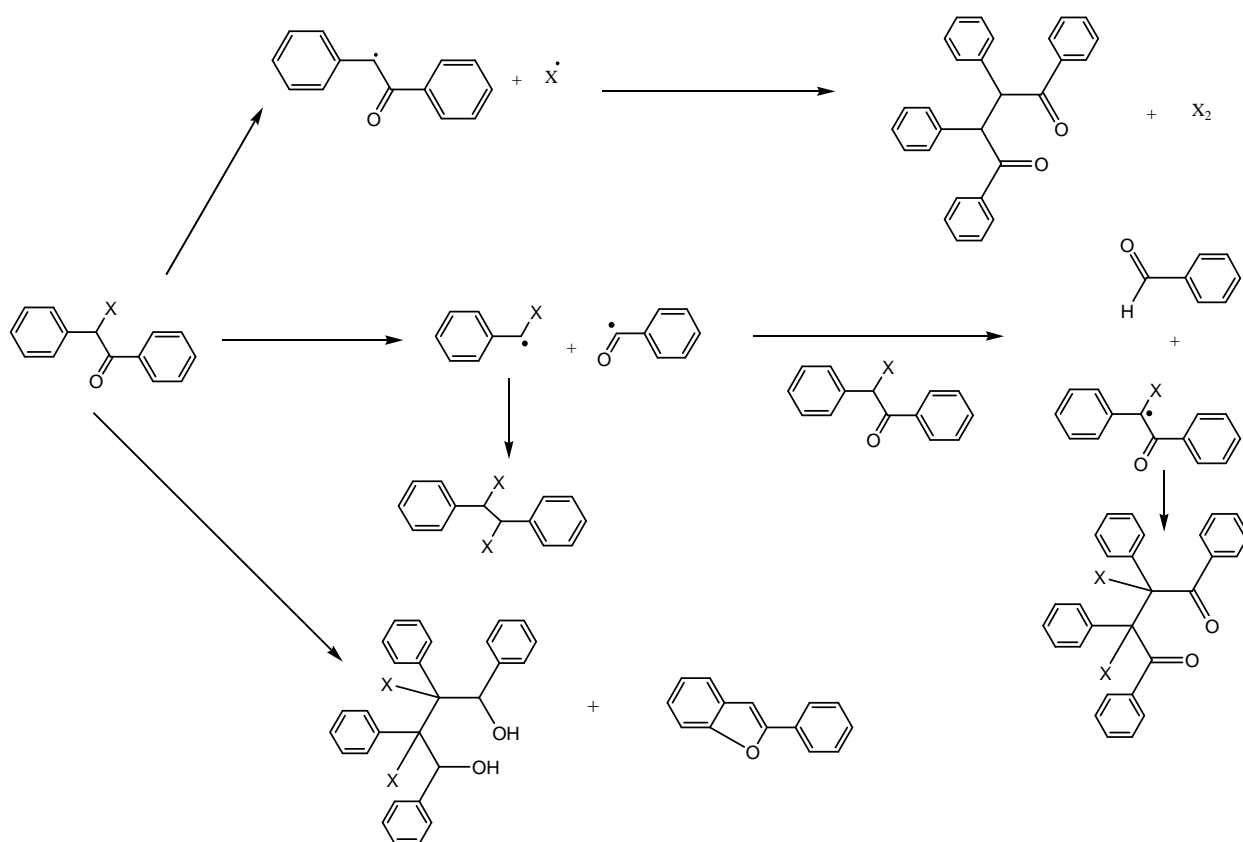
Scheme 1: Photolysis of desyl compounds.

The aim of this project was to determine the mechanism of photocyclisation of 2-fluorobenzoin (**1**) and 3',5'-dimethoxy-2-fluorobenzoin (**2**). In previous work on the photochemistry of fluoro substituted organic compounds, Sket¹ has determined that fluoride stabilizes intermediates like α -radicals or α -cations, which could be involved in the mechanism of photolysis of benzoin derivatives. This stabilization was hoped to facilitate their observation.



1. Photochemistry of benzoin compounds.

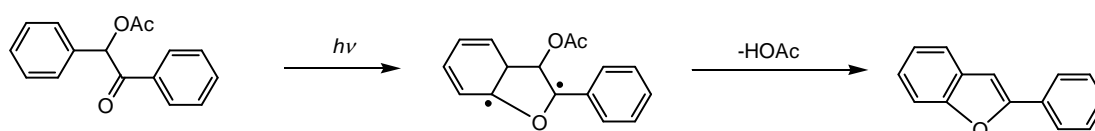
The first study about the photolysis of benzoin (desyl) compounds was made by Sheehan and Wilson² in 1964. They observed that benzoin acetate undergo photolytic cyclisation to form 2-phenylbenzofuran. They also studied the photolysis of many derivatives for which they determined the reaction yield. First, they described the various photochemical reactions that a desyl moiety^{2,3} can follow (scheme 2).



Scheme 2: Various decomposition products observed in desyl photolysis^{2,3}.

Sheehan et al. studied the photolysis of benzoin acetate. They used a high pressure mercury-vapour lamp with a Pyrex filter and isolated 2-phenylbenzofuran as the major product. Factors which should influence the cyclisation reaction were investigated. The benzofuran chemical yields are to a small extent solvent dependent (from 15% in benzene to 8 and 10 % in dioxane and isopropanol, respectively). Another important discovery is the effect of the leaving group. By replacing acetate by chloride as a leaving group, a reduction from 15 to 1% of the chemical yield is observed in benzene. Contrary to the last case, for desyldimethylamine hydrochloride ($X=\text{NH}^+(\text{CH}_3)_2\text{Cl}^-$) in aqueous solution, 67 % is converted to 2-phenylbenzofuran.

A third parameter has been studied, the substitution on the phenyl groups. Contrary to 4,4'-dimethoxybenzoin acetate photolysis in benzene, which gives only traces of the furan, 3,3'-dimethoxybenzoin acetate has a cyclisation yield of 48%. The authors tried to explain this new photolytic cyclisation mechanism by comparison of the different UV-Visible spectra of the substituted and non-substituted benzoin. The intensity of the $n-\pi^*$ band correlates with the furan yield and this effect was attributed to an interaction of the carbonyl nonbonding electrons with the π -orbitals of a β, γ -double bond. This is the reason why a mechanism with a biradical describing a strong interaction between the nonbonding oxygen orbital and the π electrons was proposed (scheme 3).



Scheme 3: Crude mechanism proposed by Sheehan for benzoin acetate photolysis.

In later work, Sheehan, Wilson and Oxford⁴ did a more extensive study on these compounds in order to understand the effect of the methoxy substitution. 4'-Methoxybenzoin acetate, 3'-methoxybenzoin acetate and 3',5'-dimethoxybenzoinacetate were photolysed. Methoxy substitution of the benzoyl group leads to significant changes in the relative energies of the $n-\pi^*$ and the $\pi-\pi^*$ carbonyl excited states. The 4'-methoxybenzoin acetate affords 2-phenyl-6-methoxybenzofuran in only 10% yield (20% for the unsubstituted derivative). The photolysis of 3'-methoxybenzoin acetate yields 88 % of benzofuran. The by-product formation is critically dependent upon the position of the methoxy substituent on the nonconjugated

phenyl group. Best results were realised with the synthesis of the 3',5'-dimethoxybenzoin acetate. The photolysis of this compound is clean and the spectra show two isobestic points at 261 and 233 nm (Figure 1).

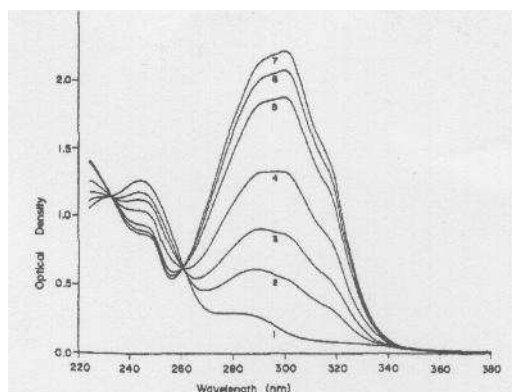
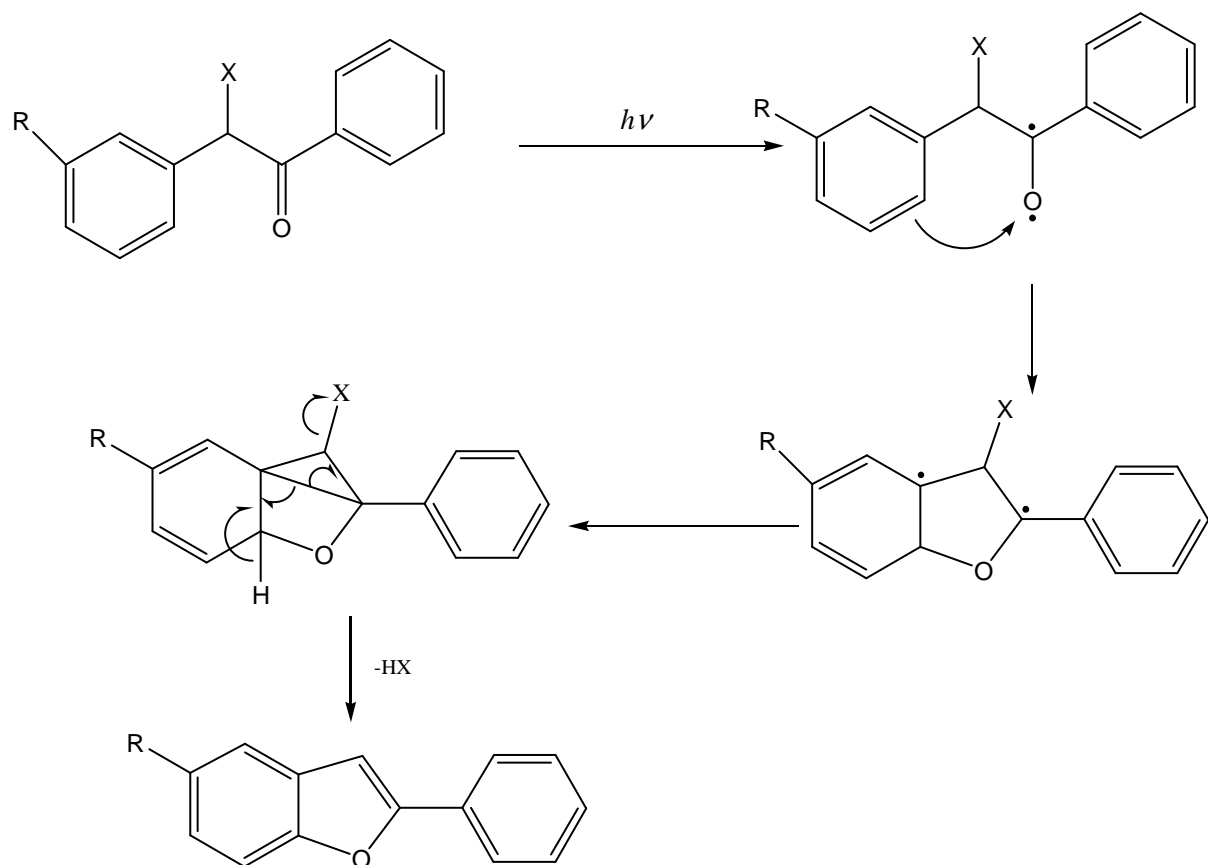


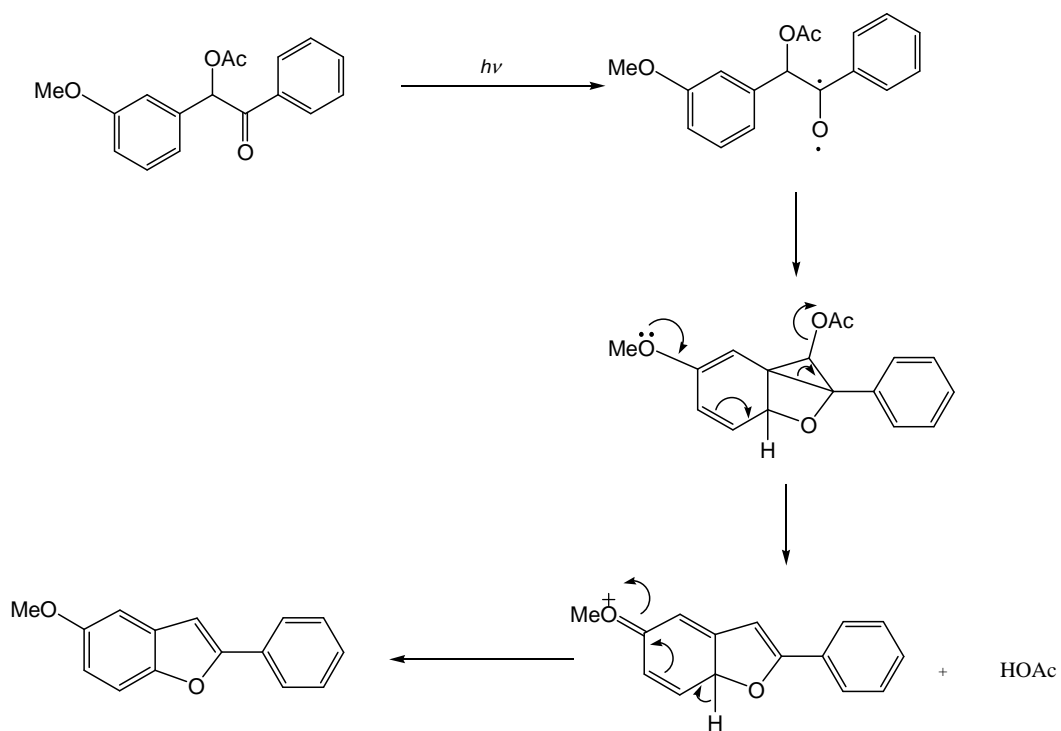
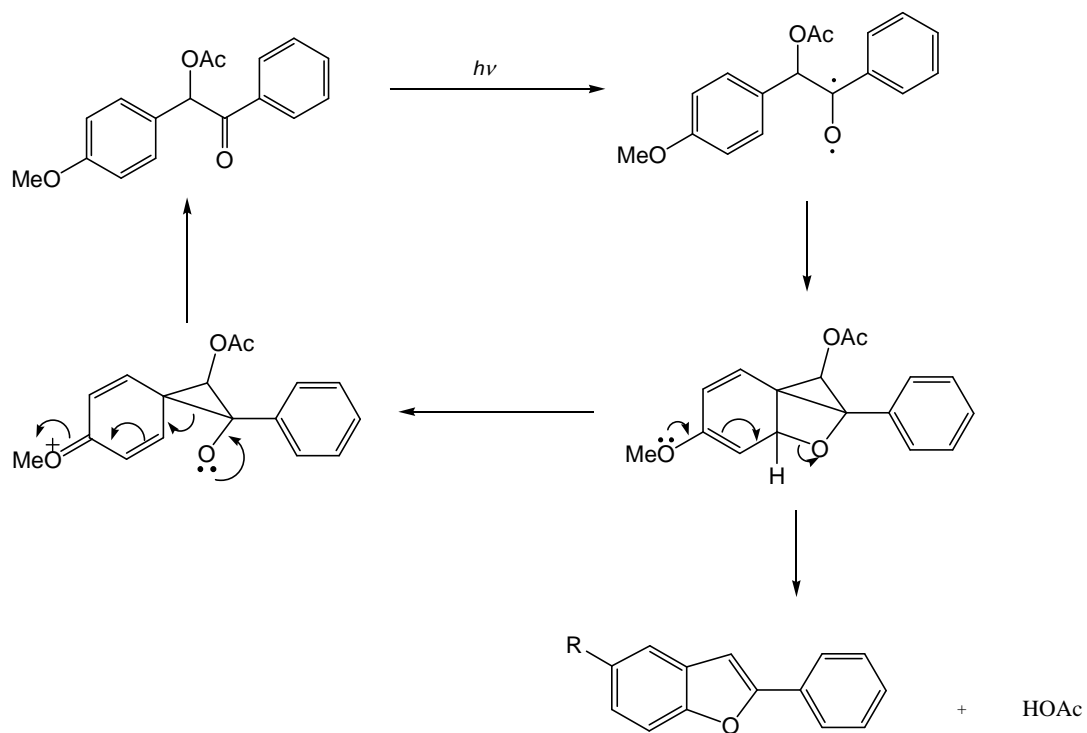
Figure 1: Course of the photolysis of 3', 5'-dimethoxybenzoin acetate to 2-phenyl-5,7-dimethoxybenzofuran, 8.22×10^{-5} M in MeCN; irradiated in a Rayonet reactor with 360 nm lamps; irradiation time in s: 0 (1); 20 (2); 40 (3); 80 (4); 180 (5); 260 (6); 420 (7) sec⁴.

The yield of 2-phenyl-5,7-dimethoxybenzofuran is close to 100%. The quantum yield of this reaction has been determined: $\Phi = 0.644 \pm 0.029$. Sheehan et al. have shown that the lowest excited state is associated with the benzoyl group and may be considered to be of $n-\pi^*$ character. The increased yield due to methoxy substitution (electron donating group) is consistent with the electrophilic nature of the $n-\pi^*$ carbonyl state. On these bases they proposed a mechanism with a strained intermediate formed just before the final benzofuran (scheme 4).



Scheme 4: Mechanism of benzofuran formation proposed by Sheehan et al ³.

Para methoxy substitution will make the electrophilic $n-\pi^*$ attack more difficult, because the attack can only take place at a meta position to the methoxy group. Meta methoxy substitution will facilitate electrophilic attack of the $n-\pi^*$ carbonyl oxygen, because the methoxy group is an ortho/para director (scheme 5).



Scheme 5: Influence of methoxy substitution (para: top, meta: bottom).

Quenching experiments have shown that para-methoxy benzoin photolysis proceeds through a triplet state ($\tau > 10^{-10}$ s). In contrast, the cyclization of meta-methoxy compounds is not quenched by triplet quenchers, so it must proceed through a very short-lived triplet state or directly from the singlet state.

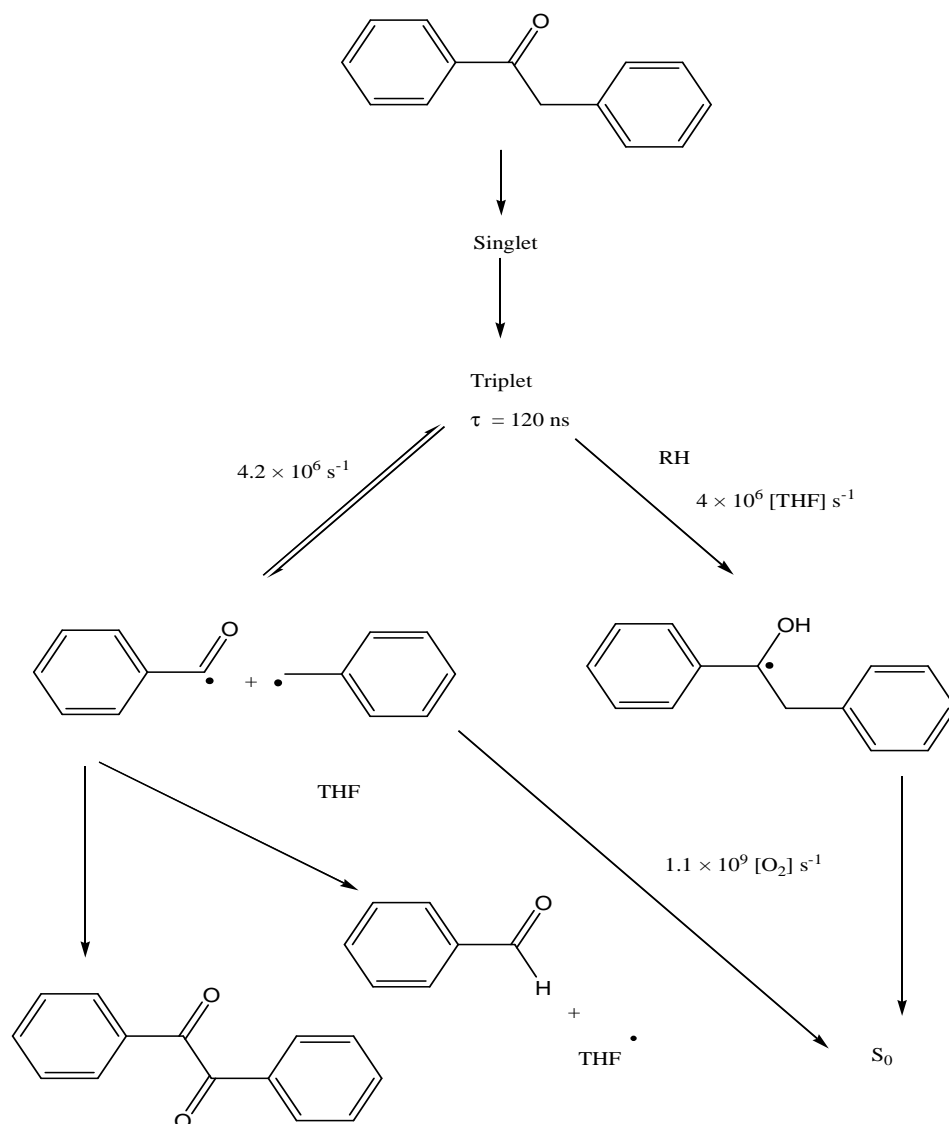
The proposed highly strained oxetane intermediate is justified by precedent. Tenney, Boykin and Lutz⁵ proposed such intermediate in the rearrangement of an α,β -unsaturated ketone to a cyclopropyl ketone. Pawda and Gruber⁶ proposed azabicyclo-[2.1.0] pentane intermediates in the conversion of benzoylazetidines to pyrroles.

Apart from giving the first mechanistic hints, Sheehan et al. were the first scientists to underline the promising potential of this benzoin group as photoremovable group. This first work has opened a lot of perspectives. One particular challenging task is to understand the mechanism of photocyclisation and in particular to measure or estimate the lifetime of the different intermediates involved. Indeed, concurrent reactions like cleavage will prevent the release of the caged compound and form some toxic by-products. Sheehan et al. conclude that 3',5'-esters of dimethoxybenzoin would satisfy the fast release and the clean by-product criteria for a good photoremovable group.

Before we discuss the details of the different mechanisms proposed in the literature, we consider the photolysis mechanism of deoxybenzoin, the parent representative of the benzoin family without a leaving group.

1.1 The deoxybenzoin case.

Few articles deal with the mechanism of deoxybenzoin photolysis. This compound is mostly studied for its applications as photoinitiator of polymerisation reactions. It is known to undergo mainly α -cleavage (Norrish I) and hydrogen abstraction from the solvent⁷ (scheme 6).



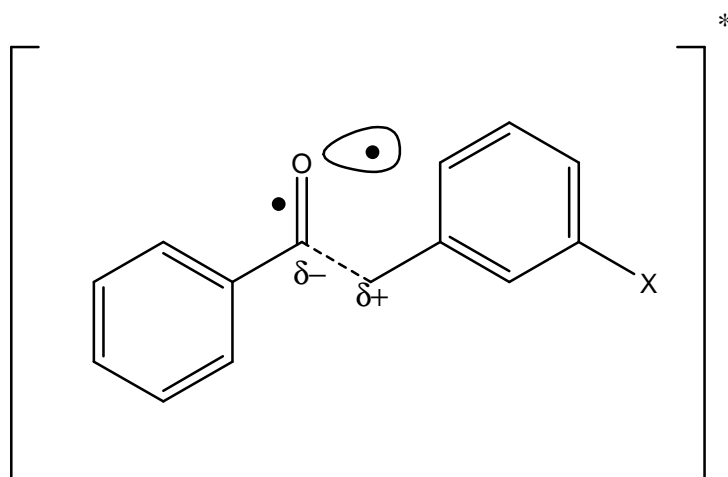
Scheme 6: Mechanism of laser flash photolysis of deoxybenzoin^{7,8}.

Lewis et al.⁸ were the first to study the photochemistry of deoxybenzoin and the fate of the free radicals generated. They concluded that α -cleavage is the only primary process observed for deoxybenzoin photolysis. Fouassier and Merlin⁷ did laser flash photolysis investigations

on deoxybenzoin photochemistry. Absorption by the triplet state, benzoyl and benzyl radicals have been observed. They also remarked that two photoprocesses can occur with similar efficiency: hydrogen abstraction and α -cleavage (scheme 6).

Lewis et al. found out that the minimum quantum yield for α -cleavage is represented by the quantum yield of benzaldehyde formation ($\Phi = 0.44$). They argue also that cage recombination of benzoyl and benzyl radicals could account for approximately half of the initially excited molecules formed⁸.

Lewis et al. also studied the effects of aromatic substitution on the α -cleavage of deoxybenzoin. Substitution affects the rate constant for α -cleavage without altering the triplet energy. From a comparison of the rate constants for photochemical α -cleavage of the deoxybenzoin and the rate constants of corresponding peresters, they concluded that the transition state for α -cleavage looks like the excited ketone rather than like a radical pair.

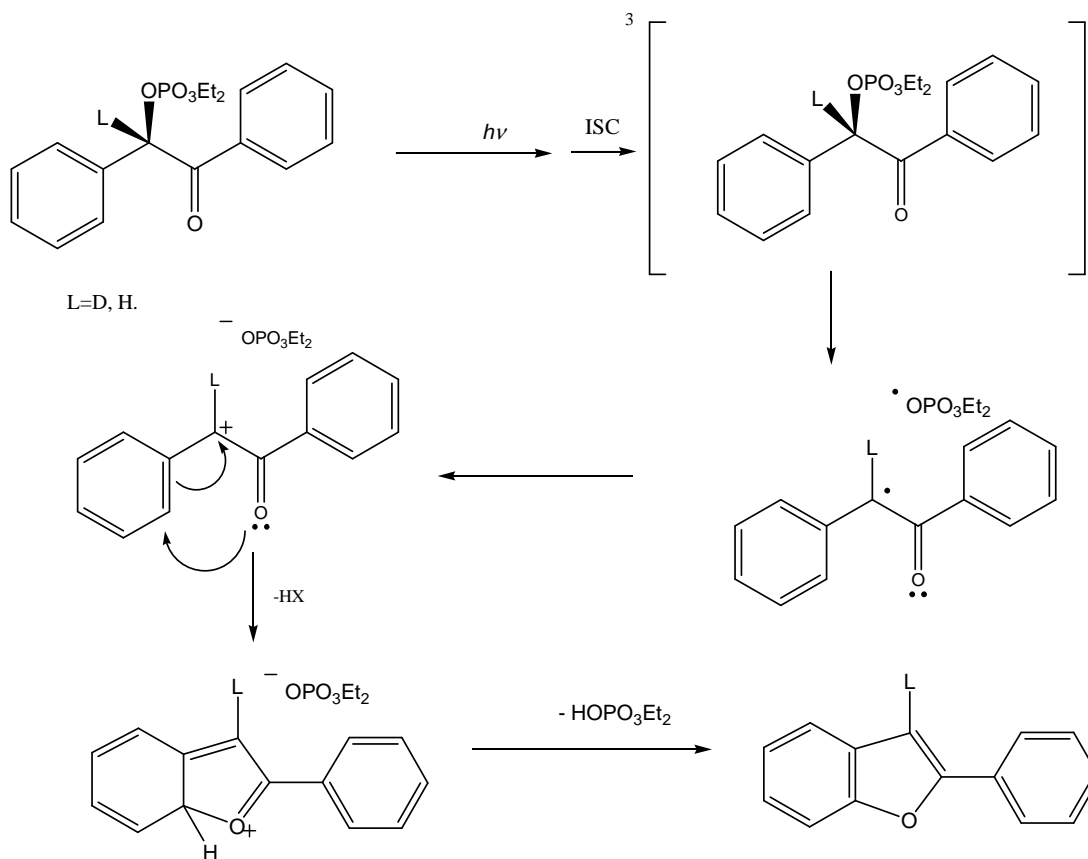


Scheme 7: Transition state for α -cleavage proposed by Lewis et al.⁸.

In this model, the partial negative charge can be stabilized by the electrophilic half-vacant non-bonding orbital on oxygen and the partial positive charge by electron donating aromatic substituents. α -Substituents which are capable of stabilizing an adjacent positive charge should accelerate the photochemical α -cleavage. The presence of a substituent may explain why cyclisation is favoured compared to α -cleavage (scheme 7).

1.2 The unsubstituted benzoin.

Two studies deal with the mechanism of unsubstituted benzoin photoremovable groups. Attention has been given to design and study new, potentially faster and less damaging caging groups than the well-known *o*-nitrobenzyl compounds that present several drawbacks. First, the release is slower than for benzoin derivatives and the final nitroso compound is not benign. Initially Givens et al.⁹ studied the benzoin phosphate, observed its efficiency and noted that benzoin is a good alternative to nitrobenzyl phototriggers. Indeed, benzoin-caged phosphates are capable of rapid release of nucleotides and other biologically active phosphates, which are used to study the kinetics of muscle action by ATP, or calcium channel activation by GTP, for example. This derivative has a triplet excited state intermediate, as shown by piperylene and naphthalene quenching experiments. Furthermore, Givens et al. caged cAMP, GABA and glutamate with benzoin esters. Photolysis at 350 nm of solutions of γ -*O*-desyl glutamate and *o*-desyl GABA in 1:1 H₂O : acetonitrile releases glutamate and GABA respectively, with rate constants of ca. 10^7 s^{-1} to give 2-phenylbenzofuran as the only by-product. Givens¹⁰ et al. studied the benzoin phosphate triester and the water soluble mono and diesters; the yield of free diester released is 30% in acetonitrile and is strongly pH dependent. The triplet lifetime has been estimated to lie between 2 and 7 ns⁹. Through their investigations, Givens et al. proved that α -keto phosphates are kinetically superior alternatives to *o*-nitrobenzyl esters for the photorelease of biologically important phosphates. They also showed that, in the triester case, photolysis was pH sensitive and more efficient at pH < 2. The release of phosphate was an order of magnitude less efficient at pH = 7-8 due to its reduced nucleofugacity in the ionized form. Photolysis of α -deuterated desyl ester ruled out a carbene intermediate. Initial homolysis followed by electron transfer and ring closure was proposed as a mechanism (scheme 8). The released phosphate ion is then able to play the role of a base toward the bridgehead proton.



Scheme 8: Mechanism proposed by Givens et al.⁹ for desyl diethyl phosphate ester photolysis.

Givens et al. synthesized and studied the photolysis of the desyl caged ester of cAMP and the rate constant for its release was estimated to be $7.1 \times 10^8 \text{ s}^{-1}$ (with a quantum yield of 0.34), which represents a progress of three orders of magnitude compared to other release reactions. The pH dependency of the photolysis reaction was suppressed by using the triester derivative instead of the diethyl one. In the case of caged amino acids from desyl esters, a rational mechanism, which illustrates the disadvantage of this caged compound in the case of the amine based leaving group, was proposed. The competing path which forms the benzyl could reduce the efficiency of the reaction because the radical is known to be a triplet quencher. Wirz et al.¹¹ have studied the kinetics and the mechanism of diethyl phosphate photorelease from benzoin by ns and ps laser flash photolysis. Steady-state irradiation of benzoin diethylphosphate gives 2-phenylbenzofuran as a main product with a quantum yield of 0.26 in benzene. In trifluoroethanol, only 25% of 2-phenylbenzofuran was formed, the major product being a solvent adduct.

Nanosecond laser flash photolysis of benzoin diethyl phosphate in degassed acetonitrile at 248, 308 or 351 nm gave a permanent absorbance around 300 nm that was formed in less than 25 ns (laser pulse width). In water or trifluoroethanol, a second absorption band was observed at $\lambda = 570$ nm, that was also formed within the duration of the laser pulse and decayed with a rate constant of $k = (2.3 \pm 0.2) \times 10^6 \text{ s}^{-1}$ in degassed aqueous solution. Addition of sodium azide accelerates the decay rate of the 570 nm transient with a quenching coefficient $k_q = (9.9 \pm 0.4) \times 10^9 \text{ M}^{-1} \text{ s}^{-1}$ and reduced the amplitude of the signal.

The decay rate constant of the transient at 570 nm was not changed by the addition of acid. A small effect of oxygen was observed (in aerated solutions $k = (2.8 \pm 0.3) \times 10^6 \text{ s}^{-1}$ and $(3.7 \pm 0.3) \times 10^6 \text{ s}^{-1}$ in oxygen-saturated solutions).

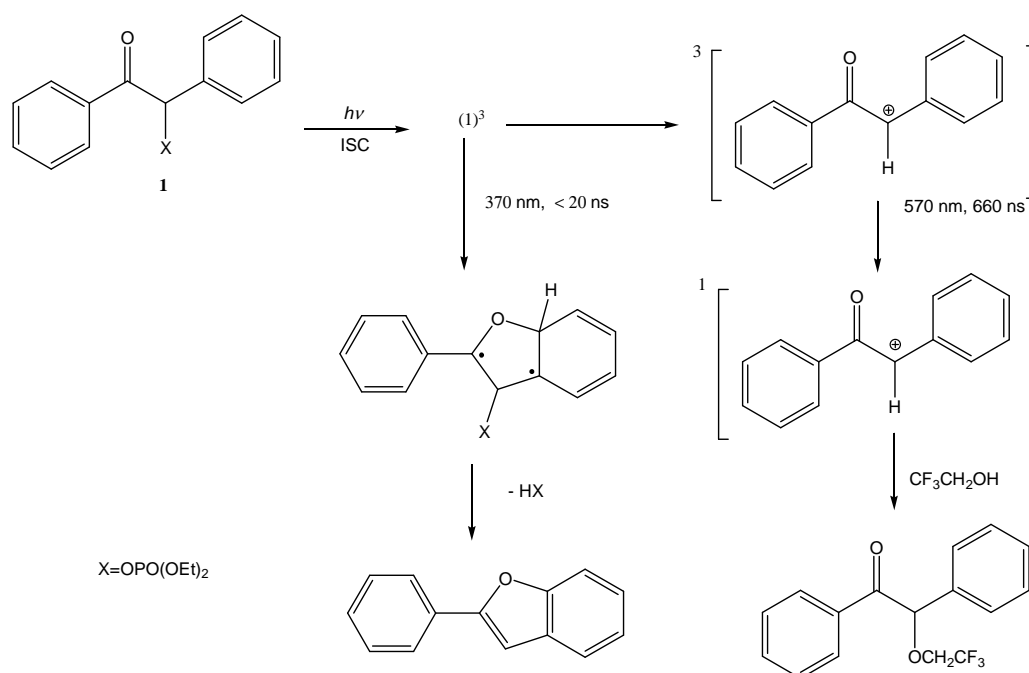
In acetonitrile, dichloromethane, chloroform, tetrahydrofuran, diethyl ether, methanol, ethanol, 2-propanol and ethyl acetate no transient was observed at 570 nm. The permanent product observed at 300 nm was identified as 2-phenylbenzofuran by comparison of its fluorescence with that of an authentic sample. 2-Phenylbenzofuran exhibits a strong fluorescence, whereas the starting material doesn't. Adiabatic formation of the 2-phenylbenzofuran was ruled out by conventional fluorescence spectroscopy. The lifetime of the triplet state of the diethyl phosphate benzoin was determined by energy transfer experiments with naphthalene ($\tau = (24 \pm 2)$ ns in trifluoroethanol).

As the rise time of the 2-phenylbenzofuran was beyond the time resolution at room temperature, Wirz et al. made some experiments at low temperature. Transient absorbance was observed a band in the region 330-430 nm region just after the flash, which was assigned to the triplet excited state of benzoin diethyl phosphate. Experiments at -100 °C in EtOH allowed a measurement of the growth rate of product absorption at 300 nm, $k = 1.8 \times 10^6 \text{ s}^{-1}$. Picosecond laser flash photolysis in acetonitrile at room temperature gave a large transient at 340 nm with a rise time of 2 – 4 ps and a lifetime of at least 5 ns.

The triplet of the starting molecule was assigned as the reactive excited state, the lifetime of which has been estimated to be between 10 and 25 ns, depending on the solvent. In solvents forming strong H-bonds (water, trifluoroethanol), the triplet state forms a triplet α -ketocation to produce the solvent addition product. In other solvents (MeCN), formation of 2-phenylbenzofuran via a cyclic biradical predominates. In both cases diethyl phosphoric acid is released (scheme 9).

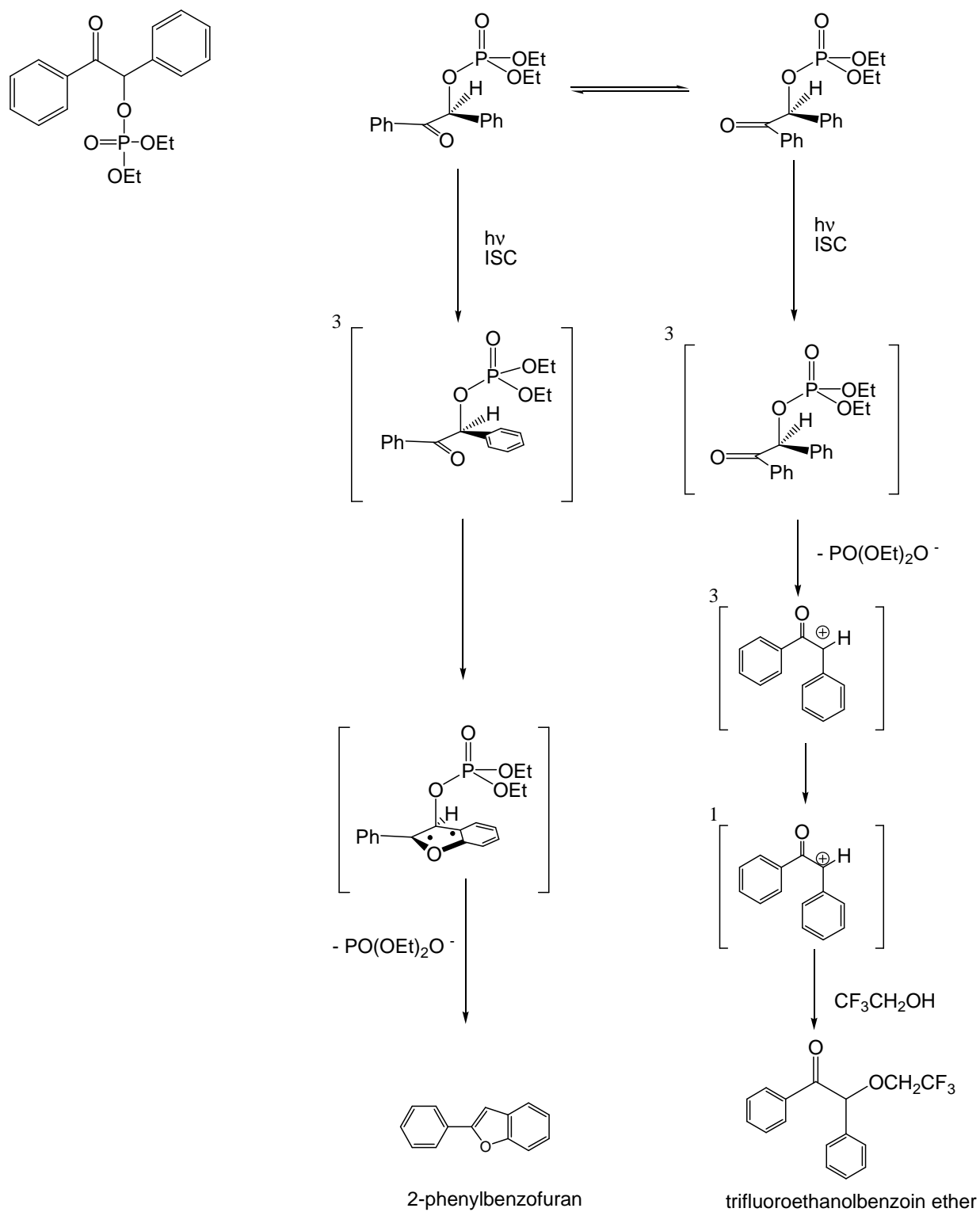
The apparent single-step transformation happened from the triplet to the final furan as a cyclization of the triplet to a biradical, which eliminates diethyl phosphoric acid faster than it

is possible to observe. Recent calculations indicate that the fast concerted elimination of diethyl phosphoric acid occurs from a *syn*-configuration¹².



Scheme 9: Mechanism proposed for benzoin diethyl phosphate photolysis¹⁰.

Quenching experiments have allowed Wirz et al. to prove that the triplet excited state of benzoin diethyl phosphate is the common precursor of 2-phenylbenzofuran and the transient at 570 nm. Radicals and carbenes were ruled out as candidates to describe this intermediate because of their incompatible reactivity, solvent dependency and absorption spectra. The effect of oxygen on the decay rate confirms the triplet multiplicity of cation. Adiabatic heterolytic dissociation of diethyl phosphate from the n,π^* triplet state was the proposed primary reaction. Solvent addition happens only after intersystem crossing to the singlet ground state. Wirz et al. also gave arguments to explain the role of the solvent. In principle a polar solvent should favour heterolytic dissociation, but no cation transient has been observed in the case of acetonitrile. The difference of conformation in the different solvents may explain the different reactivity. The α -phenyl group needs to be close enough to the carbonyl group to cyclise. This conformation is disfavoured in solvents forming hydrogen bonds (trifluoroethanol, water). The anti-conformer is favoured that facilitates the heterolytic cleavage (scheme 10).

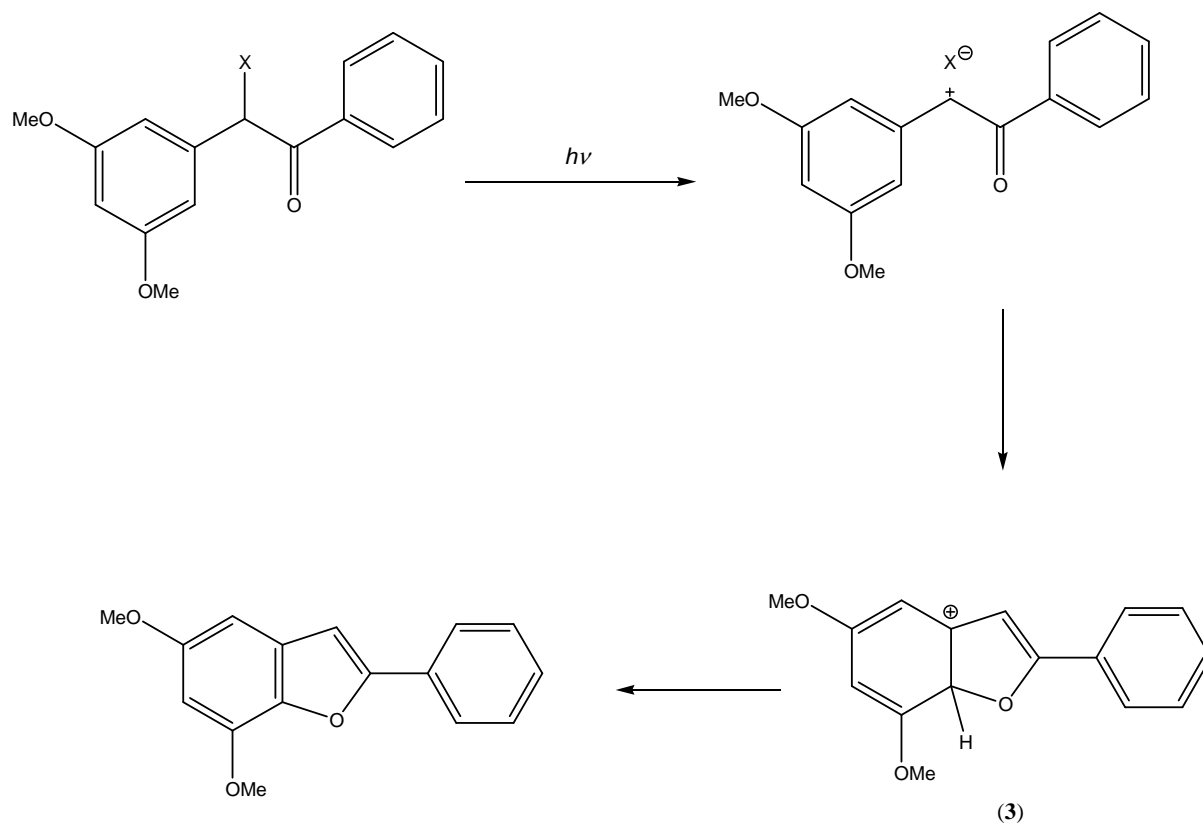


Scheme 10: Wirz's et al. mechanism for photolysis of benzoin phosphates, including the conformation effect.

The study of the dynamics of enzyme-catalysed processes by time resolved X-rays is one of the interesting applications of this type of caged compound. For this purpose, Peach et al.¹³ synthesized photolabile benzoin and furoin esters for caging active peptides. The 2-phenylbenzofuran produced is expected to be inert towards proteins.

1.3 The dimethoxybenzoin.

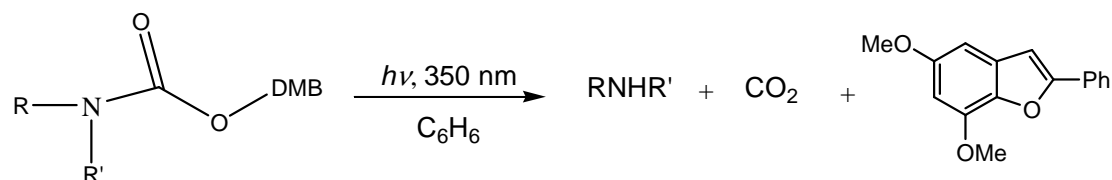
Substitution on the benzylic ring was found to make photolysis more efficient. Sheehan et al.⁴ reported that substitution at the 3'-and 5'-positions gave the best yields of benzofuran, the cleaner reaction, and that it proceeded through a singlet or a short-lived triplet state, as the quantum yield (0.64 for the acetate) was not affected by triplet quenchers. An intramolecular Paterno-Büchi reaction of the singlet excited state has been proposed by Sheehan et al.^{2, 4} (Scheme 4) to explain the formation of benzofuran product. Pirrung and Shuey¹⁵ synthesized and studied some phosphotriesters of 3',5'-dimethoxybenzoin for synthesis and caging. They tested several kinds of nonacylated aromatic ring substitutions and the best yields were again obtained with the 2',3'-dimethoxybenzoin and 3',5'-dimethoxybenzoin. They managed to develop an asymmetric synthesis of 3',5'-dimethoxybenzoin to minimize the number of diastereoisomers in phosphorylation of chiral alcohols. Following Sheehan's work on 3',5'-dimethoxy substitution on the benzoin and Zimmerman's results on the meta donor effect in benzene excited states, they suggest that the α -ketocation obtained by heterocyclic cleavage from the singlet excited state cyclises to form a cation (**3**) which deprotonates to form the final furan (scheme 11).



Scheme 11: Mechanism proposed by Pirrung et al.¹⁵ for the 3',5'-dimethoxybenzoin photolysis (X = OAc, OP(OEt₂)NR₁R₂).

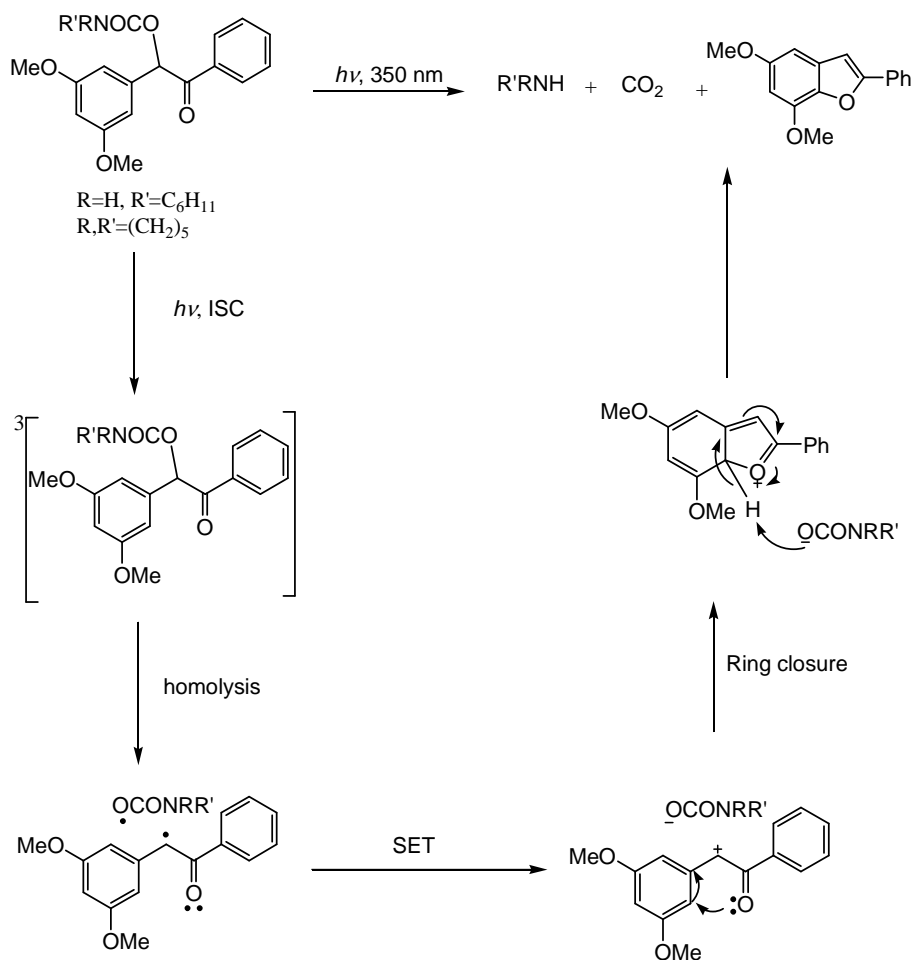
They also argue that a relatively good leaving group is necessary for the formation of benzofuran, otherwise the molecule will rather undergo α -cleavage.

Using this study, Pirrung¹⁶ et al. developed the dimethoxybenzoin (DMB) carbonate group to protect the 5'-hydroxyl groups of nucleosides, allowing the development of a photochemical version of phosphoramidite-based DNA synthesis. Dimethoxybenzoin phosphate has also been applied to prepare short DNA sequences, using light to deprotect a nucleoside 3'-phosphotriester to generate a phosphodiester used for nucleotide coupling. This technique can be applied to the preparation of surface-bound arrays of DNA probes. Experiments on parallel irradiations of DMB acetate and benzyl DMB carbonate show essentially the same rate of deprotection, so the quantum yield should be similar (0.64). They also worked on the use of DMB-carbamates¹⁷ for amine protection and photochemical deprotection (scheme 12), which can be used to produce images in polymer films.



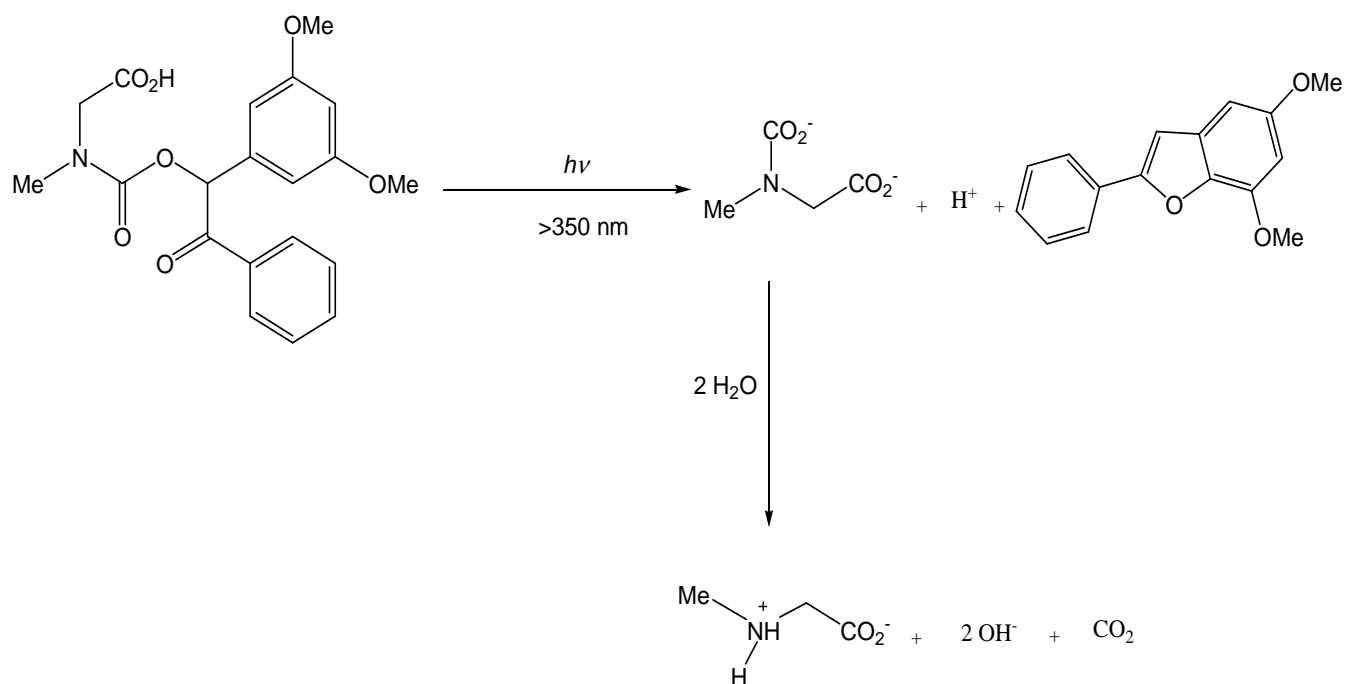
Scheme 12: Photogeneration of amines using photochemical deprotection of 3',5'-dimethoxybenzoin carbamates.

Cameron et al.¹⁸ designed a novel class of photoprecursors of organic bases. These photolabile amino protecting groups, based on 3',5'-dimethoxybenzoinyloxycarbonyl carbamates, generate free primary and secondary amines. The same authors also studied the solid state and the solution photolysis of many derivatives and found similar behaviour. The clean photochemistry and photobleachable absorption allow applications for thick films. Based on Givens' et al. work on desyl ester photocyclization and on Zimmerman's meta-effect, Cameron rationalized the photorelease of amines by an ion-pair mechanism. The proposed mechanism is shown in scheme 13. The triplet is formed by $n-\pi^*$ excitation. Then a radical pair is formed by homolysis, which is followed by single electron transfer giving an ion pair. The cation cyclizes and the free anion, acting as a base, removes the proton and the dimethoxybenzofuran is formed. Carbon dioxide is released and the amine is free.



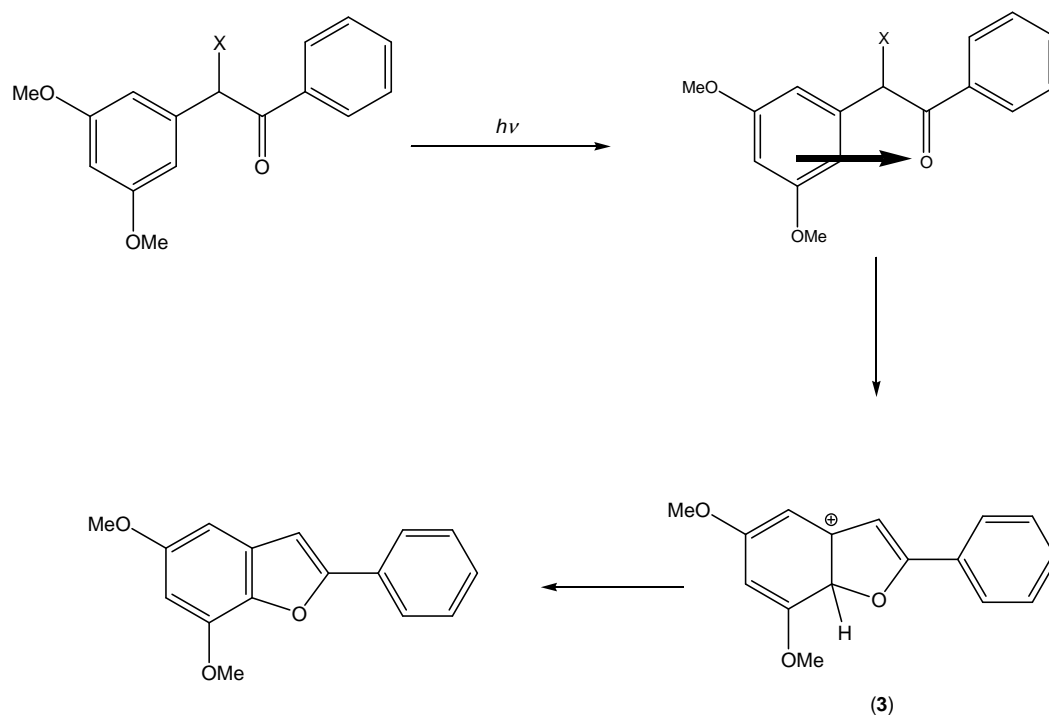
Scheme 13: Proposed mechanism for amine photogeneration from dimethoxycarbamate.

Carbamoyl derivatives of photolabile benzoin derivatives have also been synthesized and studied by Corrie and Papageorgiou. They found that the amine release rate, corresponding also to the rate of decarboxylation, was too slow (ms time scale) for applications requiring rapid release of neuroactive amino acids. At pH 7.0, rapid acidification is followed by a first order basification due to the slow amine release ($t_{1/2} = 4.5\text{ ms}$) from the carbamate anion (scheme 6). The released CO_2 is subsequently hydrated on a much longer time scale¹⁹.



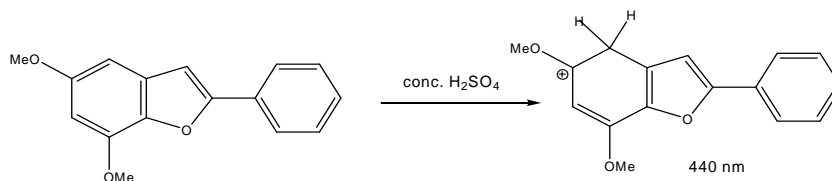
Scheme 14: Corrie's mechanism for amine photogeneration from dimethoxycarbamate.

Shi, Corrie and Wan²⁰ studied 3',5'-dimethoxybenzoin ester derivatives to understand the mechanism of photocyclisation. They agree with Pirrung for the last deprotonation step, but proposed a charge transfer interaction between the dimethoxybenzene ring and the $n-\pi^*$ singlet excited acetophenone (intramolecular exciplex) as first step (scheme 15). The last precursor in this case is the dimethoxycyclohexadienyl cation (**3**). Contrary to Pirrung et al., they exclude the α -ketocation or α -radical participation, because of the absence of solvent addition or radical-derived products.



Scheme 15: Mechanism proposed by Shi et al. for the 3', 5'-dimethoxybenzoin ester photolysis.

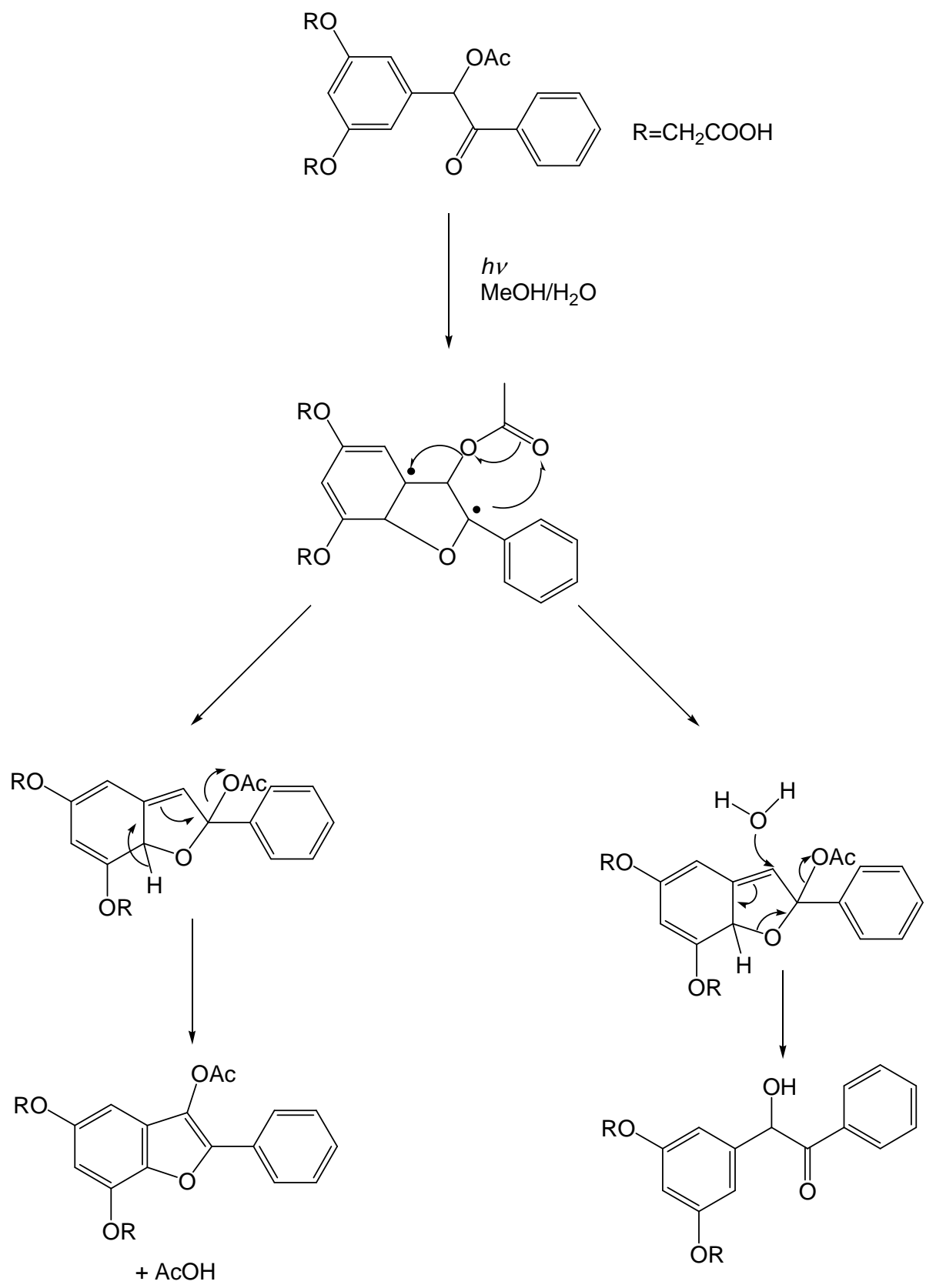
The transient absorbing at 485 nm, observed by LFP was attributed to cation **3**. This cation decays with a rate constant of $1.0 \times 10^6 \text{ s}^{-1}$. Addition of a small amount of water accelerates this decay until it was too fast for observation (5%). Protonation of the final product with concentrated sulphuric acid gave a product absorbing at 440 nm with a band shape similar to the 485-nm observed band observed by LFP of the starting dimethoxybenzoin (scheme 16).



Scheme 16: Protonation of dimethoxybenzofuran in concentrated sulphuric acid.

The authors argue that the longer λ_{\max} of **3** is due to a more extended simple polyene-type π -conjugation compared to the protonated product, similar as an allyl cation conjugated to a furan ring.

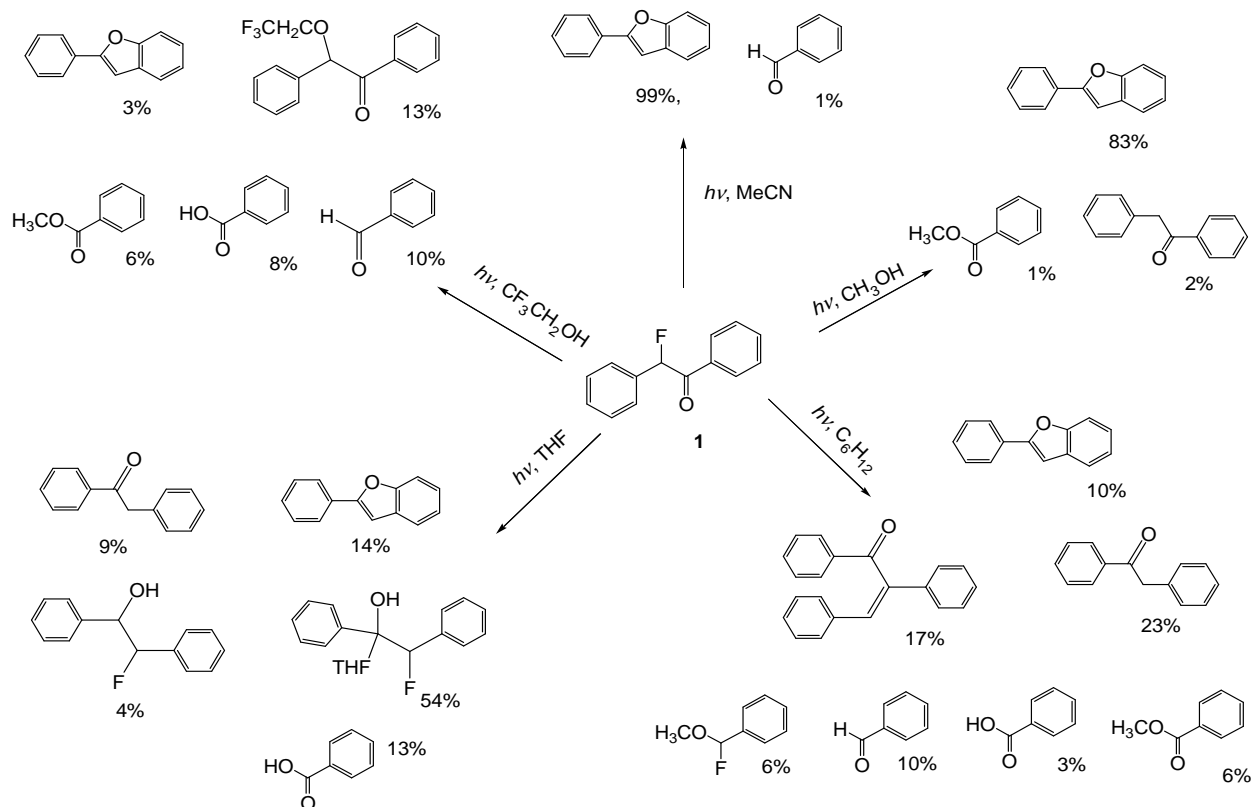
An additional transient has been observed at 330 and 420 nm. Contrary to the 485 nm signal, these new signals are affected by air (a faster decay is observed in air saturated solution). Hence, the absorptions at 420 nm and 330 nm were attributed to the triplet state of the 3',5'-dimethoxybenzoin ester. Shi et al. also concluded that the reaction proceeded from the singlet state because of the oxygen non-dependence of the yields. The main problem for biological application of benzoyl caged compounds is their poor solubility. The phenylbenzofuran photoproduct is even more insoluble and precipitates. Rock and Chan²¹ designed a dimethoxybenzoin with charged functionalities, the 3',5'-bis(carboxymethoxy)benzoin acetate (BCMBa). Photolysis of BCMBa has been done in water and methanol in aerobic conditions. They observe a lower yield of 2-phenylbenzofuran in water compared to methanol. This was explained by the formation of a second photoproduct, the 3',5'-bis(carboxymethoxy)benzoin (BCMB). With such considerations, they disfavour the possibility of the strained intermediate proposed by Sheehan, because of the necessity of the benzylic carbon to be accessible to water (or nucleophile) attack. They also argue that an α -ketocation can't participate in the cyclisation, because the heterolytic cleavage generating this cation is usually seen for $\pi-\pi^*$ excited states and not $n-\pi^*$, responsible for the cyclization. They proposed a biradical intermediate, which undergoes an acetoxy migration. This last intermediate can cyclize to form the phenylbenzofuran, or can undergo nucleophilic attack by water (scheme 17). But no spectroscopic evidence of any of those intermediates has been given.



Scheme 17: Mechanism proposed by Rock et al. for the 3', 5'-bis(carboxymethoxy)benzoin photolysis²¹.

2. Investigations on the mechanism of 2-fluorobenzoin photolysis

2.1. Preparative photolysis²²



Scheme 18: Products from preparative photolysis of **1**.

Starting materials **1** (0.01 M) were photolysed at 350 nm during 2 hours and the product distribution was determined by GC/MS by comparison with the retention time of authentic reference compounds (scheme 18).

Photolysis of **1** in CH₃CN or MeOH produces mainly 2-phenylbenzofuran. In MeOH some traces of solvent addition to the acyl radical formed by α -cleavage were detected. In trifluoroethanol several products are due to direct α -cleavage. Only 3% of 2-phenylbenzofuran and 13% of the α -ketocation solvent adduct are formed.

In apolar solvents like cyclohexane the products formed by photolysis of **1** are due to H-abstraction or recombination after α -cleavage of the starting material. In THF, the main

photoproduct is due to solvent addition to the carbonyl which has abstracted an H-atom. Quantum yields were determined for **1** in MeCN (0.01 M, at 25°C, $\lambda_{\text{irradiation}} = 350 \text{ nm}$, $I_{\text{lamp}} = 1.65 \times 10^{16} \text{ quanta (mL.s)}^{-1}$). Actinometry was done with ferrioxalate. The solution was irradiated for 5, 10, 14 and 20 min. The conversion was determined by GC using naphthalene as an internal standard. The quantum yield of disappearance was found to be 0.74. Quenching experiments showed that the photocyclisation of **1** proceeds through a triplet state^{2,4}.

2.2. Nanosecond LFP of 2-fluorobenzoin.

2.2.1. In MeCN and in water

Solutions of **1** with an absorbance of 0.25 to 0.2 per cm were excited at 248 nm (100 mJ) to observe UV-Visible spectra and kinetics of the transients. In pure MeCN, a band at 300 nm is formed immediately after the first flash (no decay was observed in either degassed or in air saturated solution), which can be attributed to formation of the end product. A second band at 400 nm (decay observed: $k_1 = (3.61 \pm 0.14) \times 10^4 \text{ s}^{-1}$, $k_2 = (1.16 \pm 0.01) \times 10^4 \text{ s}^{-1}$), seen only on second excitation, may be due to reexcitation of 2-phenylbenzofuran. In an aqueous solution containing 4% of MeCN, absorption spectra taken shortly after the laser pulse exhibit an additional absorption maximum between 500 and 600 nm (at 570 nm; decay rate constant $k = (2.58 \pm 0.09) \times 10^6 \text{ s}^{-1}$ in degassed solution) (figure 2).

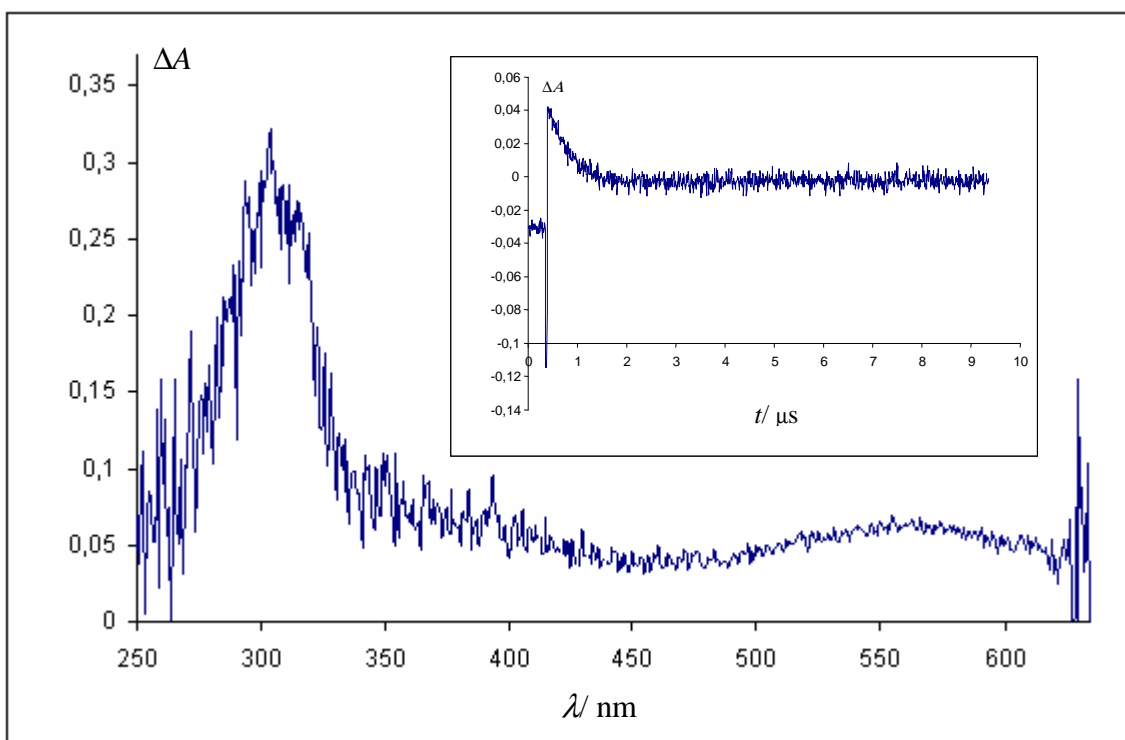


Figure 2: Kinetic trace of the absorbance at 570 nm (inset) and UV spectra of the transients 10 ns after the laser excitation.

A solution of **1** in air-saturated MeCN was studied (observation 20 ns, 200 ns, 1 μ s and 4 μ s after the laser pulse, (Figure 3)). We can see a band centred around 300 nm (observed 20 ns after the laser excitation) which represents the absorbance of the final product (2-phenylbenzofuran).

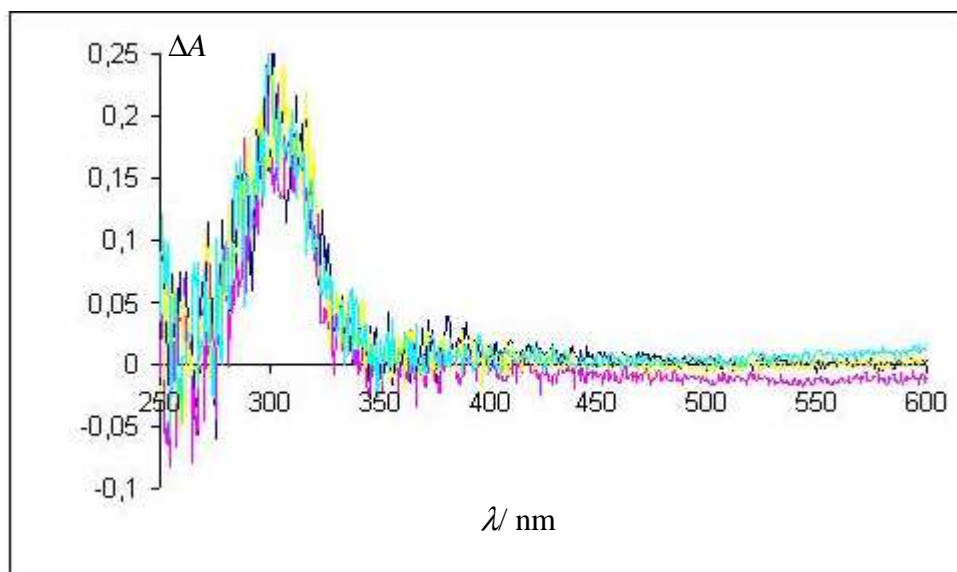


Figure 3: UV spectra of the transients 20 ns (blue), 200 ns (pink), 1 μ s (yellow) and 4 μ s (cyan) after the laser excitation of 2 FB in air saturated MeCN.

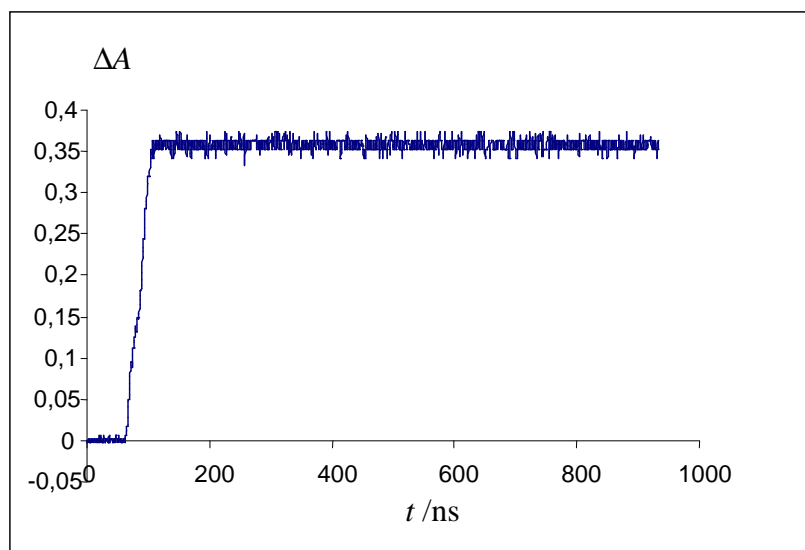


Figure 4: Kinetic traces of **1** in air-saturated MeCN observed at 301 nm (growth, formation of 2-phenylbenzofuran).

2.2.2. In ethanol at low temperature.

The goal of an experiment at low temperature was to resolve the formation and/or decay of an intermediate of short lifetime, not visible at room temperature. From quenching experiments of related compounds¹¹, we suspected that the triplet of **1** has a lifetime of less than 20 ns at room temperature. LFP of **1** in EtOH ($A_{248 \text{ nm}} = 0.97$ per cm) at -110 °C produced a transient absorbing at 370 nm with an $A_{\text{max}} = 0.012$. This signal is attributed to the triplet of **1** (Figure 5). It decayed with a rate constant of about $(1.80 \pm 0.02) \times 10^6 \text{ s}^{-1}$ to form the final product (2-phenylbenzofuran). Wirz et al.¹¹ have assumed that the rate-determining step of this transformation is the cyclization of the triplet to the biradical. At low temperature the formation of this triplet seems to be accomplished within the laser pulse, because the growth preceding the decay at 370 nm can't be resolved.

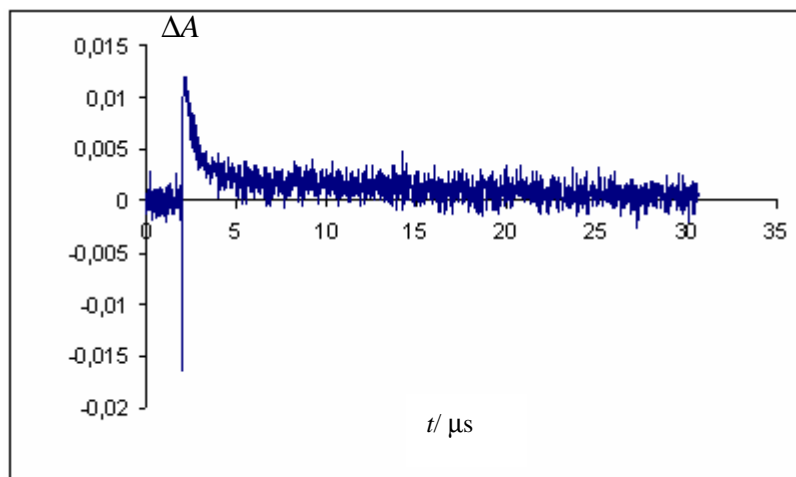


Figure 5: **1** in degassed EtOH at -110°C , kinetic trace of the absorbance at 370 nm.

At 300 nm a growth with a rate constant of $(1.7 \pm 0.8) \times 10^6 \text{ s}^{-1}$ is observed (Figure 6). Strong fluorescence from the photoproduct made kinetic analysis at 300 nm difficult. This result confirms an observation made by Wirz et al.¹¹; if another intermediate is involved, it must be shorter-lived than the triplet state, because the rate of formation of the final product is equal to the decay rate of the **1** triplet.

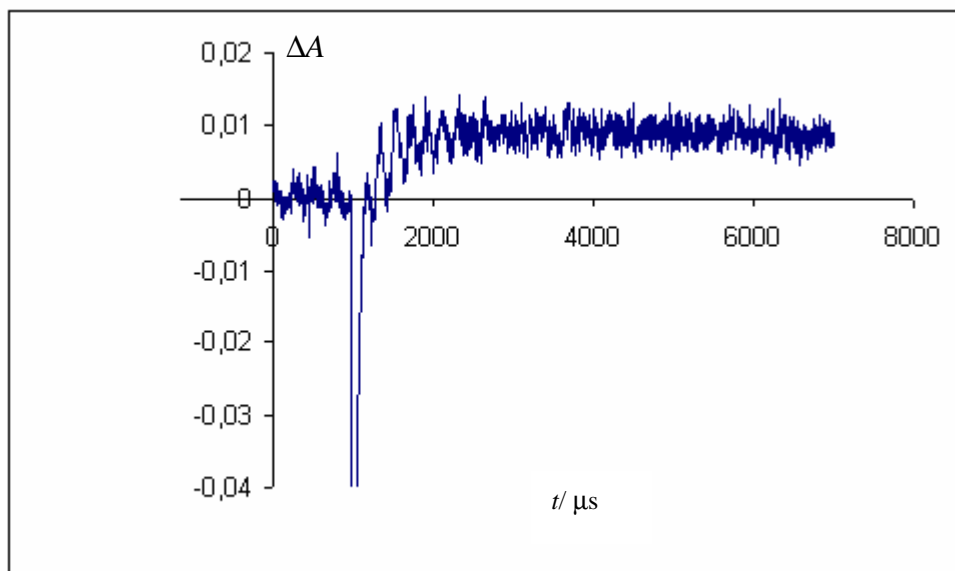


Figure 6: Kinetic trace of the absorbance at 300 nm.

2.2.3. In hexane.

In this solvent, we are looking for a biradical, formed from the triplet state of **1**, as a precursor to the cyclisation and the formation of the 2-phenylbenzofuran. The low polarity of the solvent should disfavour any heterolytic release of the leaving group. Solutions of **1** in hexane were degassed and flashed with an excimer laser 248 nm (120 mJ). UV Visible spectra were recorded 20 ns, 150 ns, 300 ns and 1 microsecond after the laser excitation (Figure 7). Just after the laser, a strong and a large band is observed with a maximum around 310 nm. Longer delays show the same band structure with a lower intensity. Kinetic analysis at 310 nm indicates that the species is formed in less than 25 ns and has a lifetime in degassed solution of (75 ± 5) ns. It's a second order decay ($k = (1.95 \pm 0.03) \times 10^8 \text{ M}^{-1} \text{ s}^{-1}$) in air-saturated hexane. In oxygen saturated hexane: $k_1 = (8.28 \pm 0.09) \times 10^6 \text{ s}^{-1}$, $k_2 = (7.22 \pm 1.06) \times 10^5 \text{ s}^{-1}$ (Figure 8). The longer lifetime in presence of oxygen may be explained by O_2 trapping of radicals and formation of peroxide radicals. These signals may correspond to absorption by radicals coming from the α -cleavage of **1**. A study of the deoxybenzoin should help to understand these signals, because this compound is known to form radicals due to α -cleavage.

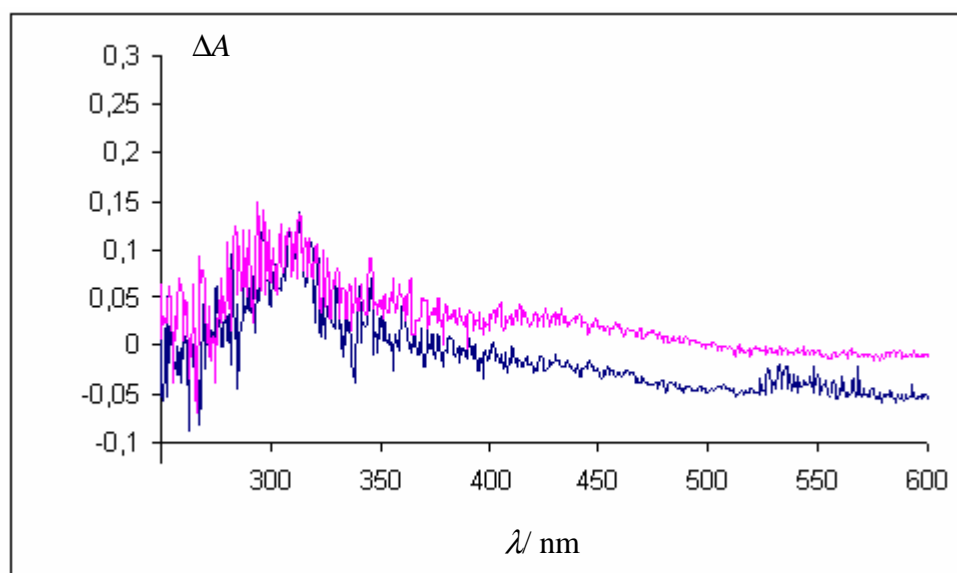


Figure 7: UV spectra of the transients 20 ns (blue), 500 ns (pink), after the laser excitation of **1** in degassed hexane.

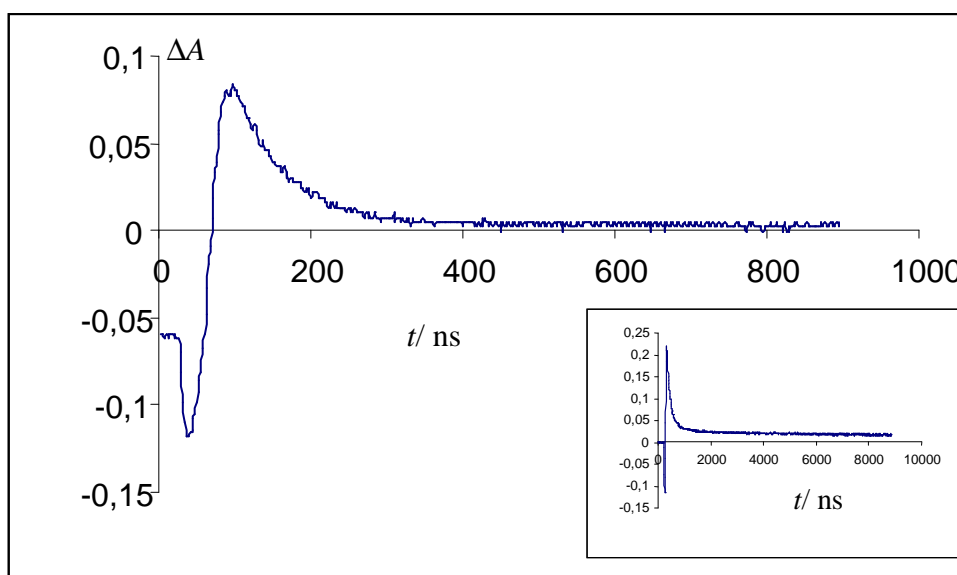


Figure 8: Kinetic traces of the **1** in degassed (air saturated in the inset) hexane observed at 310 nm.

2.3. Nanosecond LFP of diethyl phosphate benzoin in hexane.

To check whether the previously studied benzoin diethyl phosphate¹¹ (**4**) also gives the same transient absorption in hexane, LFP experiments were done with a solution of **4** in hexane (1% CH₂Cl₂) with an $A_{248} = 0.395$ per cm.

UV spectra recorded 15 ns and 1 μ s after the laser flash in air saturated and degassed solution show the same bands: one major band around 310 nm and two others with maxima at 345 and 470 nm (15 ns after the laser) (Figure 9).

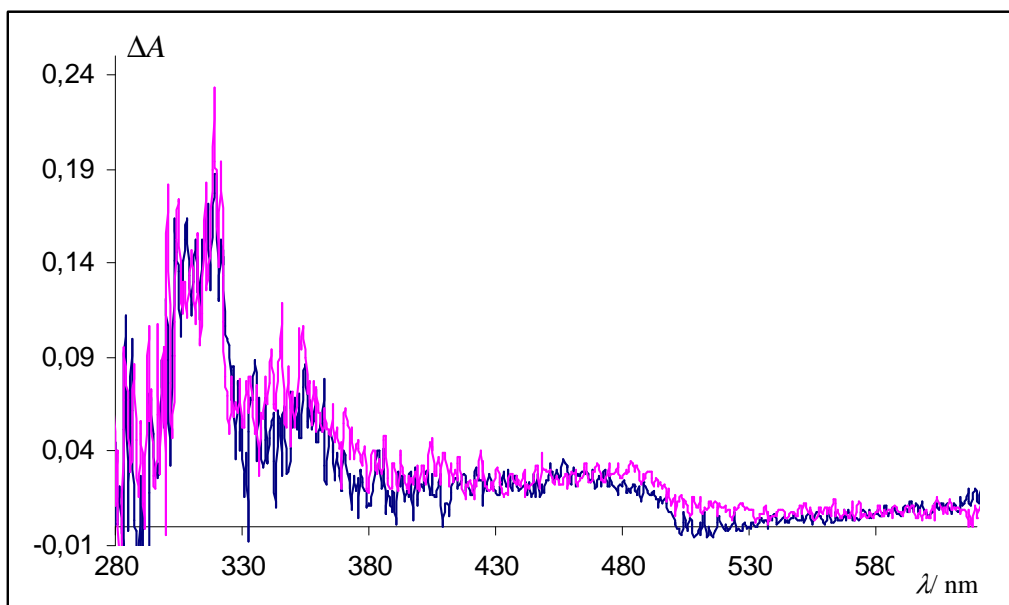


Figure 9: UV spectra of the transients 15 ns (blue), 1 μ s (pink), after the laser excitation of **4** in degassed hexane.

The decay kinetics at 345 and 470 nm are the same, but different from those at 310 nm. The transient observed at 310 nm is quenched by oxygen: the decay is faster in air saturated ($k_1 = (7.21 \pm 0.14) \times 10^6 \text{ s}^{-1}$, $k_2 = (6.44 \pm 0.07) \times 10^5 \text{ s}^{-1}$) than in degassed solution ($k = (5.32 \pm 0.04) \times 10^5 \text{ M}^{-1} \text{ s}^{-1}$) (Figure 10). In an oxygen saturated solution, we measured a rate constant of $k = (1.90 \pm 0.28) \times 10^7 \text{ s}^{-1}$. For the signals observed at 345 and 470 nm, oxygen had no influence on the second order decay ($k = (1.77 \pm 0.05) \times 10^7 \text{ M}^{-1} \text{ s}^{-1}$) (Figure 11).

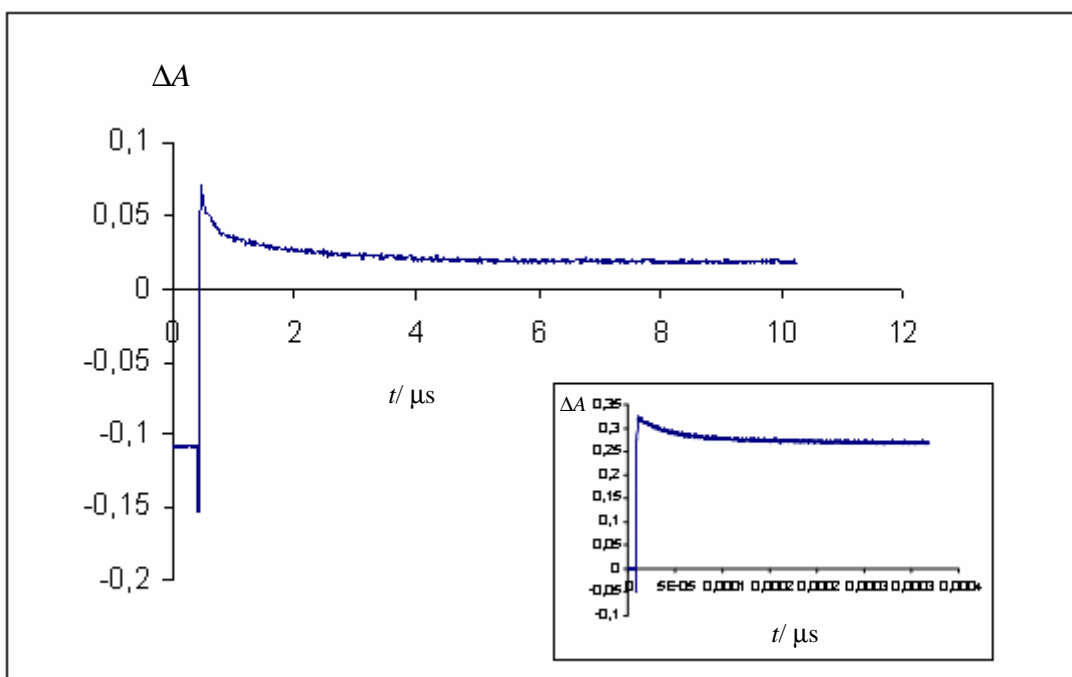


Figure 10: Kinetic traces of **4** in air saturated hexane observed at 310 nm in air saturated and degassed (inset).

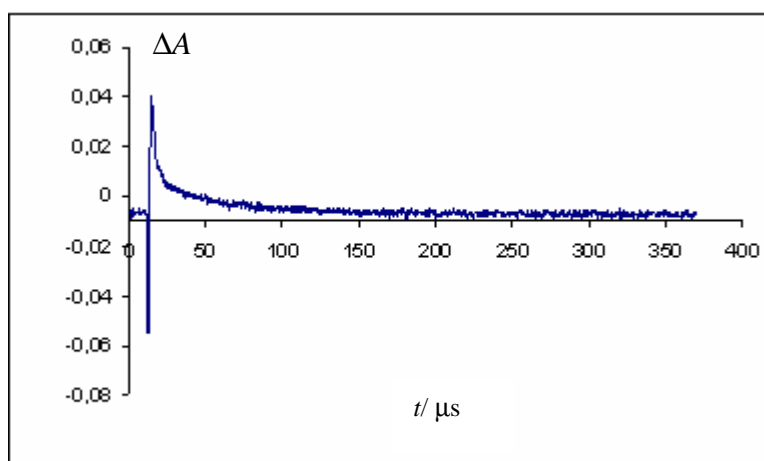
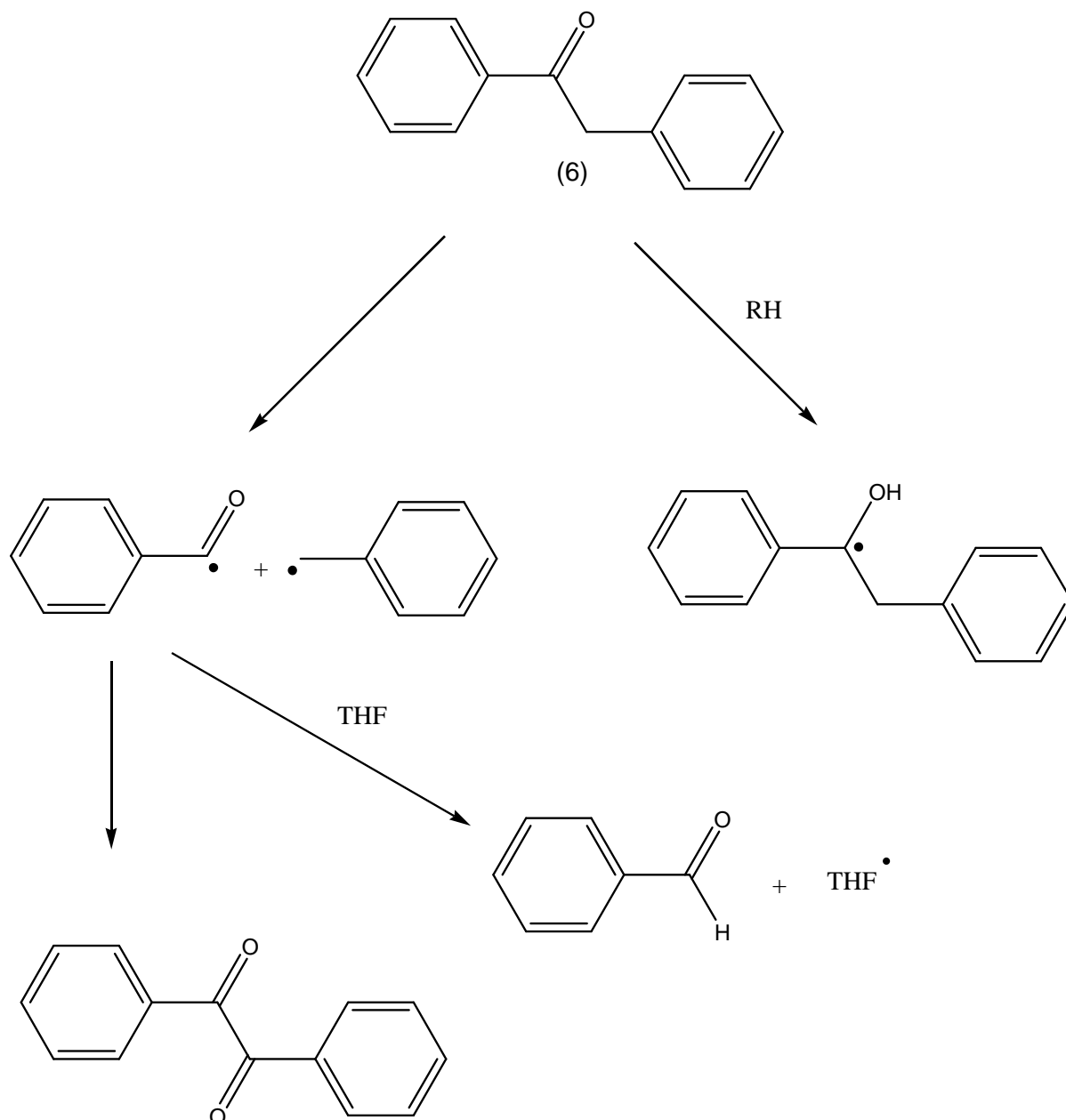


Figure 11: Kinetic trace of **4** in air saturated hexane observed at 345 nm.

If we assume that only the signal at 310 nm is due to radicals, the radicals coming from **1** have a lifetime shorter by two orders of magnitude than those formed from **4** in degassed hexane. The biexponential decay rate constants of **1** and **4** in air saturated hexane are close ($k_1 = (6.53 \pm 0.68) \times 10^5 \text{ s}^{-1}$, $k_2 = (7.78 \pm 0.16) \times 10^6 \text{ s}^{-1}$). The difference observed of the decay rate constants of the two different radicals at 310 nm in degassed solution may be attributed to the leaving group effect.

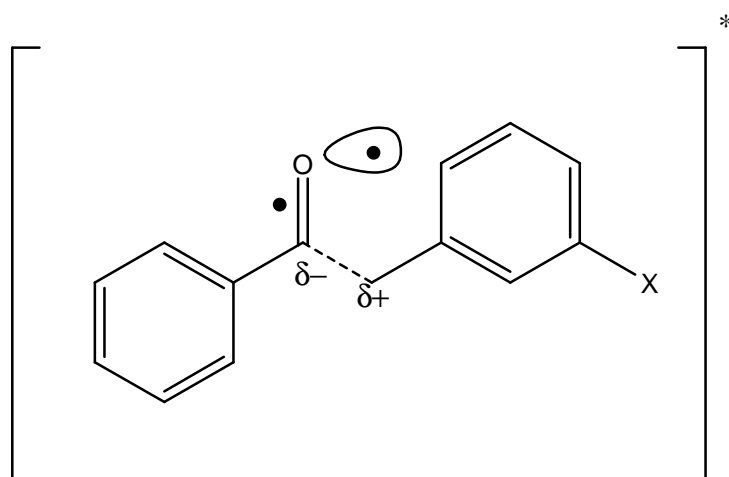
2.4. Nanosecond LFP of deoxybenzoin.

To investigate the behaviour of the radicals formed by α -cleavage, we studied deoxybenzoin (**6**) by ns laser flash photolysis. This compound is known to undergo α -cleavage (Norrish I) and hydrogen abstraction from the solvent⁷ (scheme 19).



Scheme 19: Mechanism of laser flash photolysis of **6**⁸.

We would like to check the assignments of the signal observed for **1** in hexane and see if this compound shows any other transient absorbance, like biradical. If **1** and **6** have the same photochemical behaviour, **6** should form a biradical intermediate, which decays mainly to the ground state, because most of the product observed comes from α -cleavage reaction. The cyclisation reaction, which gives the biradical, is in competition with the α -cleavage, which has to be faster. Two possible arguments may explain why a cyclisation can happen instead of the α -cleavage: the electronic character of the molecule and/or the electronic configuration of the transition state. The first argument can be discarded because the excited state involved in the cyclisation and in the α -cleavage is the same (n,π^*)^{2, 4}. An interesting argument from Lewis et al.⁸ may explain why **1** and **2** rather cyclise than forming a radical pair as observed for deoxybenzoin. Lewis described the transition state for α -cleavage of deoxybenzoin derivatives (scheme 20).



Scheme 20: Transition state for α -cleavage proposed by Lewis et al.⁸

In this model, the partial negative charge can be stabilized by the electrophilic oxygen (half-vacant non bonding orbital) and the partial positive charge by electron donating aromatic substituents. Substituents, which are capable of stabilizing an adjacent positive charge should accelerate the photochemical α -cleavage. In **1** and **2**, the α -F substituent will not stabilize the positive charge (compared to H), so it should disfavour α -cleavage relatively to cyclisation.

2.4.1 In hexane.

LFP experiments were done with a solution of **6** in hexane ($A_{248} = 0.35$ per cm). The transient spectrum (20 ns after the laser) shows two bands, one centred at 310 nm and another one at 430 nm (Figure 12). The 310 nm and 430 nm absorptions are due to formation of radicals from α -cleavage of the deoxybenzoin⁷ (ketyl, benzoyl and benzyl radical). Lewis et al.⁸ argued that the minimum quantum yield for α -cleavage is represented by the quantum yield of benzaldehyde formation ($\Phi = 0.44$) and that cage recombination of benzoyl and benzyl radicals could account for approximately half of the initially excited molecules⁸. This would indicate that α -cleavage can be considered to be the dominant primary photochemical process for **6**.

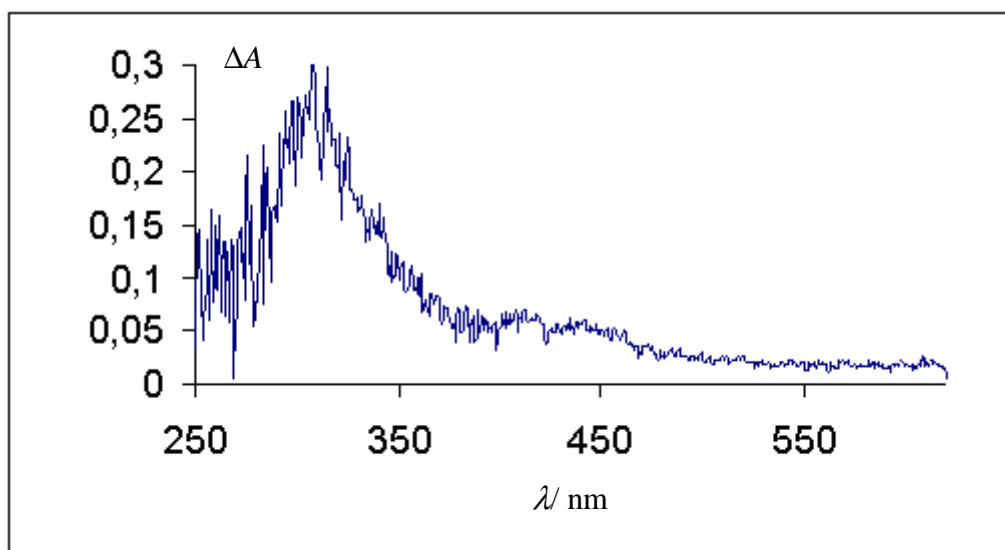


Figure 12: UV spectra of the transients 20 ns after the laser excitation of **6** in degassed hexane.

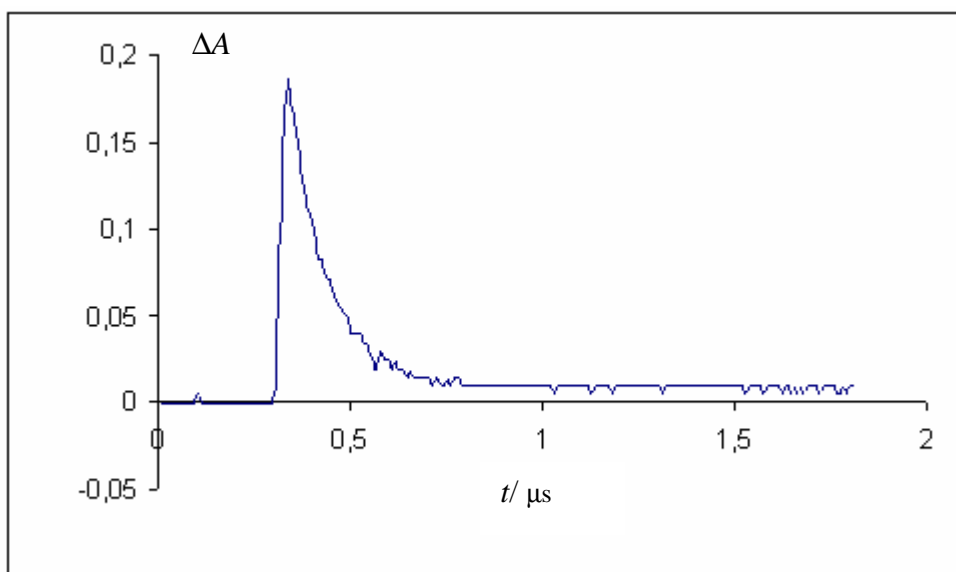


Figure 13: Kinetic trace of **6** in air saturated hexane observed at 310 nm.

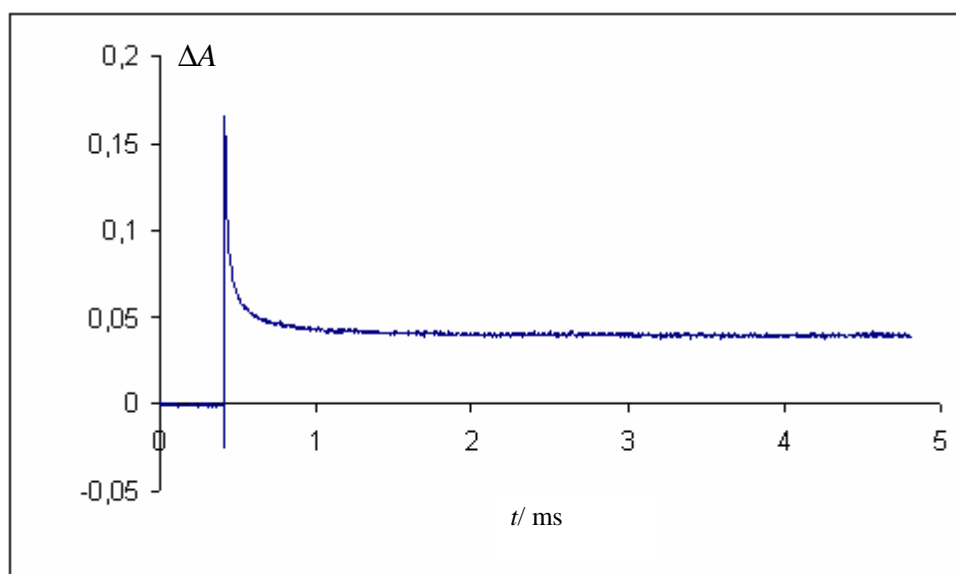


Figure 14: Kinetic trace of **6** in degassed hexane observed at 310 nm.

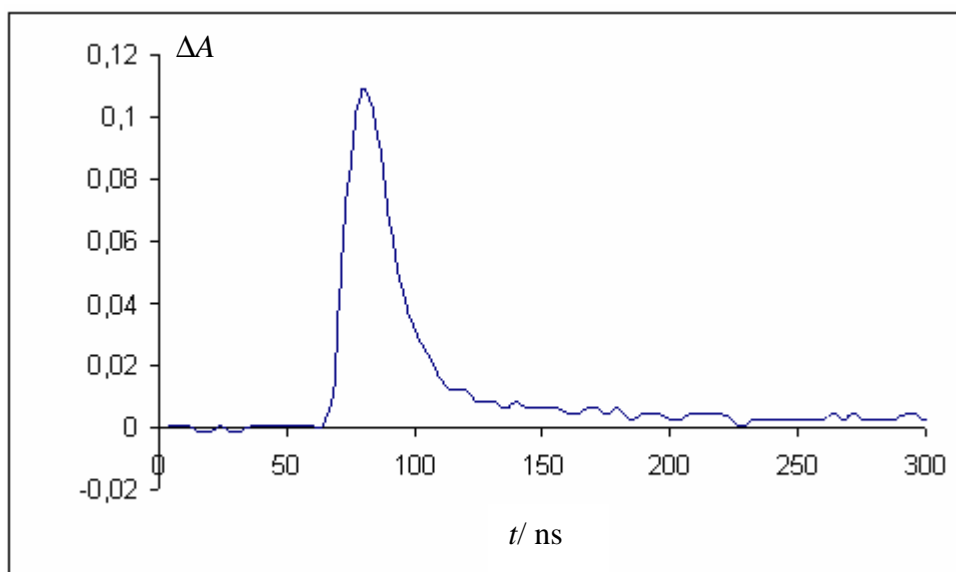


Figure 15: Kinetic trace of **6** in oxygen-saturated hexane observed at 310 nm.

Kinetic measurement at 310 nm gave a monoexponential decay ($k_1 = (9.93 \pm 0.09) \times 10^6 \text{ s}^{-1}$) in air saturated solution (Figure 13), a second order decay in degassed hexane $k = (1.98 \pm 0.02) \times 10^5 \text{ M}^{-1} \text{ s}^{-1}$ (Figure 14). In oxygen saturated solution $k = (6.50 \pm 0.14) \times 10^7 \text{ s}^{-1}$ (Figure 15).

2.4.2 In MeCN.

In degassed, air and oxygen saturated MeCN, the UV-Visible transient spectra show a large band centred around 320 nm (Figure 16). At 320 nm, in degassed solution the decay follows second order kinetics ($k = (1.75 \pm 0.01) \times 10^5 \text{ M}^{-1} \text{ s}^{-1}$, Figure 17). In air and oxygen saturated solution the decay is monoexponential, $k = (8.69 \pm 0.05) \times 10^6 \text{ s}^{-1}$ and $k = (2.47 \pm 0.06) \times 10^7 \text{ s}^{-1}$, respectively (Figure 18 and 19).

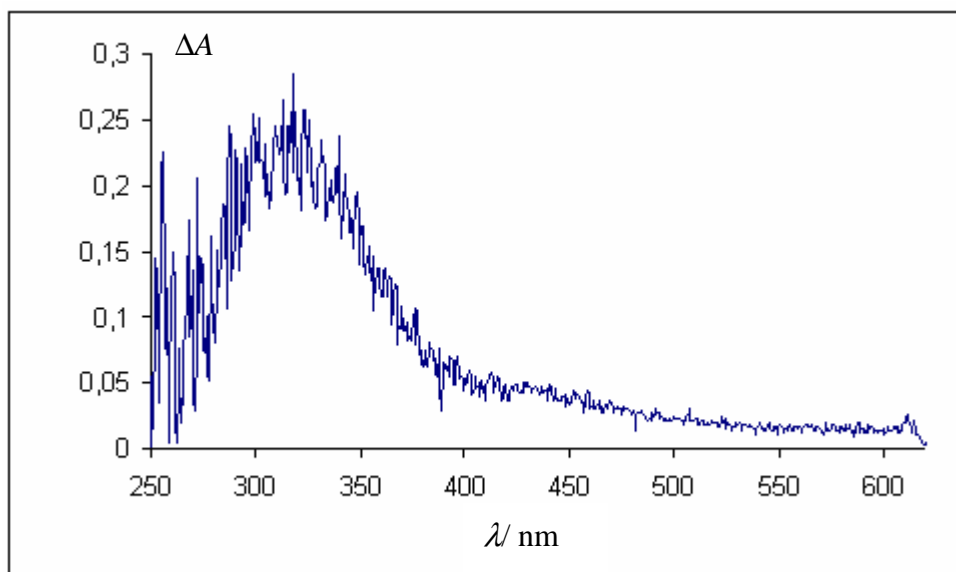


Figure 16: Transient UV spectrum 20 ns after 248 nm laser excitation of **6** in degassed acetonitrile.

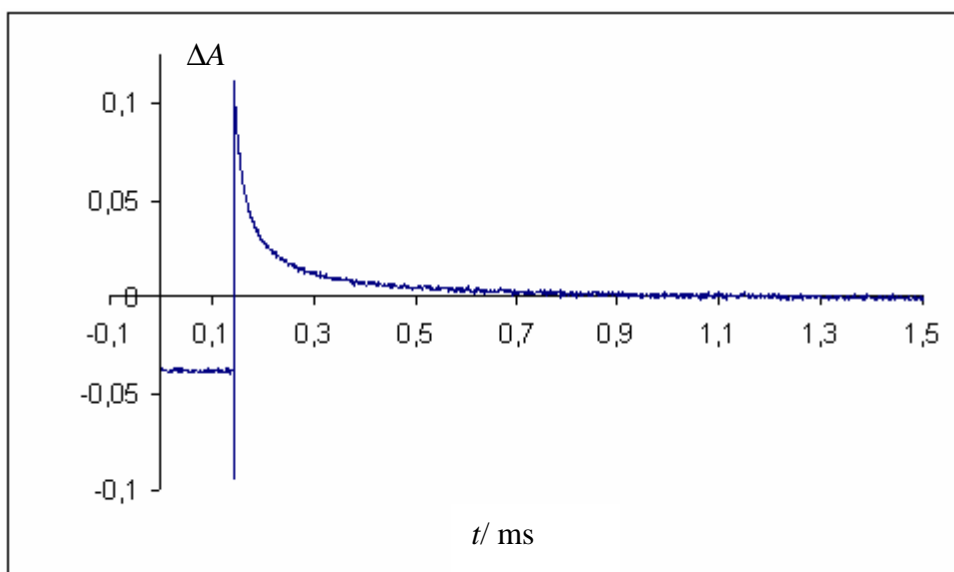


Figure 17: Kinetic trace of **6** in degassed acetonitrile observed at 310 nm.

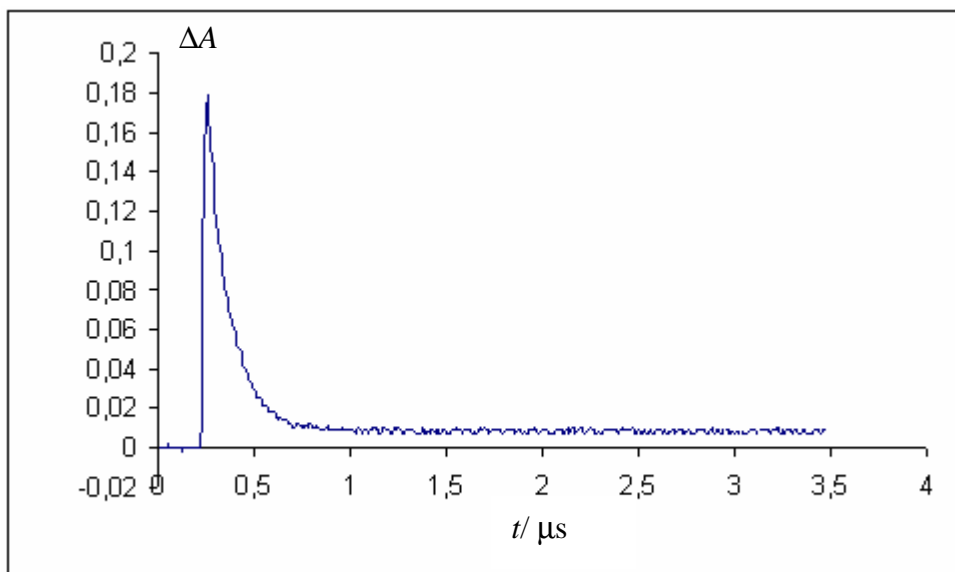


Figure 18: Kinetic trace of **6** in air-saturated acetonitrile observed at 310 nm.

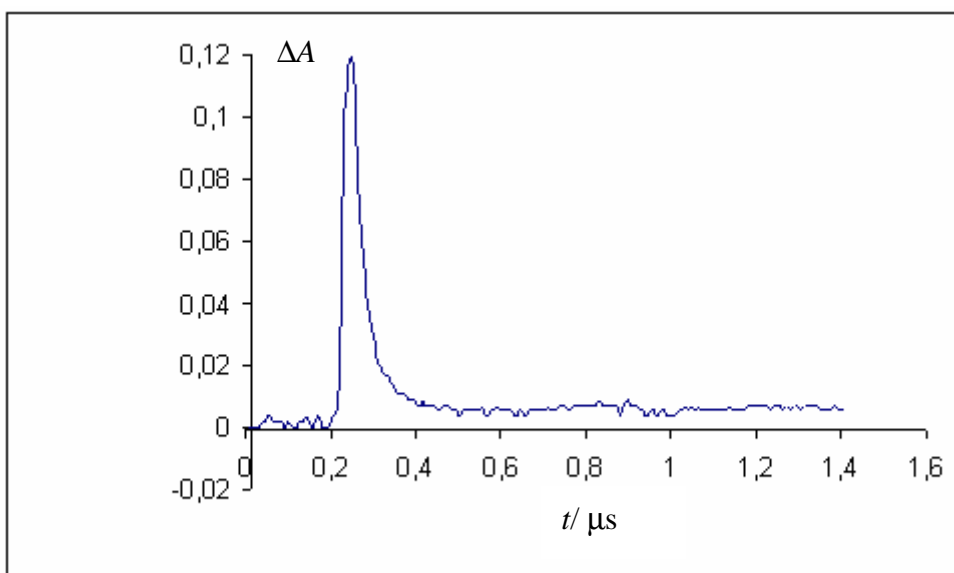


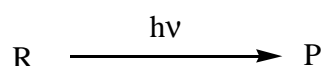
Figure 19: Kinetic trace of **6** in oxygen-saturated acetonitrile observed at 310 nm.

Compounds **1**, **4** and **6** show the same transients, which are attributed to radicals from α -cleavage. This fact is confirmed by chemical analysis of the photolysis products of **1** in hexane, which show a large distribution of products issued from radicals. So the use of a solvent like hexane is not of great help for slowing down the photocyclisation, because in this solvent the photochemistry of **1** is dominated by α -cleavage.

2.5. Quantum yield determination of 2-fluorobenzoin and diethyl phosphate benzoin photolysis in hexane.

Air saturated solutions of **1** and **4** in hexane were irradiated and the ensuing absorption changes were followed. Changes in the UV spectra were slower than in acetonitrile, where **1** was completely converted (99%) within 20 min, compared to 55 min for 10% conversion in hexane. The higher polarity of acetonitrile may favour the release of the leaving group, contrary to hexane which may favour α -cleavage and be a good solvent for back reaction to the starting material. In both solvents we observe the formation of a new band at 300 nm, indicating formation of benzofuran. The reaction quantum yields were measured at 300 nm, where the maximum of the end product should be.

If we consider that the reaction is a simple process:



We can deduce a quantum yield of benzofuran formation using the kinetic equation²⁴:

$$\frac{-dA}{dt} = -\phi_p I F \epsilon_p (A - A_\infty)$$

Where:

ϕ_p is the quantum yield of formation of the end product

ϵ_p is the extinction coefficient of P at 300nm.

I is the intensity of light source

$F = \frac{1-10^{-A}}{A}$ is the photokinetic factor at the wavelength of irradiation, $\lambda_{\text{irr}} = 254 \text{ nm}$

A_∞ is the absorbance at the wavelength of observation when the reaction is complete ($t = \infty$)

Assuming that the photokinetic factor can be considered constant in a short time interval, integration of the kinetic equation gives:

$$\ln\left(\frac{A_1 - A_\infty}{A_2 - A_\infty}\right) = \phi_p I \bar{F} \varepsilon_p (t_2 - t_1)$$

\bar{F} is the average between the photokinetic factors calculated at times t_1 and t_2 . Quantum yields were calculated for several short time intervals, from 30 s to 10 min, and then averaged.

A_∞ was obtained at the end of the photoirradiation reaction, when the value of the absorbance over time became constant. The intensity of the light source was measured using the trans→cis isomerisation of azobenzene as an actinometer, as described in the IUPAC Technical report on chemical actinometry²³ by Gauglitz and Hubig²⁴.

The actinometry was performed, right after the photolysis experiment. It was carried out under conditions of total absorption where the photochemical back reaction (cis→trans isomerisation) can be neglected. Then a linear relationship can be used between absorbance changes and the irradiation time:

$$E_p = \frac{1}{\phi_A \varepsilon_A} \frac{\Delta A_{358 \text{ nm}}}{\Delta t} = \frac{W}{\phi_A \varepsilon_A} \frac{\Delta A_{358 \text{ nm}}}{\Delta t}$$

E_p is the photon flux (Einstein $\text{cm}^{-2} \text{s}^{-1}$)

$$W = \phi_A \times \varepsilon_A$$

$I = 1000 E_p$ is the flux of photon $\text{mol cm}^{-2} \text{s}^{-1}$

ε_A is the extinction coefficient of the actinometer at the excitation wavelength

ϕ_A is the quantum yield of the photoreaction

Using the value of W reported, (IUPAC publication for determination of chemical actinometry^{23, 24}) irradiation at 254 nm and reaction monitoring at 358 nm,

$$W^I = 2.30 \times 10^{-6} \text{ mol cm}^{-2}.$$

The light intensity is calculated by linear regression of $\Delta A_{358 \text{ nm}}$ vs. time (Figure 20)

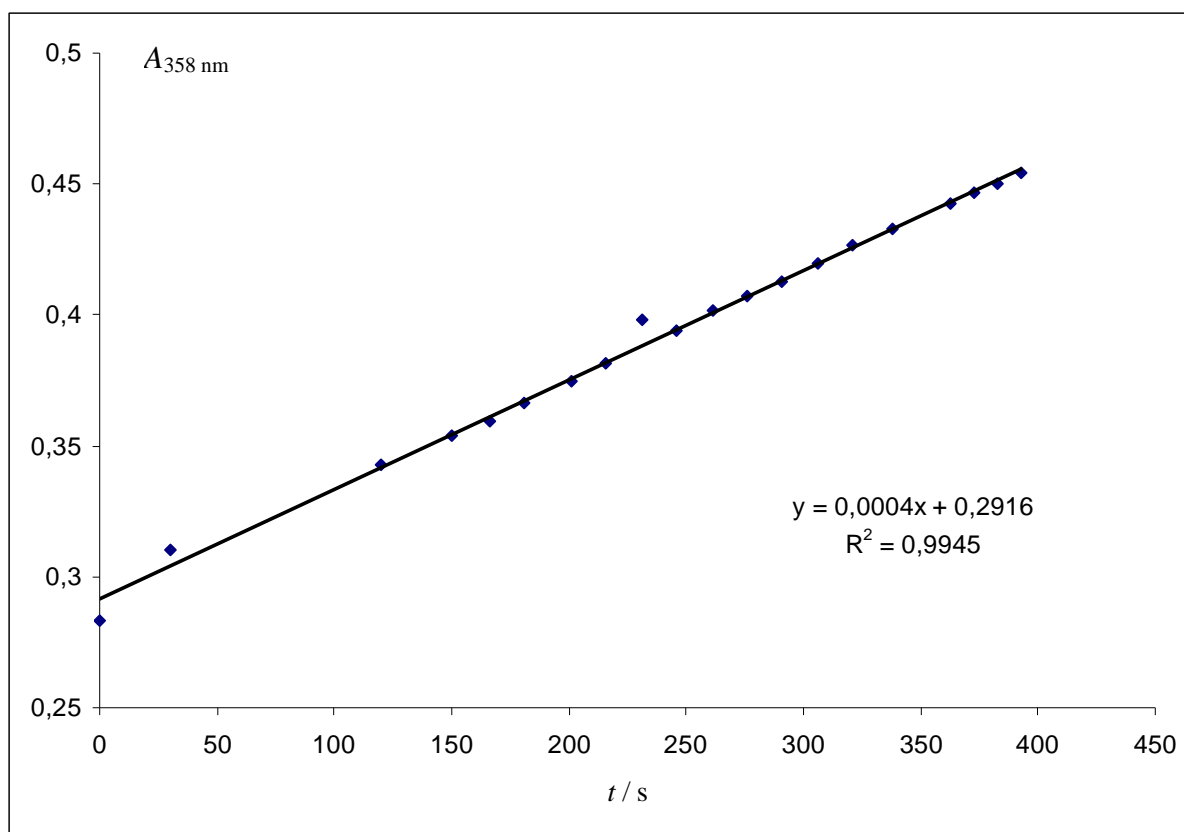


Figure 20: Azobenzene actinometry. Irradiation at 254 nm, observation at 358 nm.

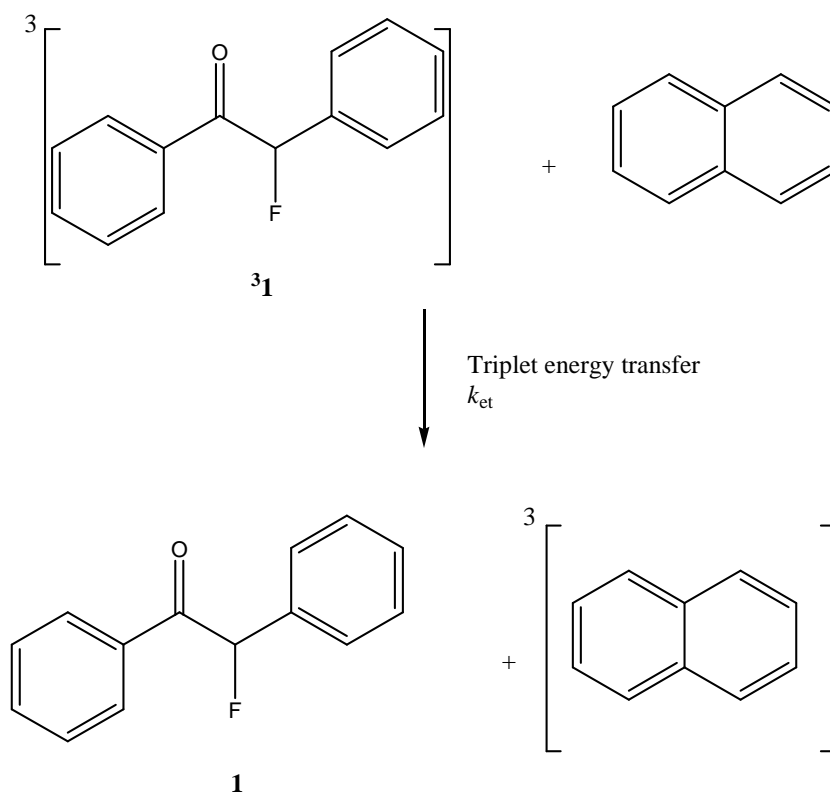
$$\frac{\Delta A_{358 \text{ nm}}}{\Delta t} = 4 \times 10^{-4} \text{ s}^{-1}$$

$$\text{So } I = 9.20 \times 10^{-7} \text{ mol cm L}^{-1} \text{ s}^{-1}$$

The averaged quantum yield in aerated hexane is $(15.5 \pm 1.5) \%$ for **4** and $(2.3 \pm 0.3) \%$ for **1**. The quantum yield of **1** is lower than in acetonitrile (0.64^{22}).

2.6. 2-Fluorobenzoin triplet lifetime determination.

The triplet lifetime of 2-fluorobenzoin was too short to be observed with our nanosecond apparatus. Quenching of the triplet state of **1** by naphthalene was used to determine its lifetime. A solution of **1** in MeCN was excited by 351-nm laser pulses in the presence of naphthalene, and the amount of energy transfer was monitored by the triplet absorbance of naphthalene at 413 nm at the end of the laser pulse (scheme 21).



Scheme 21: Mechanism of photoinduced energy transfer between **1** and naphthalene.

Two different pathways are possible for the decay of $^3\mathbf{1}$:

- Energy transfer to naphthalene
- Decay to the ground state

The lifetime of $^3\mathbf{1}$ can be defined as follows:

$$\tau_{^3\mathbf{1}} = \frac{1}{k_0 + k_{\text{et}} \times c_{\text{N}}}$$

c_{N} is the naphthalene concentration (M)

k_{et} is the energy transfer reaction rate constant ($\text{M}^{-1} \text{s}^{-1}$)

k_0 is the decay rate constant of triplet excited state naphthalene to its ground state (s^{-1})

$$A(^3\text{N}) = \varepsilon_{^3\text{N}} \times l \times c_{^3\text{N}_{t=0}}$$

$$C^3_{N_{t=0}} = C^3_N \frac{k_{et} \times c_N}{k_0 + k_{et} \times c_N}$$

$$\frac{A_{\max}({}^3N)}{A({}^3N)} = \frac{\varepsilon_{3N} \times l \times c_{3N}}{\varepsilon_{3N} \times l \times c_{3N} \frac{k_{et} \times c_N}{k_0 + k_{et} \times c_N}}$$

This expression can be simplified:

$$\frac{A_{\max}({}^3N)}{A({}^3N)} = \frac{k_0 + k_{et} \times c_N}{k_{et} \times c_N} = 1 + \frac{k_0}{k_{et} \times c_N}$$

A linear regression of $\frac{A_{\max}({}^3N)}{A({}^3N)}$ versus $\frac{1}{c_N}$ give a straight line (figure 21).

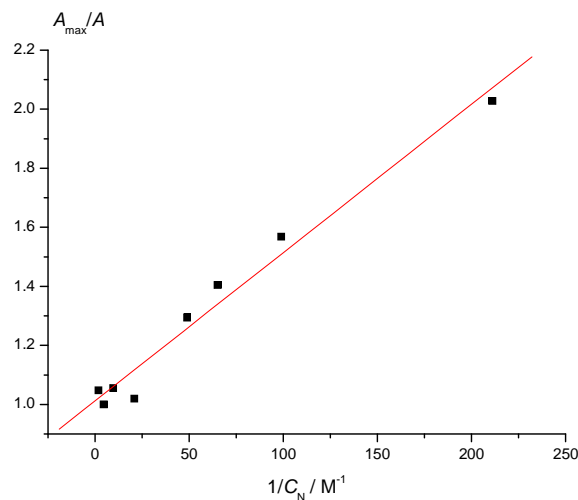


Figure 21: Data treatment of the quenching experiment of ${}^3\mathbf{1}$ by energy transfer reaction with naphthalene.

A_{\max} is the triplet absorbance at high concentration of naphthalene

k_0 is the rate constant for the triplet decay of $\mathbf{1}$ in the absence of naphthalene

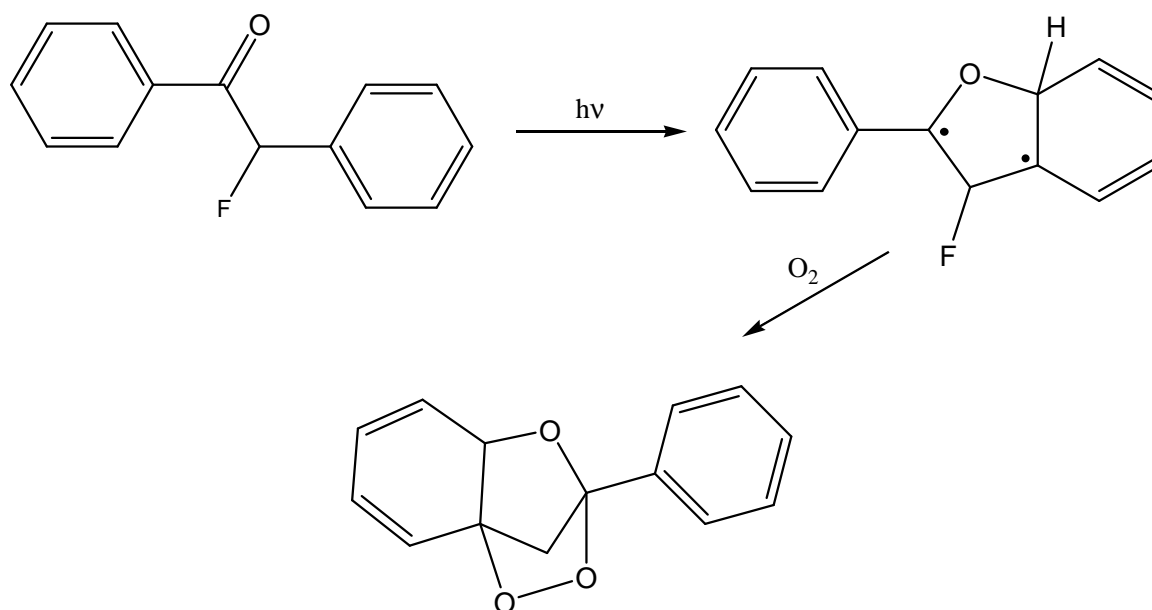
k_{et} is the rate constant for energy transfer (bimolecular).

Linear regression of $\frac{A_{\max}({}^3\text{N})}{A({}^3\text{N})}$ versus $\frac{I}{C_{\text{N}}}$ gave a slope of $\frac{k_0}{k_{\text{et}}} = (5.02 \pm 0.33) \times 10^{-3} \text{ M}$.

A rate constant for triplet-triplet energy transfer between benzophenone or acetophenone (in benzene and isooctane respectively) of $k_{\text{et}} = 1.0 \times 10^{10} \text{ M}^{-1} \text{ s}^{-1}$ has been determined and naphthalene by Porter and Wilkinson²⁵. By assuming this value, the triplet lifetime of **1** is then 20 ns in MeCN. This triplet lifetime is in the same order of magnitude as the one found for diethyl phosphate benzoin by Rajesh¹¹ et al. (24 ± 2 ns in trifluoroethanol).

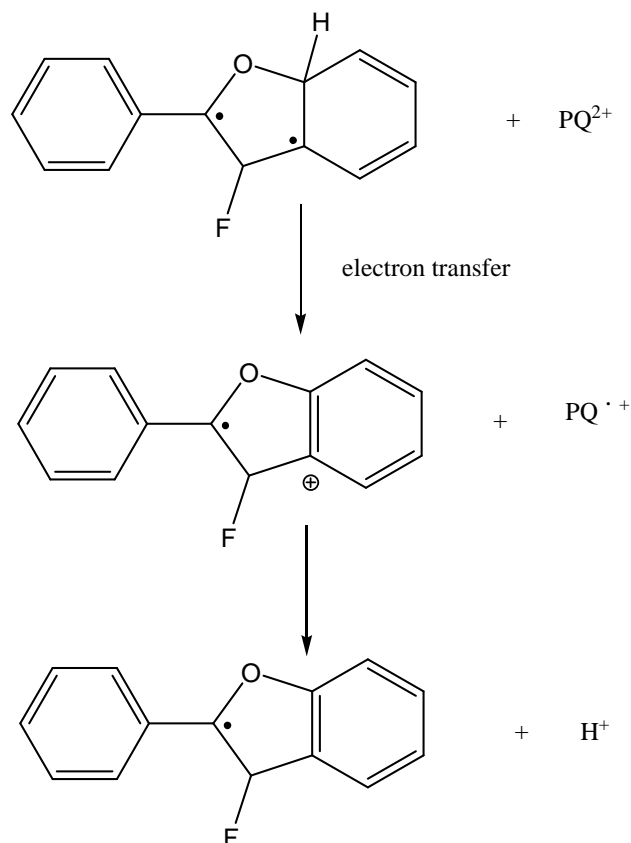
2.7. Diradical trapping experiments.

The main intermediate expected for photolysis of **1** in MeCN is a biradical. I tried, without success, two different techniques to trap it (Scheme 22). The first one is based on the use of oxygen to react with the biradical to form the dioxo adduct. In oxygen saturated CD₃CN at -40°C , **1** was irradiated with an Hg lamp during 30 min. No change was observed in the NMR spectra. A new, oxygen saturated solution at -40°C was flashed 120 times with 248 nm laser (100 mJ) with no success, only formation of benzofuran was observed. The same solution was then irradiated with 1800 flashes at ambient temperature but still only formation of benzofuran was observed.



Scheme 22: Mechanism of diradical (from **1** photolysis) trapping with O₂.

A biradical intermediate can be investigated by laser flash photolysis using the paraquat dication (1,1'-4,4'-bipyridinium, PQ^{2+}) as an electron transfer trapping agent (scheme 23).

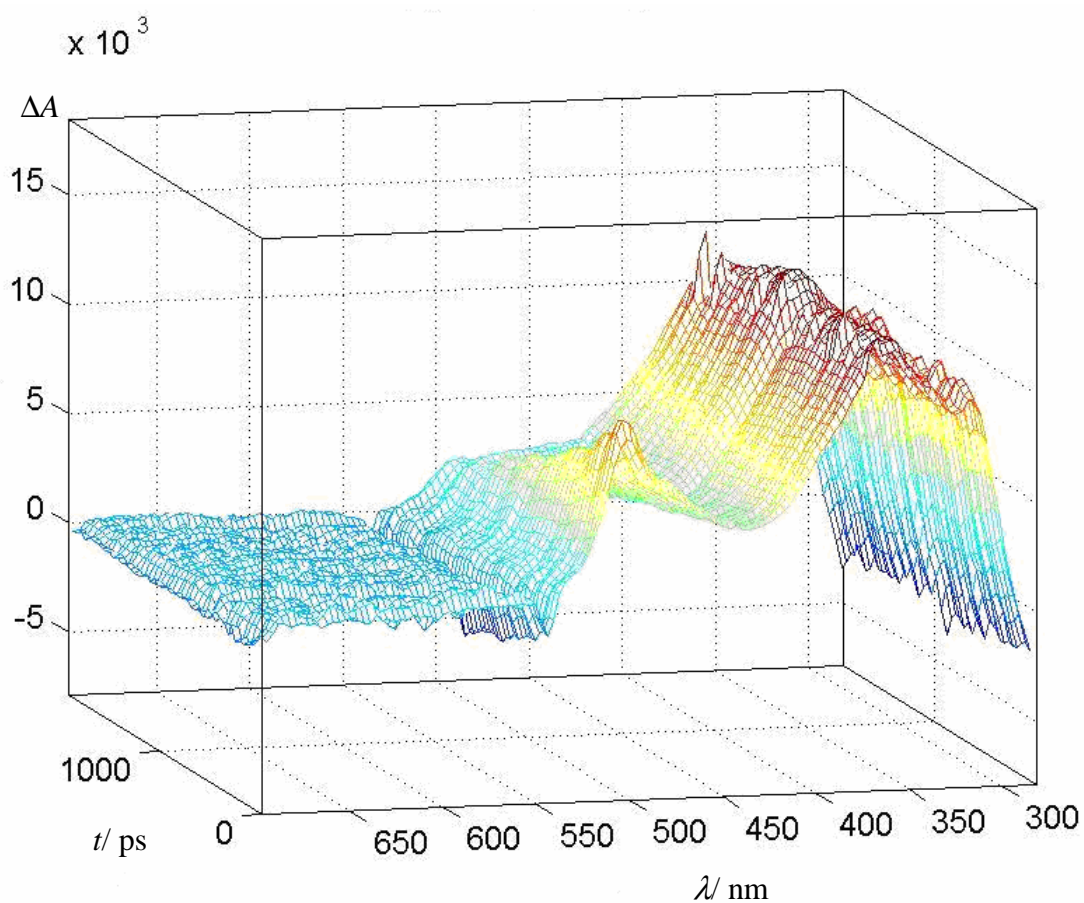


Scheme 23: The electron transfer reaction between intermediate issue of **1** and paraquat dication.

When an electron transfer occurs between PQ^{2+} and the biradical, we should observe a transient at 603 nm, due to $PQ^{\cdot+}$ absorption. Only weak signals have been observed. Two explanations are possible. First the biradical formed may be a poor electron donor. The other explanation could be that the lifetime of the biradical is too short for interception.

2.8. Femtosecond LFP of 2-fluorobenzoin in MeCN and in trifluoroethanol.

Femtosecond experiments were carried out using solutions of **1** in acetonitrile and trifluoroethanol. Pump-probe spectra, covering a time range from 0 to 1.9 ns, and from 0 to 100 ps to resolve the formation of the transients, were done and shown before their factor analysis in the different figures. On excitation by a subpicosecond pulse at 263 nm, all solutions showed a broad transient absorption in the near-UV, $\lambda_{\text{max}} = 310$ nm in MeCN (315 nm in $\text{CF}_3\text{CH}_2\text{OH}$) (Figure 22 and 24).



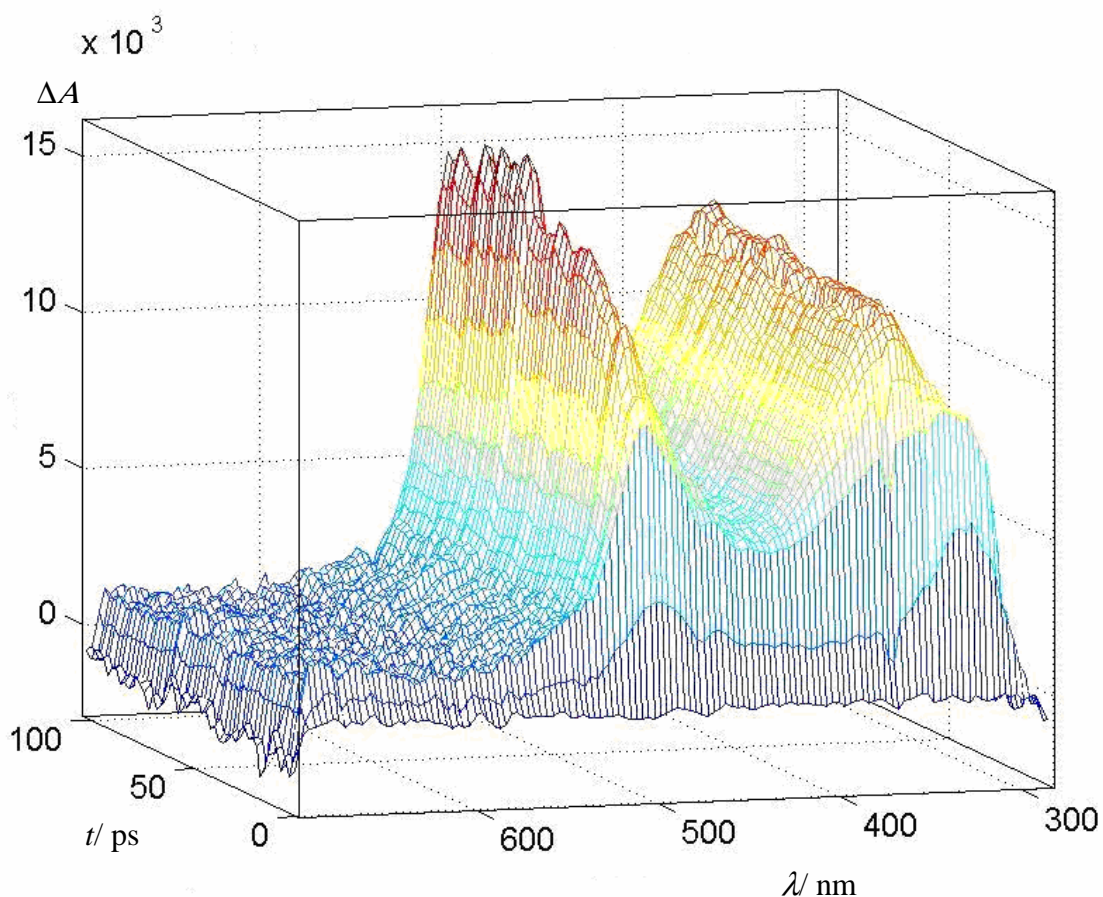


Figure 22: Femtosecond pump-probe spectra of **1** in acetonitrile solution (excitation with a subpicosecond flash at 263 nm) with delays between 0 and 1.9 ns (top), and 0-120 ps (bottom).

This transient (310 nm) is formed within the first measurement step (Figure 23 and 25) and observable up to 1.9 ns, hence its lifetime must be at least 2 ns. The data were accumulated through 500 pulses and the final spectrum is an average of 3 experiments. The transient at 310 nm is attributed to the superposition of the singlet absorbance to the triplet absorbance of **1** (growth of the triplet and decay of the singlet).

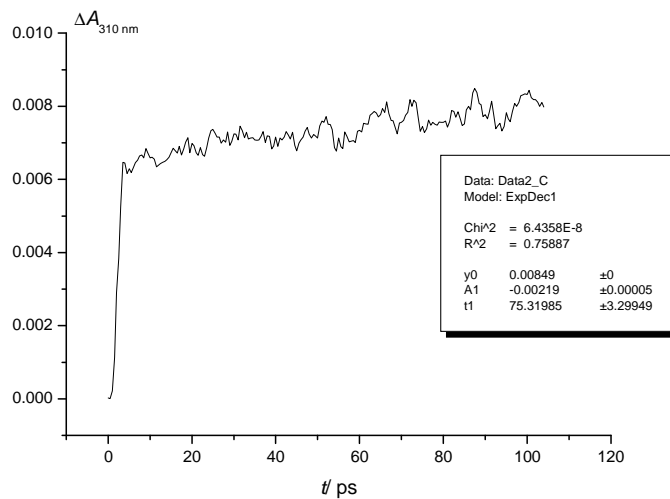
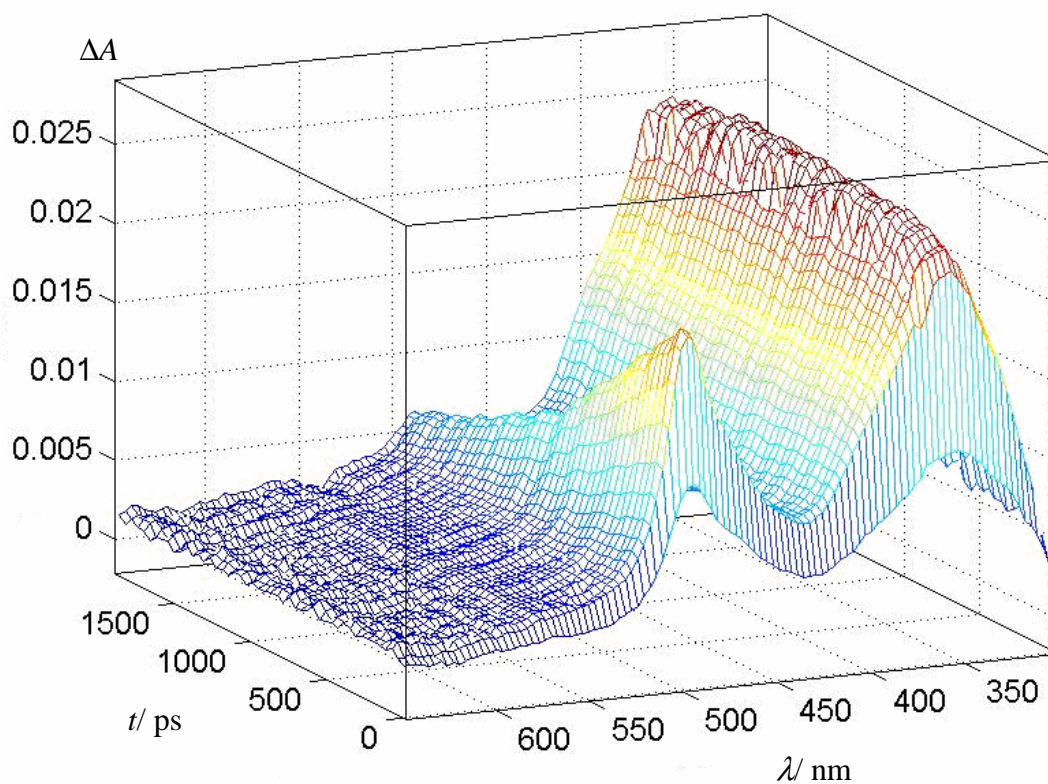


Figure 23: Kinetic trace of the absorbances at 310 nm extracted from femtosecond pump-probe spectra of **1** in acetonitrile solution (excitation with a subpicosecond flash at 263 nm) with delays between 0 and 120 ps.



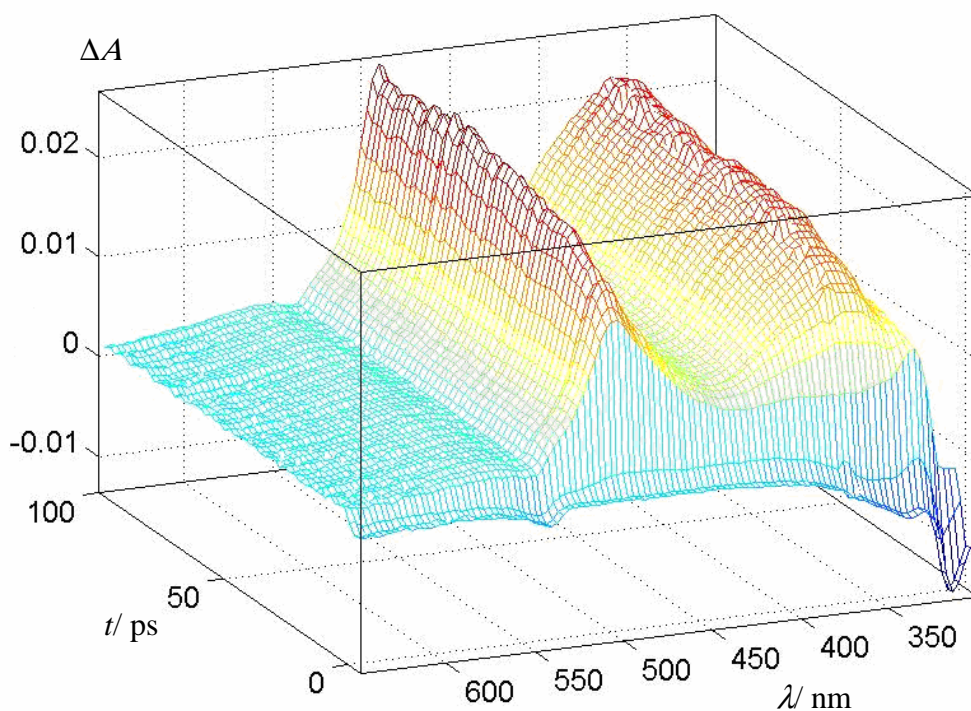
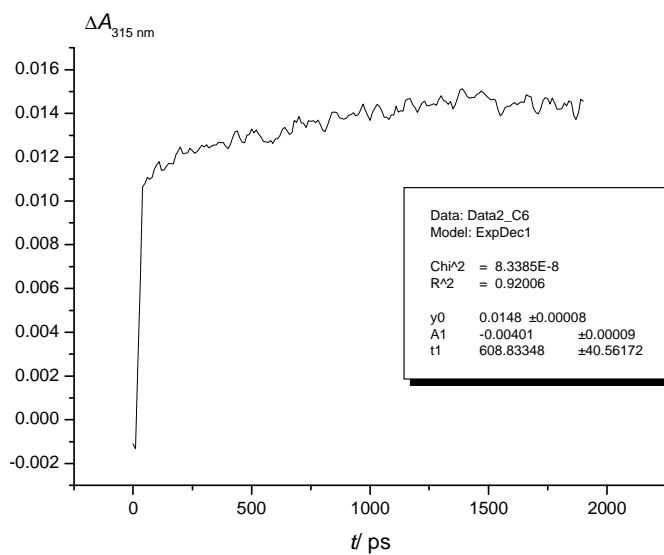


Figure 24: Femtosecond pump-probe spectra of **1** in trifluoroethanol solution (excitation with a subpicosecond flash at 263 nm) with delays between 0 and 1.9 ns (top), and 0-120 ps (bottom).



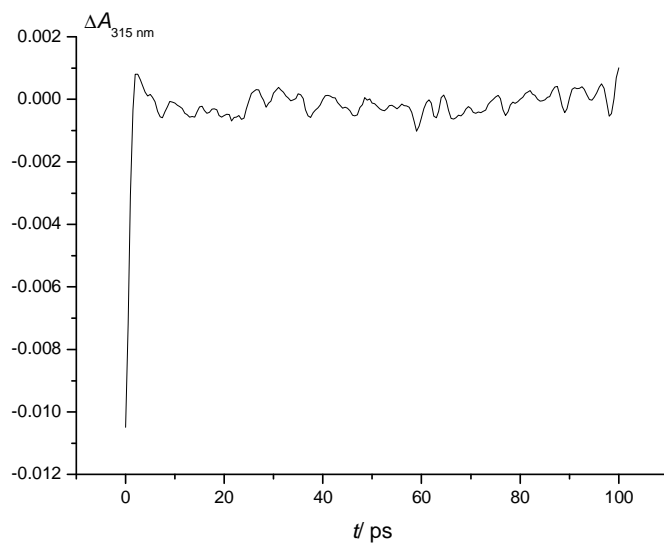


Figure 25: Kinetic traces of the absorbance at 310 nm extracted from the femtosecond pump-probe spectra of **1** in trifluoroethanol solution (excitation with a subpicosecond flash at 263 nm) with delays between 0 and 1.9 ns (top) and 0-120 ps (bottom).

The pump-probe spectra of **1** in acetonitrile and trifluoroethanol showed a second absorbance band around 355 nm (Figure 24). This band is attributed to the triplet of **1**, because it was still observable after 1.9 ns and corresponds to the signal around 360 nm observed in nanosecond laser flash photolysis at low temperature. Another argument for the triplet assignment is the similarity of the chromophore of **1** with acetophenone. Triplet acetophenone is known to absorb around 330 nm²⁶, which is relatively close to the triplet band observed for **1**. This transient is formed in 4.5 ps in acetonitrile, and 22 ps in trifluoroethanol (Figure 26 and 27).

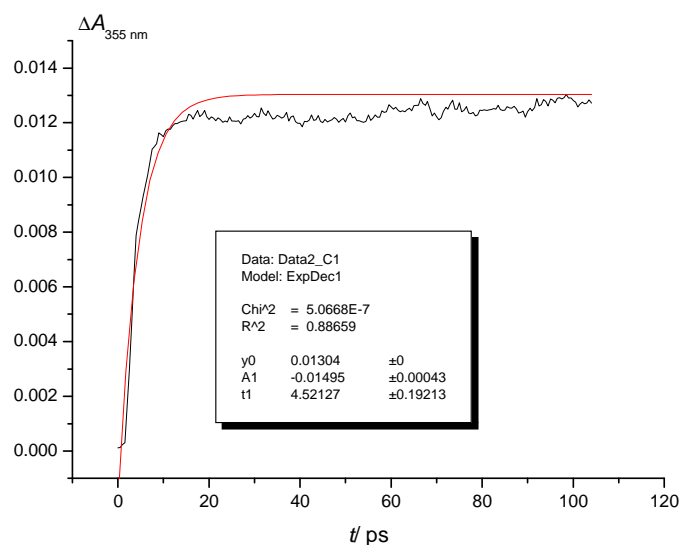


Figure 26: Kinetic traces of the absorbance at 355 nm extracted from the femtosecond pump-probe spectra of **1** in acetonitrile solution (excitation with a subpicosecond flash at 263 nm) with delays between 0 and 120 ps (bottom).

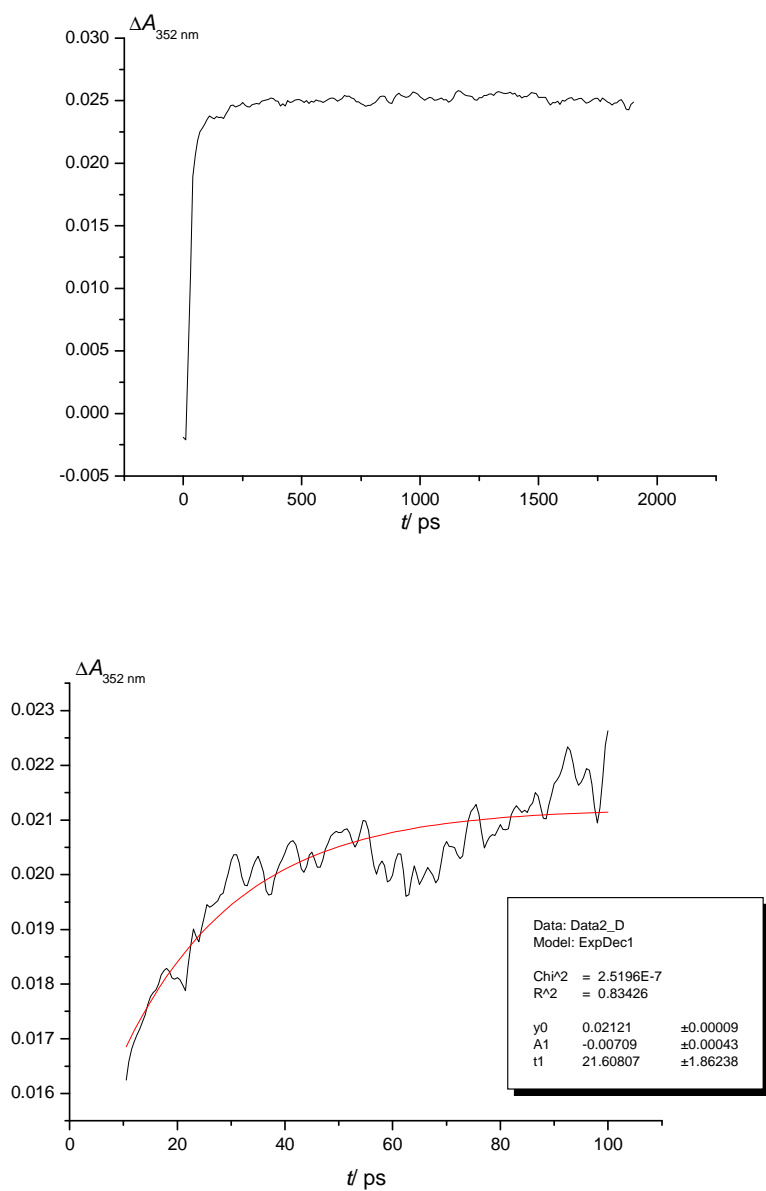


Figure 27: Kinetic traces of the absorbance at 352 nm extracted from the femtosecond pump-probe spectra of **1** in trifluoroethanol solution (excitation with a subpicosecond flash at 263 nm) with delays between 0 and 1.9 ns (top) and 0-120 ps (bottom).

In addition, a short-lived transient absorbing around 497 nm in acetonitrile (490 nm in trifluoroethanol) was observed (lifetime: 2.3 and 1.2 ns in acetonitrile and trifluoroethanol respectively, and formation in 21 and 18 ps in acetonitrile and trifluoroethanol respectively) (Figure 28 and 29)). This transient may be due to the presence of another intermediate formed from the singlet in competition with the triplet, or it could be due to accumulation and reexcitation of the photoproduct (2-phenylbenzofuran) in the recycled solution of the flow cell.

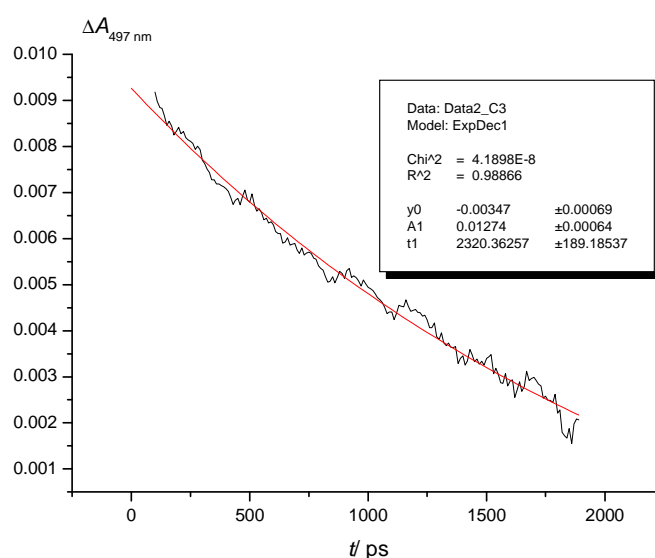
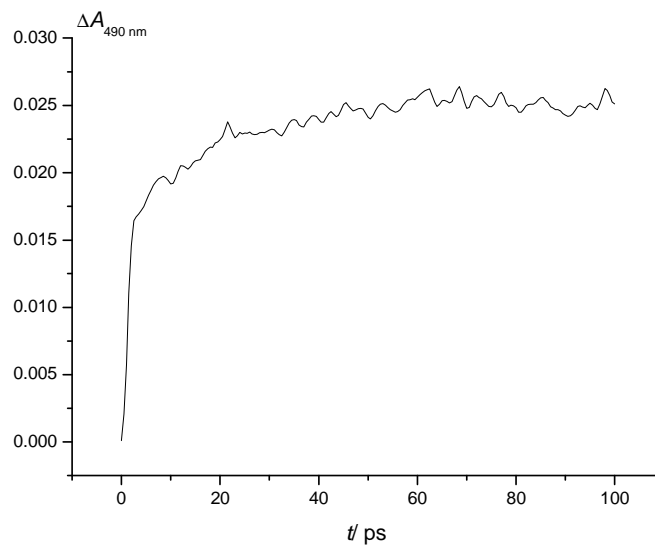
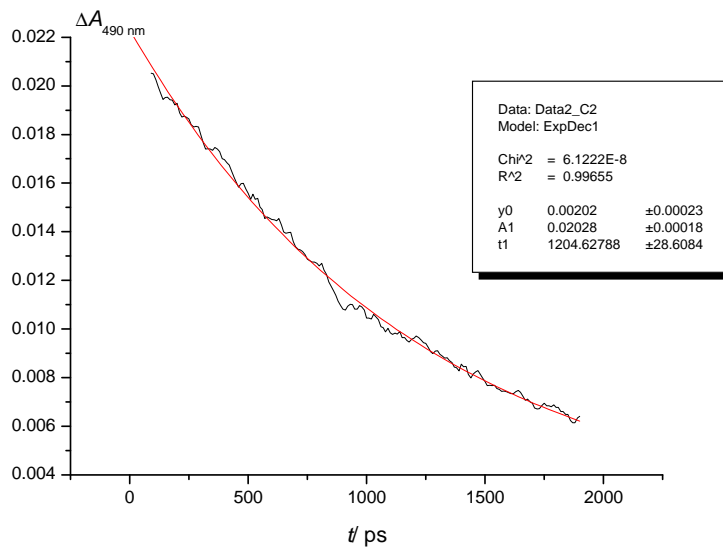


Figure 28: Kinetic traces of the absorbance at 497 nm extracted from the femtosecond pump-probe spectra of **1** in acetonitrile solution (excitation with a subpicosecond flash at 263 nm) with delays between 0 and 1.9 ns (top) and 0-120 ps (bottom).



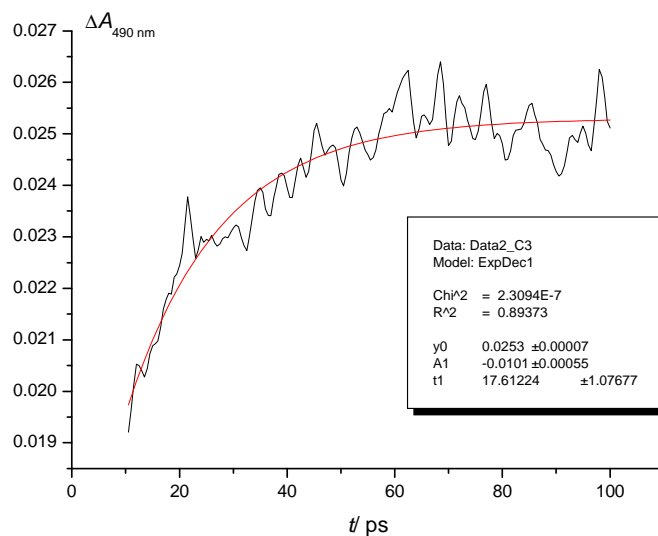
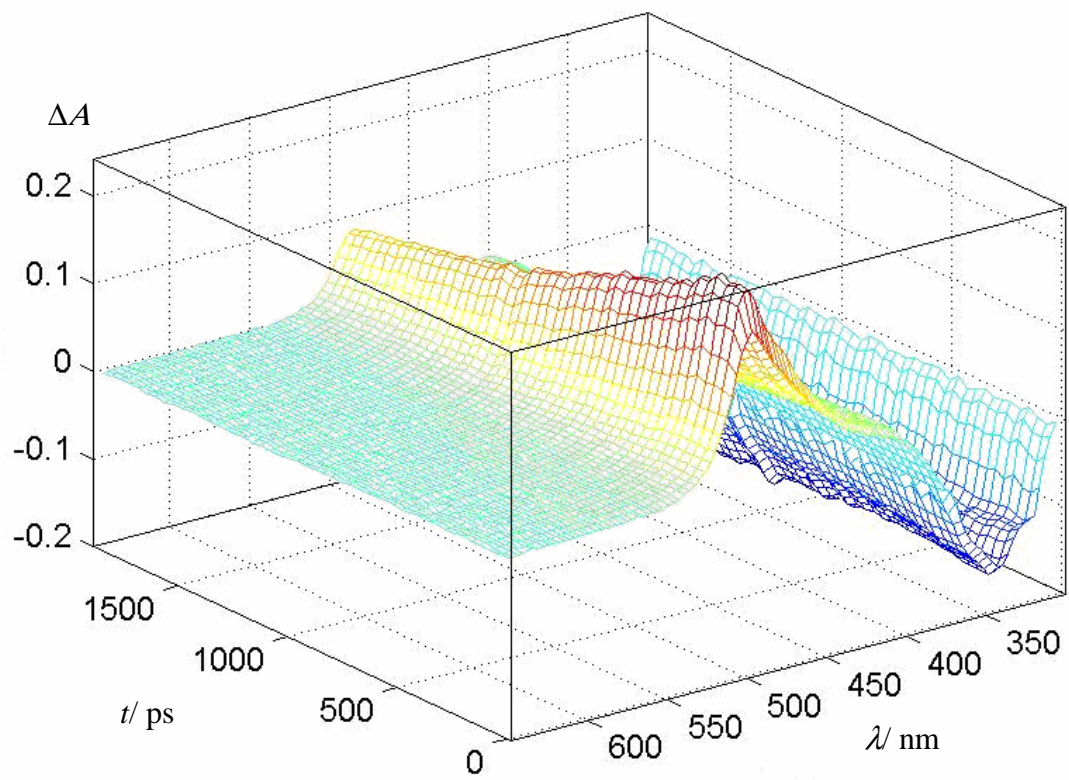


Figure 29: Kinetic traces of the absorbance at 490 nm extracted from the femtosecond pump-probe spectra of **1** in trifluoroethanol solution (excitation with a subpicosecond flash at 263 nm) with delays between 0-1.9 ns (top) and 0-120 ps (bottom).

To check if the transient observed at 490 nm is due to reexcitation of 2-phenylbenzofuran, we did femtosecond LFP of 2-phenylbenzofuran in $\text{CF}_3\text{CH}_2\text{OH}$. We can see a transient at 490 nm (lifetime of 1.6 ns in trifluoroethanol, rise time of 10 ps), due to the singlet excited state of 2-phenylbenzofuran (Figure 30 and 31). The shape of the band and kinetics are similar to the one observed for **1** in the same solvent. A higher intensity maximum has been observed when the spectra have been recorded from 1.9 ns to 0 ns delay, compare to the spectra recorded from 0 to 1.9 ns delay. This means that photoproduct accumulates (due to prolonged exposure) during the measurements and the signal observed at 490 nm is due to its reexcitation.



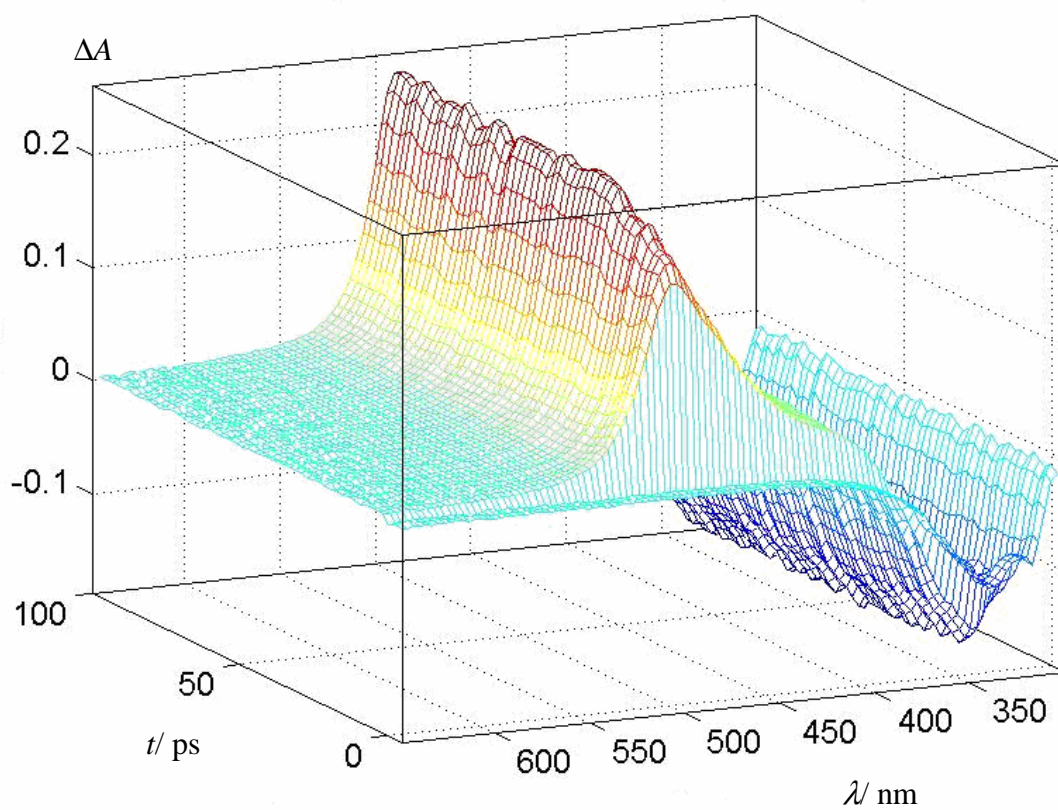
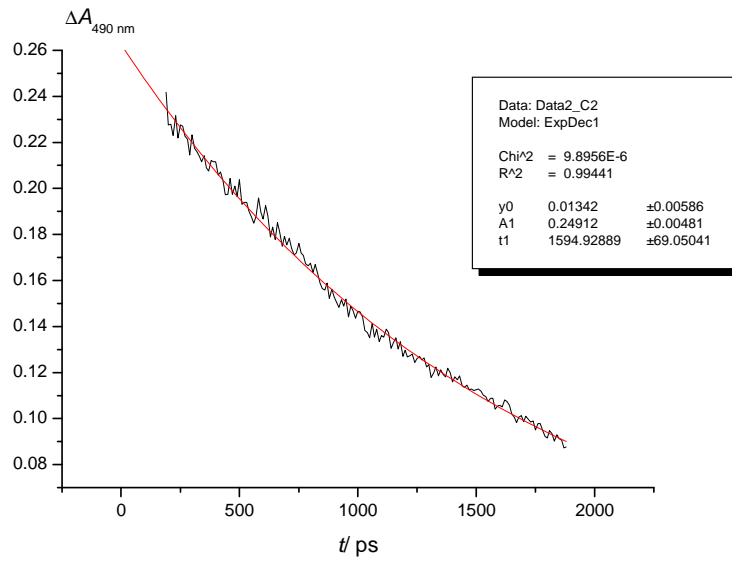
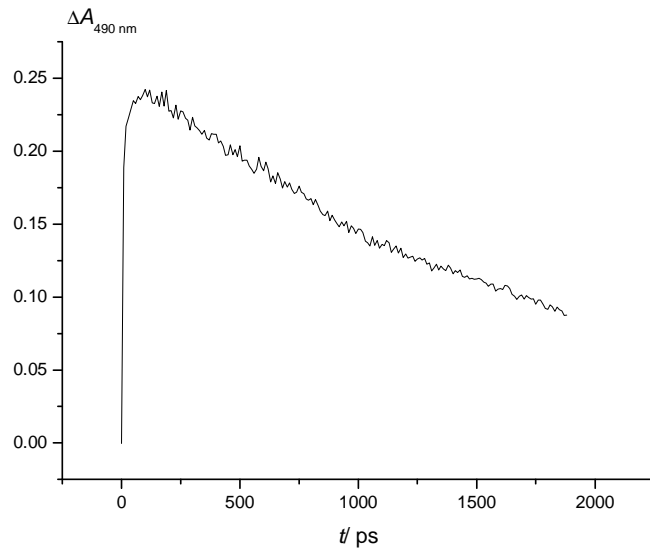


Figure 30: Femtosecond pump-probe spectra of 2-phenylbenzofuan in trifluoroethanol solution (excitation with a subpicosecond flash at 263 nm) with delays between 0 and 1.9 ns (top), and 0-100 ps (bottom).



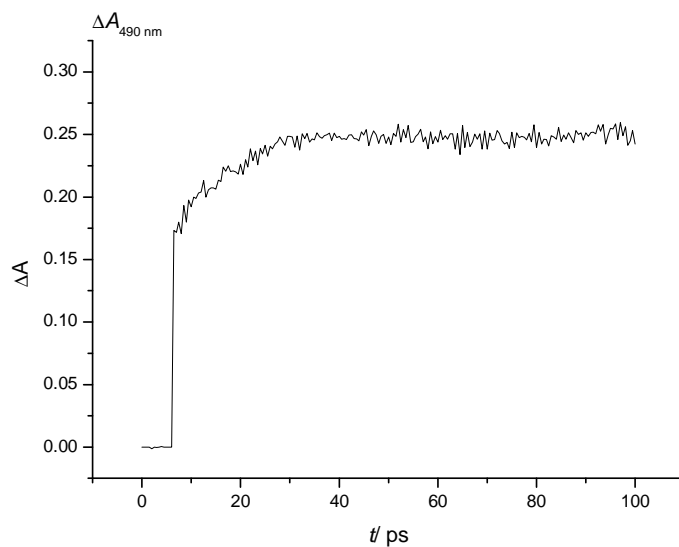
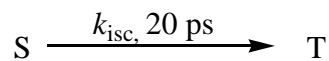


Figure 31: Kinetic traces of the absorbance at 490 nm extracted from the femtosecond pump-probe spectra of 2-phenylbenzofuan in trifluoroethanol solution (excitation with a subpicosecond flash at 263 nm) with delays between 0 and 1.9 ns (top) and 0-120 ps (bottom).

Global Analysis of the three dimensional absorption spectra for the two different solvents, using factor analysis, indicated two main factors. A model including two coloured species was then applied to do the global kinetic fits (scheme 24).



in MeCN or $\text{CF}_3\text{CH}_2\text{OH}$

Scheme 24: Proposed scheme for global kinetic fits of the femtosecond pump-probe spectra of **1** in MeCN and in $\text{CF}_3\text{CH}_2\text{OH}$.

Following this model, the software is able to fit the different parts of the three dimensional curves and give an accurate rate constant of ¹**1** decay.

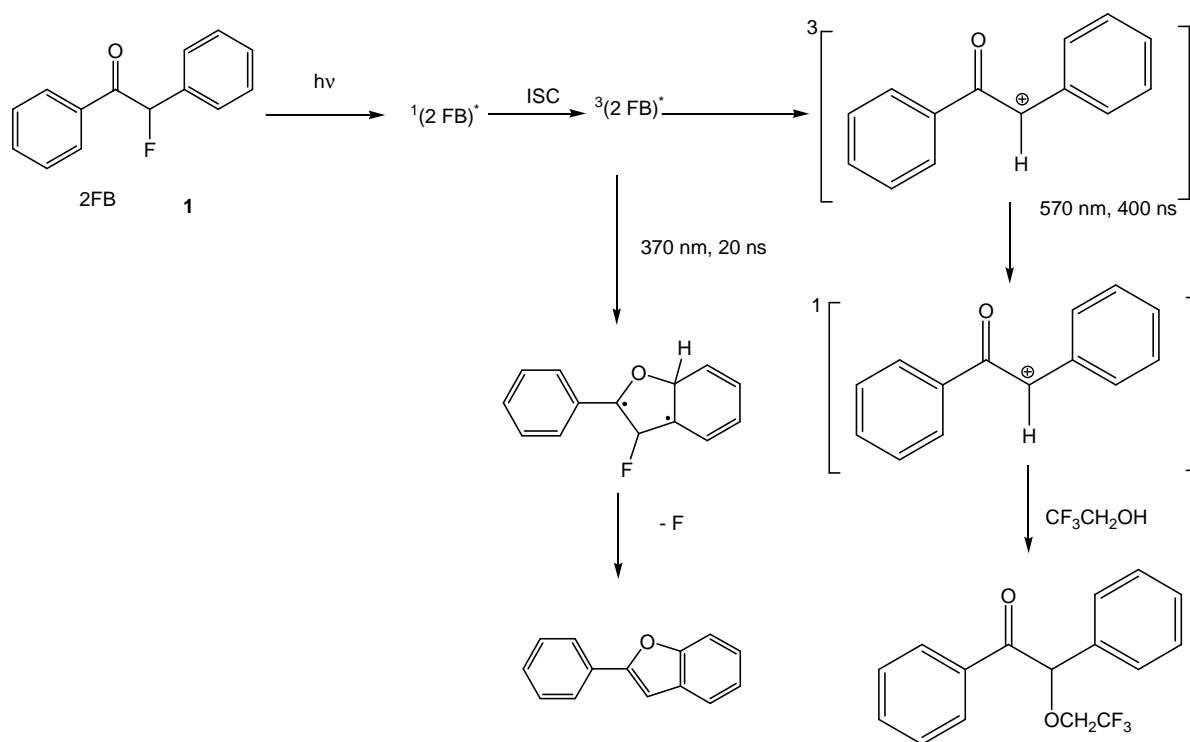
	MeCN	CF ₃ CH ₂ OH
$k_{\text{decay}}/ \text{s}^{-1}$	$(3.45 \pm 0.15) \times 10^{11}$	$(7.68 \pm 0.30) \times 10^{11}$

The 485-650 nm range was not analysed in detail with the software, because it contains the signal of the transient due to the reexcitation of the final product and not the intermediates involved in the mechanism.

2.9. Discussion.

The observations with **1** (2-fluorobenzoin) are quite similar as those reported¹¹ for **4** (benzoin diethyl phosphate). We observed the triplet of **1** at 370 nm with a lifetime of 550 ns at -110 °C in EtOH and the formation of the 2-phenylbenzofuran at 310 nm. Observation of the assumed biradical intermediate was not possible, in spite of a lot of effort. A triplet α -ketocation was observed at 570 nm with a lifetime of 400 ns by LFP of **1** in water (4% MeCN). Product analysis indicates that 2-phenylbenzofuran is mainly formed in MeCN, and that solvent addition on α -ketocation occurs in trifluoroethanol. We propose the mechanism shown in scheme 25. The triplet state of **1** observed in nanosecond experiment at low temperature has been confirmed in femtosecond experiments. The triplet is formed quite fast at 370 nm (rise time: 4.5 ps in acetonitrile, and 22 ps in trifluoroethanol) and is stable up to 1.9 ns (a lifetime of 20 ns has been determined by quenching experiments with naphthalene). This study has shown that replacement of diethyl phosphate by F leaving group doesn't affect the mechanism of photocyclization and doesn't slow the reaction, compare to diethylphosphate benzoin¹¹ (**4**). The acidity constants of F (pK_a (HF) = 3.17) has also a pK_a value rather close to diethylphosphate (pK_a (diethylphosphate) = 1.39) to consider that nucleofugacity will have a substantial effect on the transient kinetics.

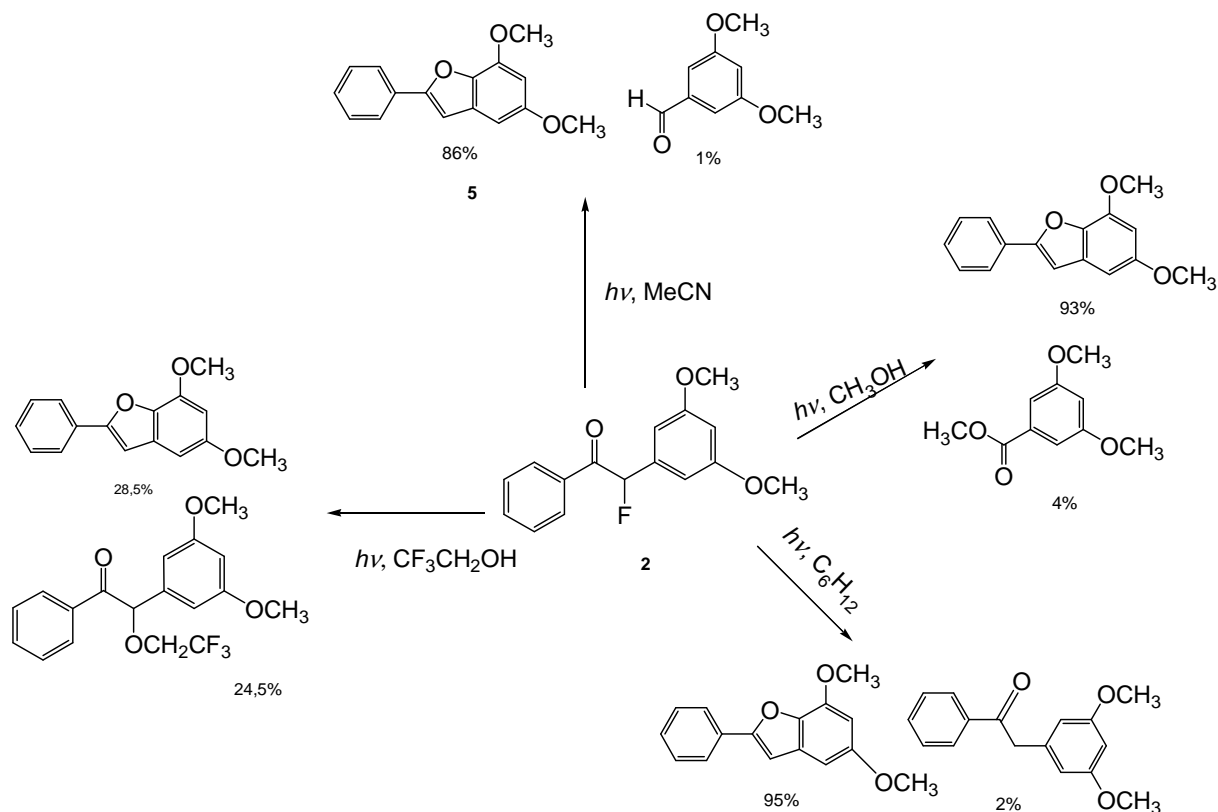
Proposed mechanism:



Scheme 25: Proposed mechanism for LFP of **1**.

3. Investigations on the mechanism of 2-fluoro-3',5'-dimethoxybenzoin (2).

3.1. Preparative photolysis²².



Scheme 26: Products from preparative photolysis of **2**.

The starting material **2** (0.01 M) was photolysed at 350 nm during 2 hours and the product distribution was determined by GC/MS. Products were identified by comparison with retention time of standards (scheme 26). Photolysis of **2** produces mainly dimethoxy-2-phenylbenzofuran (**5**) in CH₃CN, in methanol and in hexane. In MeOH some traces of solvent adduct to the α -cleavage product have been detected. Indeed, photolysis of **2** forms two main products: dimethoxybenzofuran and the α -solvent adduct. From this experiment, two main reaction pathways can be put forth to describe the photolysis of **2**: nucleophilic attack of the solvent at the leaving group position, and cyclization.

Quantum yields have been determined for **2** in MeCN. The number of photons was measured by ferrioxalate actinometry (0.01 M, at 25°C, $\lambda_{\text{irradiation}} = 350 \text{ nm}$, $I_{\text{lamp}} = 1.65 \times 10^{16} \text{ quanta (mL s)}^{-1}$). The solution was irradiated for 5, 10, 14, 20 min. The conversion was determined by GC (naphthalene was used as an internal standard). The quantum yield of disappearance was found to be 0.74. Quenching experiments have been also done: photocyclisation of **2** proceeds from the singlet state, because conversion of **2** remained the same with or without naphthalene in solution.

3.2. Nanosecond LFP of 2-fluoro-3',5'-dimethoxybenzoin in MeCN and in water.

UV spectra of a solution of **2** in MeCN ($A_{248} = 0.34$) taken before and after a single flash show that the photochemical reaction is very efficient: a massive band appears at 320 nm. Transient spectroscopy of **2** in degassed MeCN shows two bands with maxima ca. 470 and 320 nm (Figure 32). One microsecond after the laser, we can still see the same band at 320 nm and a shifted band at 430 nm (Figure 32) (instead of 470 nm, 20 ns after the pulse). In air saturated solution, we observed bands at 320 and 485 nm (470 nm in degassed solution), just after the excitation, and only one band at 320 nm 1 μs after the laser pulse (Figure 33).

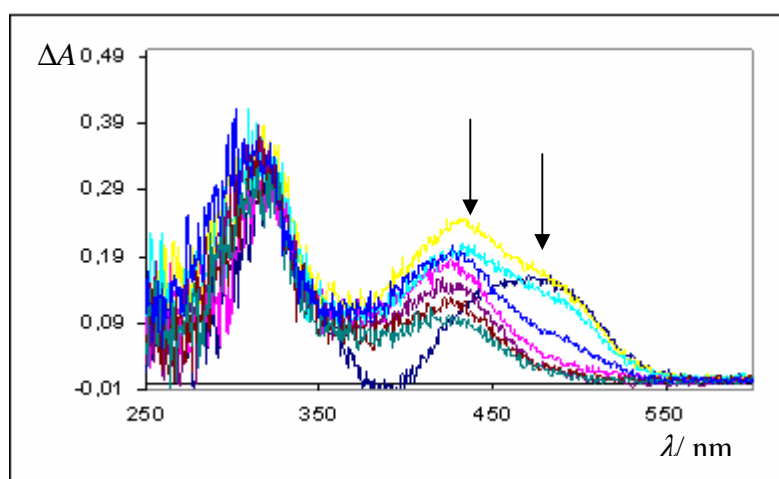


Figure 32: UV spectra of the transients, after the laser excitation of **2** in degassed MeCN (20 ns (deep blue, max ca. 470 nm), 60 ns (yellow), 100 ns (cyan), 500 ns (blue), 1 μs (pink), 2 μs (violet), 5 μs (brown), 16 μs (green-blue)).

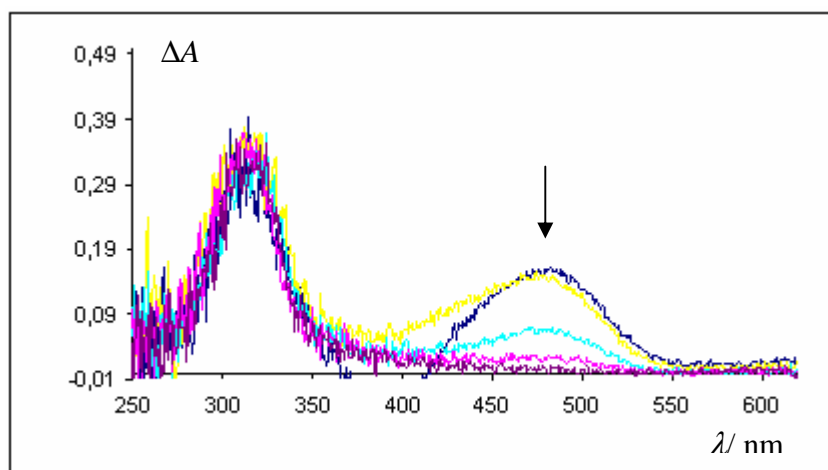


Figure 33: UV spectra of the transients, after the laser excitation of **2** in air saturated MeCN (5 ns (blue), 100 ns (yellow), 500 ns (cyan), 1 μ s (pink), 2 μ s (violet)).

Absorbance growth is observed at 305 nm in degassed MeCN, $k_1 = (3.21 \pm 0.09) \times 10^6 \text{ s}^{-1}$, which could represent the formation of the final furan product **5**. In an air-saturated solution of **2** ($A_{248} = 0.33$), the observed rate constant is $(4.27 \pm 0.13) \times 10^6 \text{ s}^{-1}$ at 305 nm (figure 34 (A)). The decay of the transient at 485 nm is monoexponential: $k = (2.34 \pm 0.07) \times 10^6 \text{ s}^{-1}$ in air saturated solution (Figure 34 (B)) ($k = (2.29 \pm 0.01) \times 10^6 \text{ s}^{-1}$ in degassed solution). The growth rate constant at 305 nm and the decay rate constant at 485 nm are relatively close, to argue that the transient at 485 nm (cation **3**) is the precursor of the final product observed at 305 nm (final product).

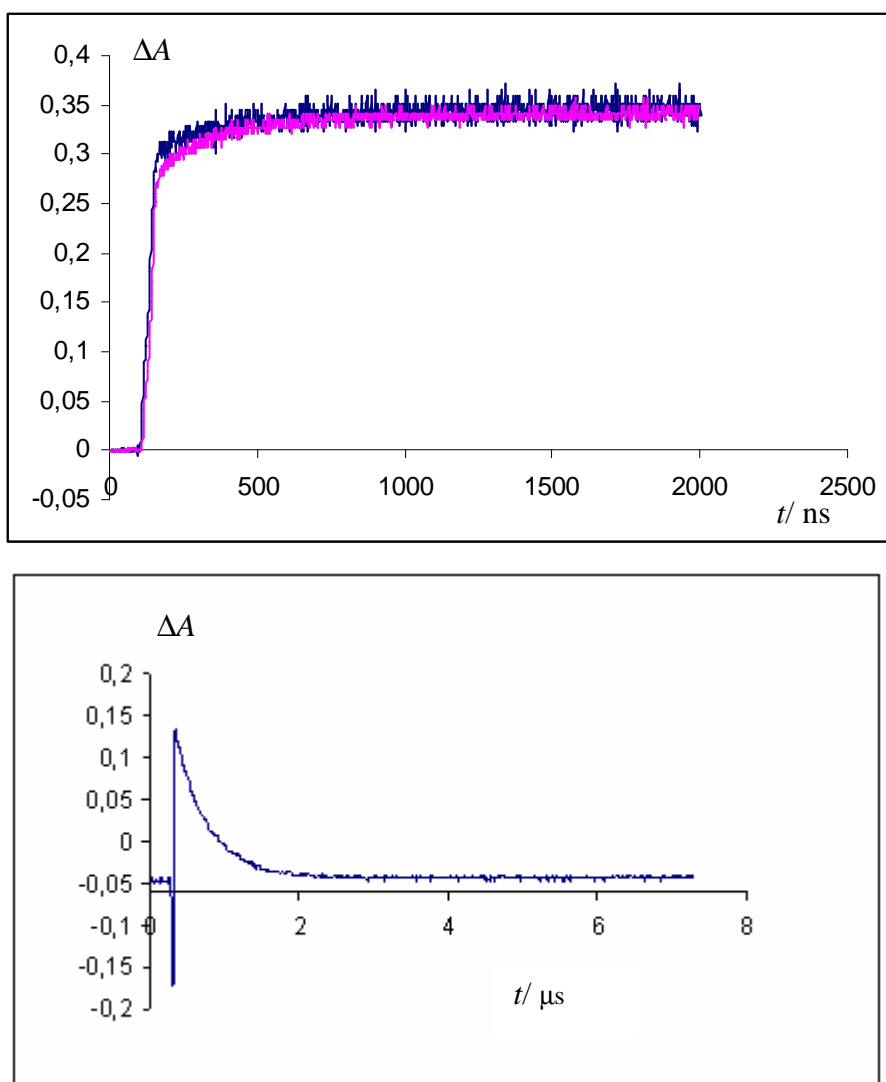


Figure 34: Kinetic traces of **2** photolysis observed at 305 nm (A), in degassed (blue) and air saturated (pink) MeCN, at 485 nm (B), in air saturated MeCN.

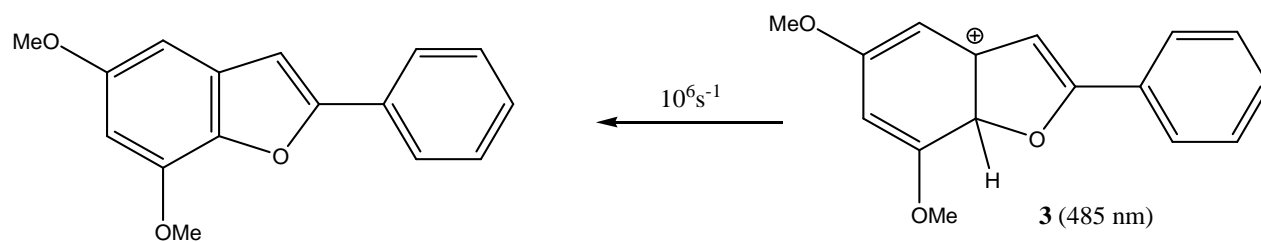
The kinetics of the band observed at 430 nm was probed (Figure 35). A fast growth (less than 60 ns), followed by a slower decay ($k_1 = (1.50 \pm 0.02) \times 10^6 \text{ s}^{-1}$, in degassed solution) is detected (in air saturated solution, $k_1 = (6.40 \pm 0.20) \times 10^6 \text{ s}^{-1}$, $k_2 = (1.00 \pm 0.01) \times 10^6 \text{ s}^{-1}$). Introduction of air did not affect the 485 nm signal. Shi et al.²⁰ have assigned a band at 420 nm (in air saturated MeCN) to the triplet state of the 3',5'-dimethoxybenzoin ester.

Addition of small amounts of water increases the decay rate of the 485 nm signal.

water concentration		decay rate constant, k / s^{-1}
$c / \mu\text{M}$	% (vol)	
0	0	$(4.60 \pm 0.02) \times 10^6$
0.133	0.0002	$(4.78 \pm 0.01) \times 10^6$
0.266	0.0005	$(4.63 \pm 0.02) \times 10^6$
0.665	0.0012	$(4.79 \pm 0.01) \times 10^6$
1.330	0.0025	$(5.43 \pm 0.02) \times 10^6$
2.660	0.0050	$(5.95 \pm 0.02) \times 10^6$
6.650	0.0125	$(7.85 \pm 0.03) \times 10^6$
9.980	0.0190	$(9.98 \pm 0.05) \times 10^6$

Linear regression of the decay rate constant, k , versus water concentration, C , gave a slope of $= (5.27 \pm 0.15) \times 10^6 \text{ M}^{-1} \cdot \text{s}^{-1}$

Shi observed an increase of the decay rate constant at 485 nm, after addition of water till 5%, the decay was then too fast for observation²⁰. In our case we observe an increase of the rate till 10 μM water (4% volume). The acceleration of the decay indicates that water molecules trap the dimethoxycyclohexadienyl cation (**7**) (formed in the sub nanosecond time scale).



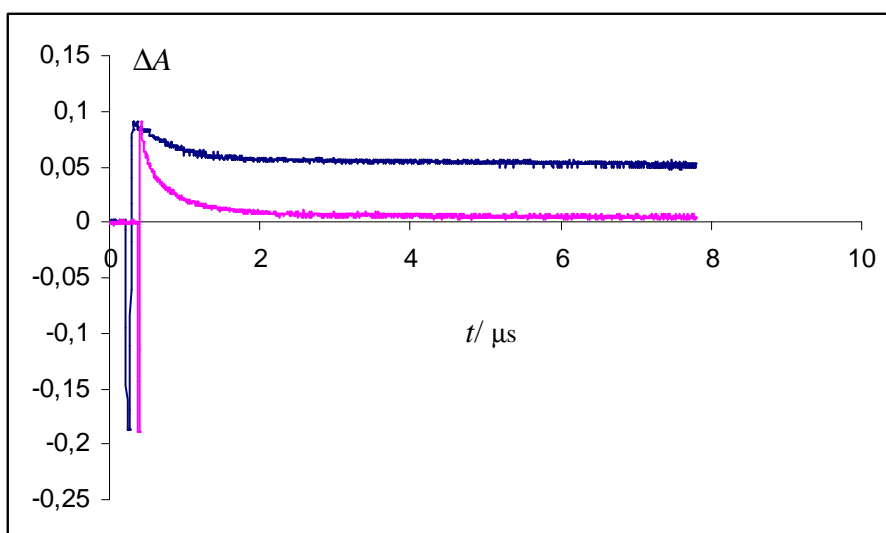


Figure 35: Kinetic traces after excitation of **2** in air saturated (pink) and degassed (blue) MeCN observed at 430 nm.

An aqueous solution of **2** was also studied by LFP ($A_{248} = 0.18$, 5 % MeCN as a cosolvent) (248 nm, 110 mJ/pulse). UV spectra, in degassed and air saturated water solution, 20 ns, 1 μ s and 2 μ s after the laser excitation, show only a weak band around 300 nm in degassed solution 2 μ s after the flash. After several flashes, the band intensity at 300 nm increases, assigned to formation of **5** (spectra were taken with the same reference: the starting material spectrum before photolysis).

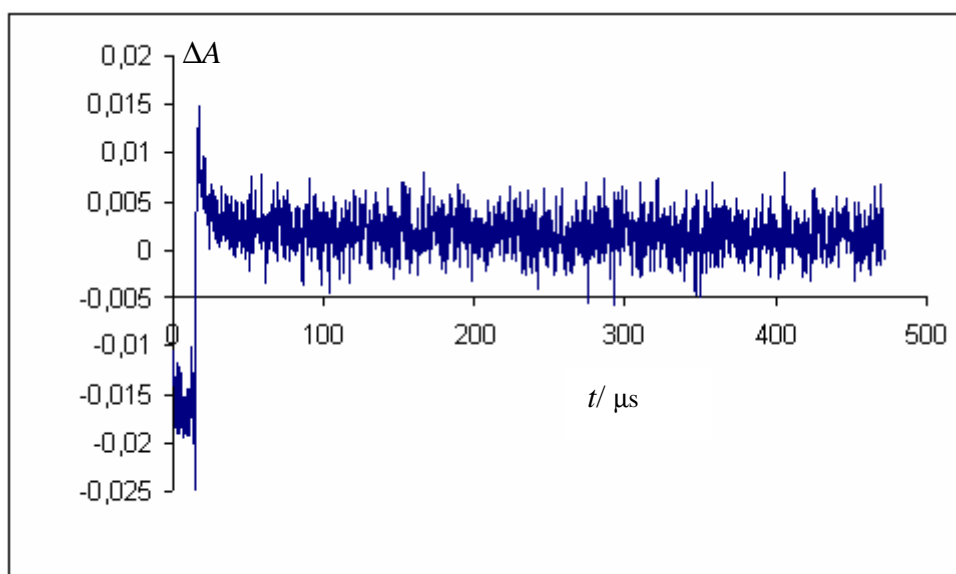


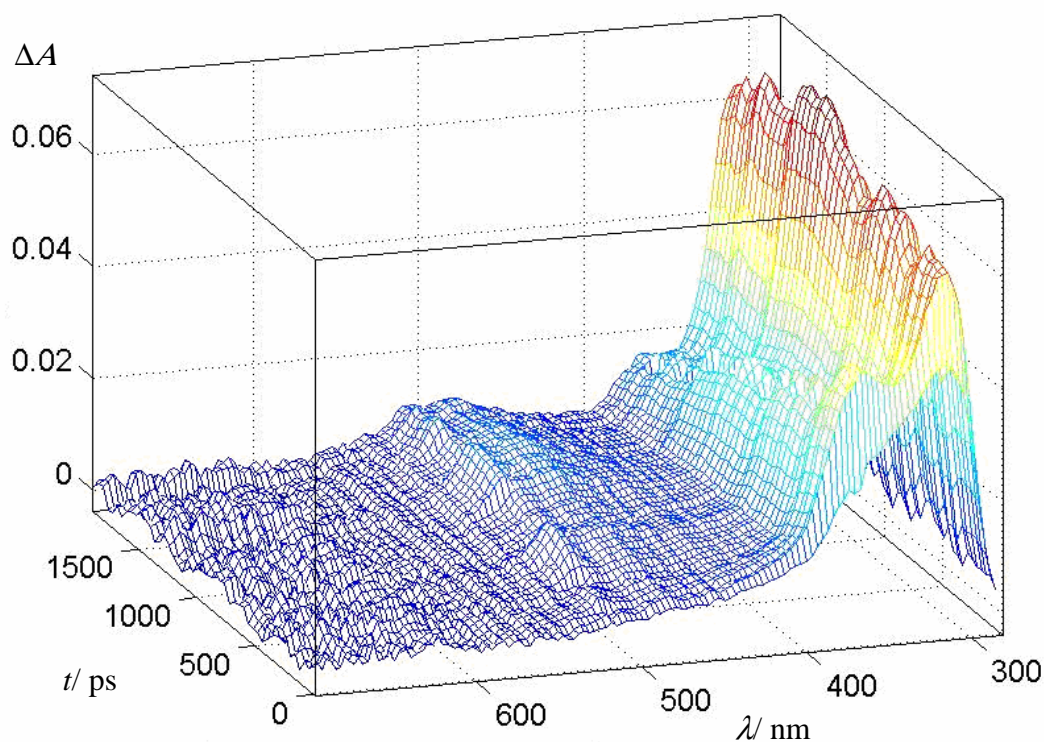
Figure 36: Kinetic traces of **2** photolysis in degassed H₂O observed at 310 nm.

Even if no substantial transient in air saturated water was observed in the different time resolved UV spectra, kinetic traces were recorded at several wavelengths in order to look for weak signals. In air saturated solution a weak transient was detected at 310 nm. The species is formed within the laser flash and decays slowly ($k_1 = (5.25 \pm 0.22) \times 10^5 \text{ s}^{-1}$) (Figure 36). No significant signal has been detected at 430, 470, 485 and 650 nm. In degassed solution ($k_1 = (1.29 \pm 0.34) \times 10^5 \text{ s}^{-1}$), the decay at 310 nm is slower than the one observed in aerated solution. This transient is probably due to the reexcitation of the final product formed after photolysis of **2**: the dimethoxy-2-phenylbenzofuran (**5**), within the duration of flash.

3.3. Femtosecond LFP of 2-fluoro-3',5'-dimethoxybenzoin (**2**) in MeCN and in trifluoroethanol.

Femtosecond experiments were carried out using solutions of **2** in acetonitrile and trifluoroethanol. Pump probe spectra covered a time range from 0 to 1.9 ns, and from 0 to 100 ps to resolve the formation of the transients.

On excitation by a subpicosecond pulse at 263 nm (200 fs), all solutions showed a broad transient absorption in the near-UV, $\lambda_{\text{max}} = 315 \text{ nm}$ in MeCN (Figure 37) and 312 nm in $\text{CF}_3\text{CH}_2\text{OH}$ (Figure 38).



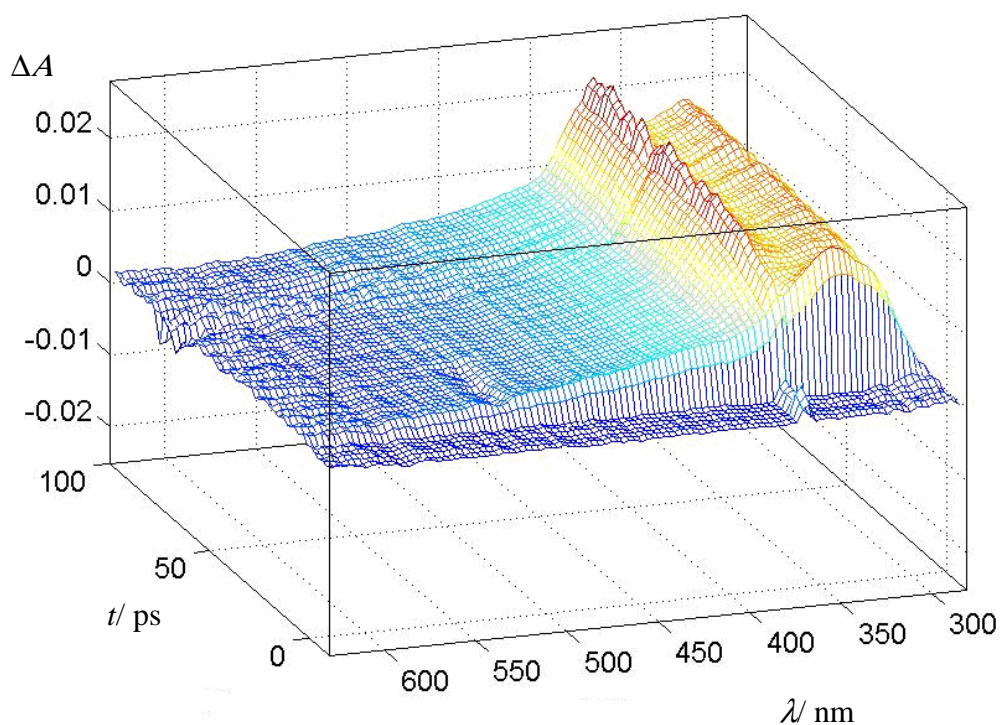


Figure 37: Femtosecond pump-probe spectra of **2** in acetonitrile solution (excitation with a subpicosecond flash at 263 nm) with delays between 0 and 1.9 ns (top), and 0-120 ps (bottom).

The transient observed (ca 315 nm) in the two different solvents is formed within the time-resolution of the instrument (500 fs) and observable up to 1.9 ns (Figure 37 and 38). The data were accumulated through 500 pulses and the final spectrum is an average of 3 experiments. The transient at 315 nm is attributed to the superposition of the singlet absorbance to the triplet absorbance of **2**.

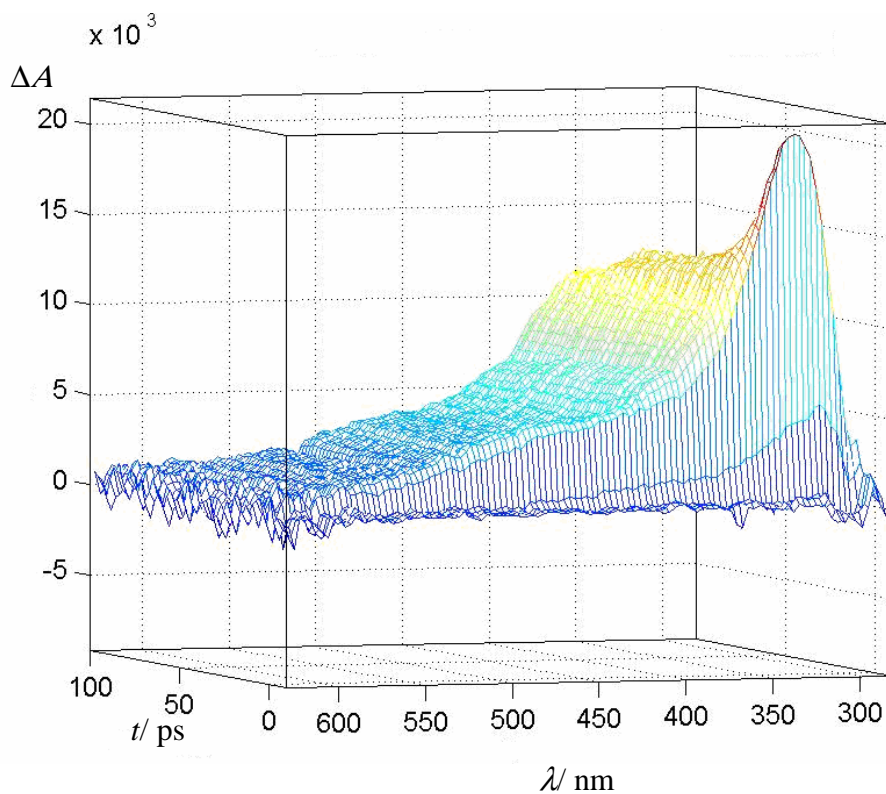
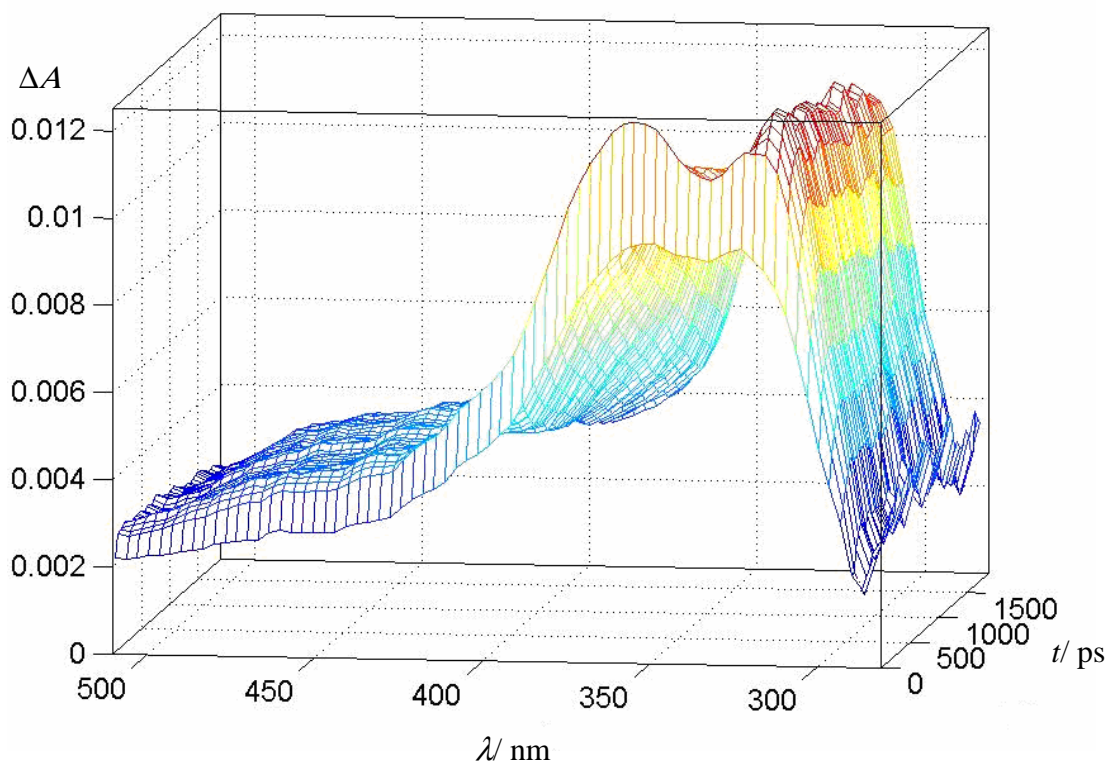


Figure 38: Femtosecond pump-probe spectra **2** in trifluoroethanol solution (excitation with a subpicosecond flash at 263 nm) with delays between 0 and 1.9 ns (top), and 0-120 ps (bottom).

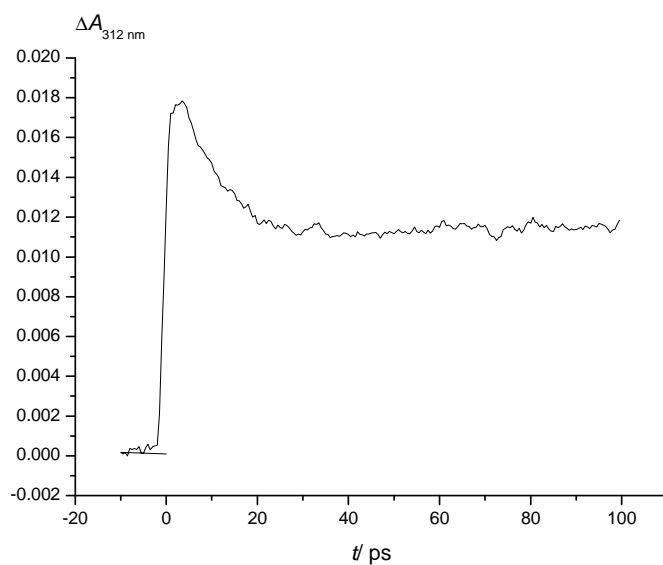
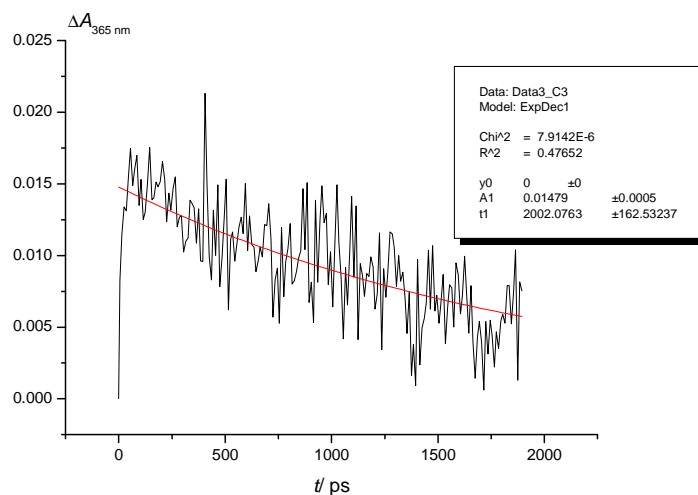


Figure 39: Kinetic traces of the absorbance at 312 nm extracted from the femtosecond pump-probe spectra of **2** in trifluoroethanol solution (excitation with a subpicosecond flash at 263 nm) with delays 0 and 120 ps.

The signal at 312 nm (formed in less than 500 fs) decays ($\tau = 10$ ps) to an end absorbance (Figure 39). This fast reaction is attributed to the intersystem crossing of **2**.



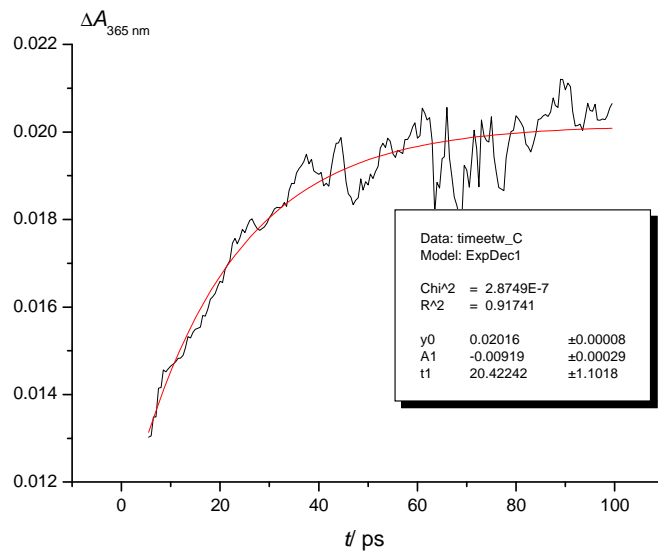
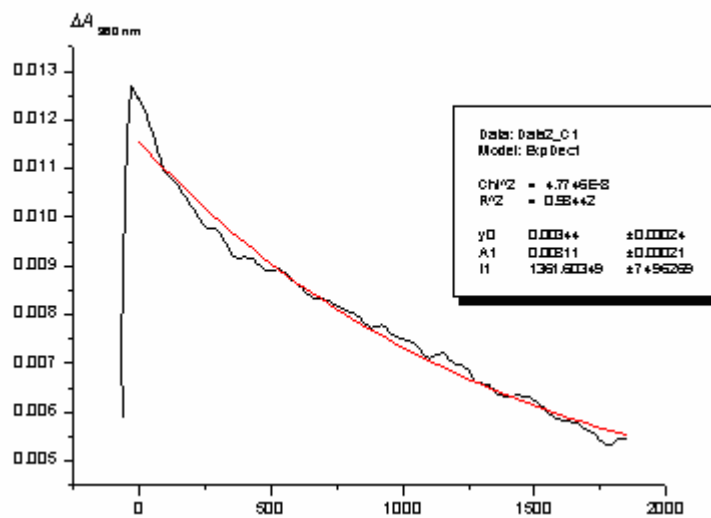


Figure 40: Kinetic traces of the absorbance at 365 nm extracted from the femtosecond pump-probe spectra of **2** in acetonitrile solution (excitation with a subpicosecond flash at 263 nm) with delays between 0 and 1.9 ns (top) and 0-100 ps (bottom).



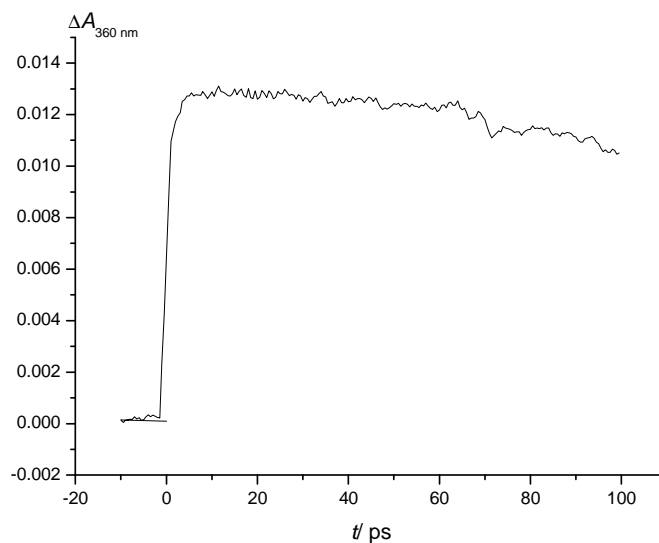
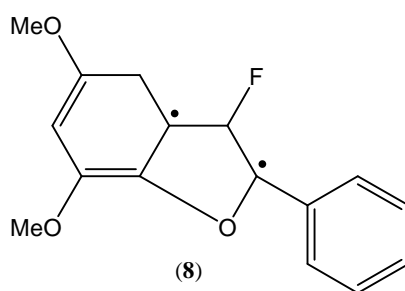


Figure 41: Kinetic traces of the absorbance at 365 nm extracted from the femtosecond pump-probe spectra of **2** in trifluoroethanol solution (excitation with a subpicosecond flash at 263 nm) with delays between 0 and 1.9 ns (top) and 0-100 ps (bottom).

A solution of **2** in acetonitrile and trifluoroethanol showed the formation of an other absorbance band around 360 nm (in acetonitrile: $\lambda_{\text{max}} = 365$ nm, formation in 20 ps (Figure 40) and lifetime of > 2 ns (Figure 40); in trifluoroethanol, $\lambda_{\text{max}} = 360$ nm, rise time less than 500 fs and lifetime of 1.4 ns (Figure 41)). An additional, short-lived absorbance around 490 nm in acetonitrile (also in trifluoroethanol) has been observed. After its growth (less than 500 fs in acetonitrile and trifluoroethanol respectively (Figure 42)), the weak signal was still observable after 1.9 ns in acetonitrile and trifluoroethanol (Figure 43)). In this case the position of the band maximum matches well with the position of the band centred at 485 nm observed on the ns time scale and assigned to the dimethoxycyclohexadienyl cation (**3**).



The transient observed at 360 nm is attributed to the biradical **8**, as the only plausible intermediate able to form the cation **3** and absorbing in this UV region (360 nm). Such intermediate has been proposed in several papers^{11, 21}, but never observed, so this is the first time that this intermediate is detected.

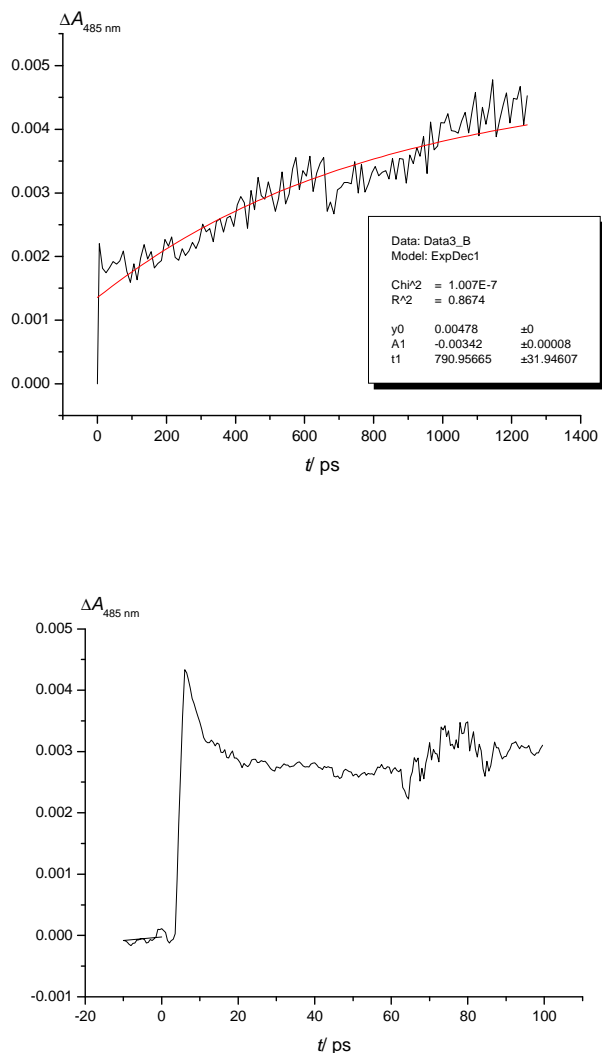


Figure 42: Kinetic traces of the absorbance at 485 nm extracted from the femtosecond pump-probe spectra of **2** in acetonitrile solution (excitation with a subpicosecond flash at 263 nm) with delays between 0 and 1.9 ns (top) and 0-100 ps (bottom).

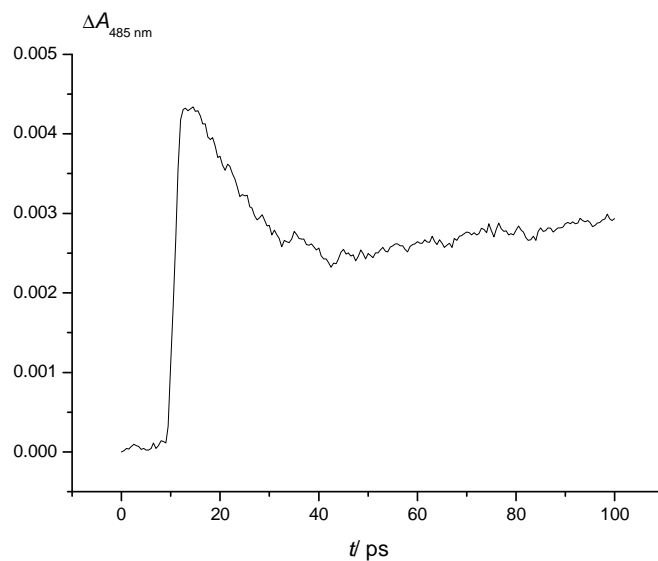
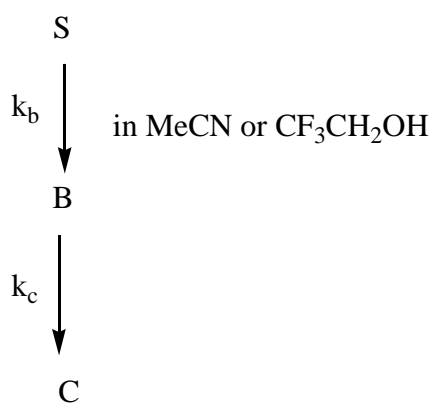


Figure 43: Kinetic traces of the absorbance at 485 nm extracted from the femtosecond pump-probe spectra of **2** in trifluoroethanol solution (excitation with a subpicosecond flash at 263 nm) with delays between 0 and 100 ps (bottom).

Global Analysis of the different three dimensional curves, using the singular value decomposition, gave two dominant factors. A model including two colored species (the radical **8** (B) and the cation **3** (C)) was then applied to do the kinetic fits (scheme 27).

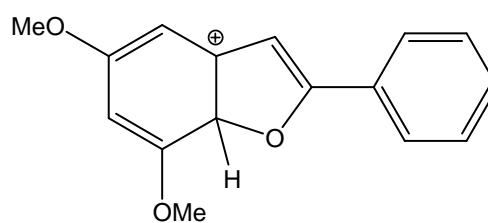
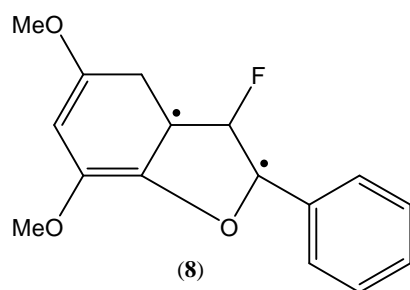


Scheme 27: Proposed scheme for kinetic fits after global analysis of the femtosecond pump-probe spectra of **2** in MeCN and in CF₃CH₂OH.

Following this model, the software is able to do a global fit and give accurate rate constants k_b , k_c .

	MeCN	CF ₃ CH ₂ OH
k_b / s^{-1}	$(4.23 \pm 0.28) \times 10^{10}$	$(5.81 \pm 0.36) \times 10^{10}$
k_c / s^{-1}	$(5.05 \pm 0.89) \times 10^8$	$(6.48 \pm 0.63) \times 10^8$

The proposed mechanism includes one pathway to form the final benzofuran from the first singlet excited state, through the biradical **8** and the cation **3**.



Addition of small amount of water (5 %) accelerates the decay rate constant of the 360 nm signal, which has been assigned to the biradical **8**. This can explain that the biradical **8**, precursor of the cation **3**, can react with water in a different pathway. Biradical **8** seems to be the parent intermediate of dimethoxybenzofuran **5** and the product due to nucleophilic attack of the solvent (at the leaving group position).

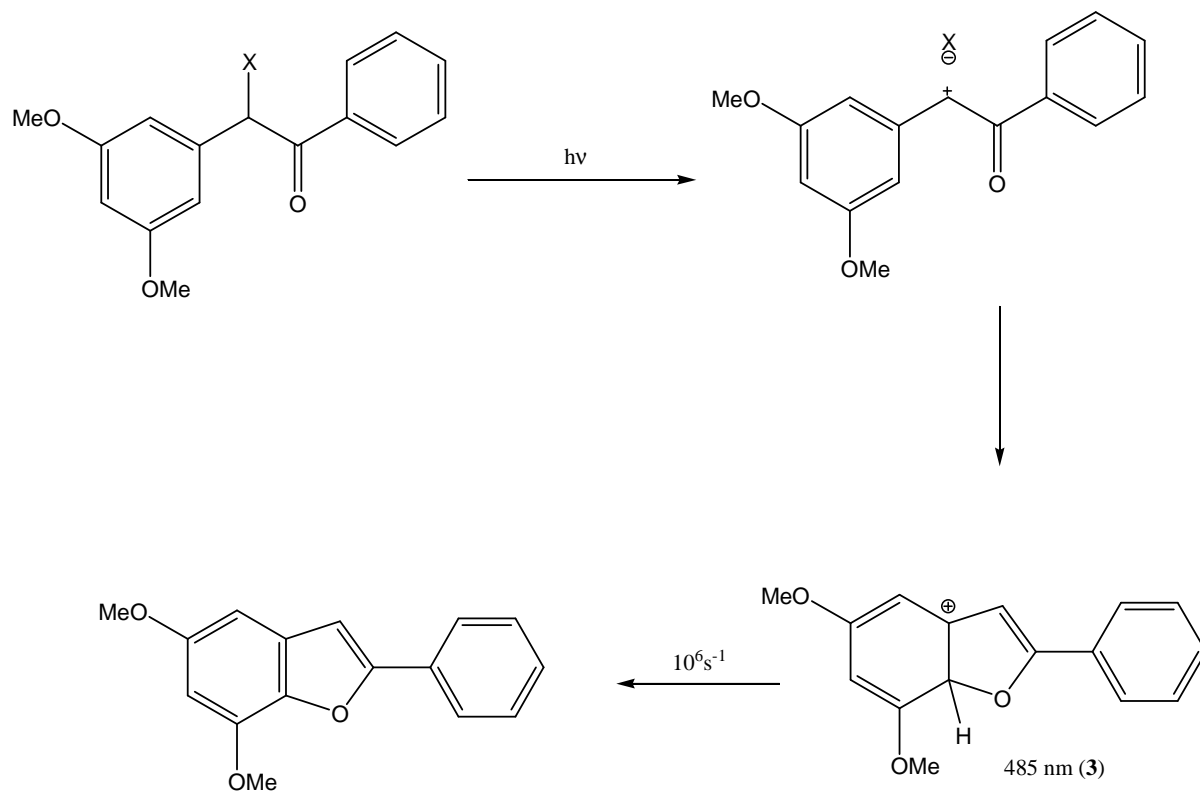
% water	k_{obs} / s^{-1}
0	$(4.21 \pm 1.06) \times 10^8$
5	$(9.09 \pm 1.53) \times 10^8$

3.4. Discussion.

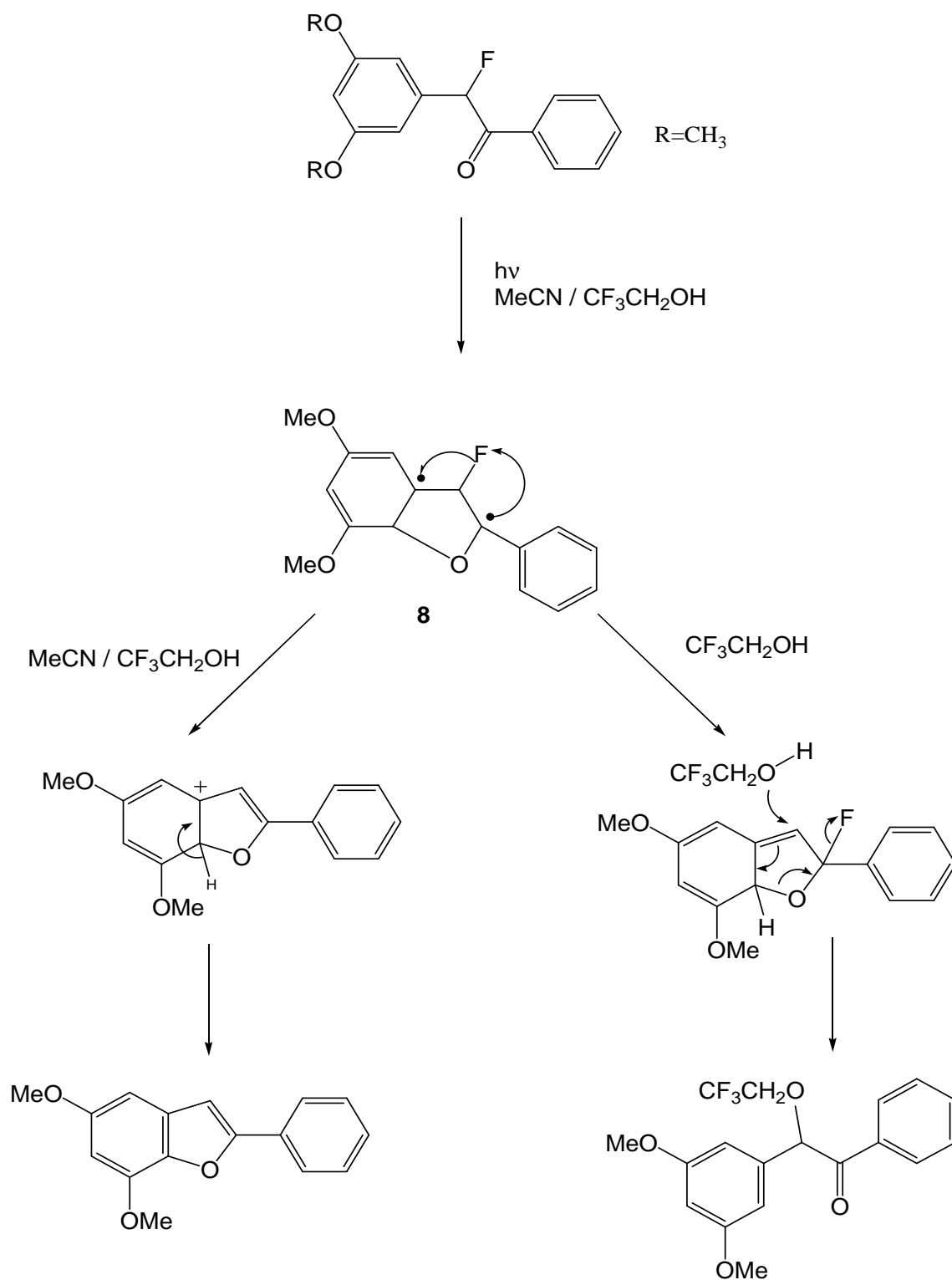
Quenching experiments indicate that the reactive excited state involved in the photolysis of **2** (2-fluoro-3',5'-dimethoxybenzoin) is the singlet state. A transient observed solvent at 485 nm, with a lifetime of 500 ns, can be assigned to a short lived cation **3** (scheme 29), a precursor of the dimethoxy-2-phenylbenzofuran²⁰. Configuration Interaction calculations (CIS: configuration interaction-singles; the CIS wave function is a linear combination of electronic configurations, obtained by monoexcitations from the Hartree-Fock wave function), after B3LYP/6-311G(d) optimization of the structure in gas phase, predict an absorption band of this cation at 456 nm. By photolysis of **2** in trifluoroethanol, 24.5% is converted to solvent adduct at the α -position of the keto group (28.5% in benzofuran), which indicates the formation of a trappable ketocation. Shi et al.²⁰ eliminate this first intermediate to favour a charge transfer complex between the ring and the carbonyl, because they observe no trace of solvent trapping product from the acetate derivative, contrary to our case. The proposal by Rock and Chan²¹, which consists on a common biradical **8** intermediate cyclising to benzofuran **5** or attacked by water, is consistent with our experiments. They argued that heterolytic cleavage is usually seen for a $\pi-\pi^*$ excited states of benzyl esters, whereas lowest excitation state of **2** is n,π^* . Biradical **8** corresponds to that proposed by Wirz et al.¹¹ in the case of **4**, and the lifetime of the species was less than 25 ns. We observe a species absorbing at 365 nm, with a lifetime of about 2 ns. This transient, observed during the femtosecond LFP experiments, is tentatively assigned to the biradical **8**, because its decay corresponds to the growth of the cation **3** at 485 nm and gives the rate of F release ($k = (5.05 \pm 0.89) \times 10^8$ in air saturated MeCN).

Nanosecond and femtosecond laser flash photolysis experiments show no transient above 550 nm. So the intermediate generating our product may not be an α -ketocation proposed by Pirrung et al.^{16, 17} (Scheme 28). The structure **8** suggested by Rock and Chan²¹ rationalizes the two possible pathways to access to the final products. The first one is the solvent addition, in the subnanosecond time scale. The second path proceeds via the cation **3** which deprotonates to form the 3'-5'-dimethoxy- 2-phenylbenzofuran **5**. Scheme 29 summarizes the different pathways involved in the photolysis of **2**.

Proposed mechanism:



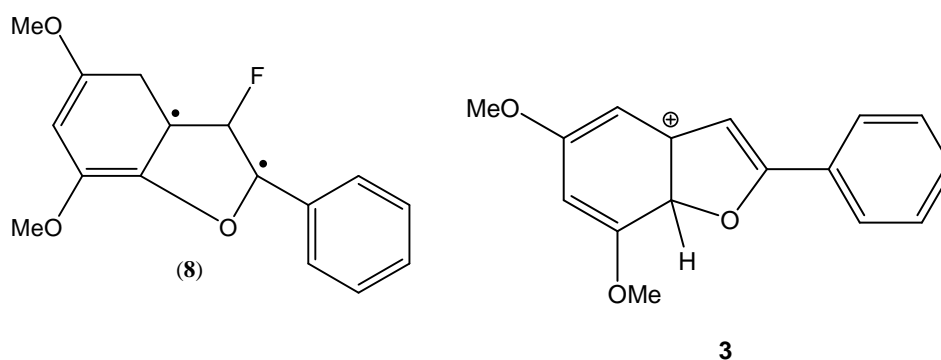
Scheme 28: First hypothetic mechanism proposed for LFP of **2**.



Scheme 29: Second mechanism proposed for LFP of **2**.

4. Conclusion.

Our studies on 2-fluorobenzoin (**1**) and 3',5'-dimethoxy-2-fluorobenzoin (**2**) showed that replacement of the leaving group by fluoride has little influence on the reaction mechanism. Three differences in the photolysis mechanism can be observed between **1** and **2**. The photochemistry of caged compound **1** proceeds through the triplet state, that of **2** through a photoreactive singlet state. In the photocyclisation of **2**, the final benzofuran is mainly formed through a slow deprotonation of a cation **3**, contrary to **1**, for which the main precursor seems to be a biradical. The solvent adduct is formed directly from the biradical in the case of **2** and from an α -cation in photolysis of **1**. Laser flash photolysis experiments with **2** have permitted to observe the long-sought biradical **8**, decaying to form the cyclohexadienyl cation **3** which deprotonates to give the 5,7dimethoxy-2-phenylbenzofuran.



5. Experimental.

5.1 Irradiation

Solutions were irradiated with a Hanau medium pressure mercury lamp. A band-pass filter was used to isolate the desired excitation wavelength (254 nm for actinometry).

5.1 Nanosecond laser flash photolysis.

Laser flash photolysis experiments were carried out by exciting the sample solutions (absorbances of $<0.5 \text{ cm}^{-1}$ at the excitation wavelength) with 20-ns, ca 100-mJ pulses of an excimer laser (248 nm, KrF; 308 nm, XeCl; 351 nm, XeF; Lambda Physik Compex 205). A pulsed Xenon arc was used as the monitoring light source (cell path length 4.5 cm, orthogonal to the excitation pulse). The detection system allowed monitoring of either the kinetics at a single wavelength using a transient digitizer, or the whole transient spectrum, with a gated diode array²⁷. Measurements were made with fresh solutions, which were replaced after each flash.

5.2 Femtosecond laser flash photolysis.

Pump - probe spectroscopy was used to investigate processes on the subnanosecond time-scale. The measurements were done with solutions in acetonitrile, trifluoroethanol. Experiments were carried out by exciting of the sample solutions with the 150-200 fs pump pulse (at 263 nm, CPA-2001 Laser System manufactured by Clark-MXR .Inc) of a titanium:sapphire amplified laser system. The remainder of the laser output was used to generate a white light continuum in a thick piece of calcium fluoride and used as probe beam. Transient spectra were collected within the wavelength range from 300 to 600 nm. A more detailed description can be found elsewhere²⁸.

5.3 Calculations.

SPECFIT 32 and origin 7.0 were used for global analysis and kinetics fitting respectively. CIS and DFT calculation were carried out with the GAUSSIAN 03 package.

6. References

- (1) S. Stavber, T. S. Pečan, M. Zupan, *J. Chem. Soc., Perkin Trans. 2*, (2000), 1141-1145
- (2) J. C. Sheehan, R. M. Wilson, *J. Am. Chem. Soc.*, **86**, (1964) 5277-5281
- (3) A. Schönberg, A. K. Fateen, S. M. A. R. Omran, *J. Am. Chem. Soc.*, **78**, (1955) 1224-1225
- (4) J. C. Sheehan, R. M. Wilson, A. W. Oxford, *J. Am. Chem. Soc.*, **93**, (1971) 7222-7228
- (5) L. P. Tenney, D. W. Boykin, Jr., R. E. Lutz, *J. Am. Chem. Soc.*, **88**, (1966) 1835-1836
- (6) A. Padwa, R. Gruber, *J. Am. Chem. Soc.*, **92**, (1977) 100-114
- (7) J. P. Fouassier, A. Merlin, *Can. J. Chem.*, **57**, (1979) 2812-2817
- (8) F. D. Lewis, C. H. Hoyle, J. G. Magyar, *J. Org. Chem.*, **40**, (1975) 488-492
- (9) R. S. Givens, P. S. Athey, L. W. Kueper III, B. Matuszewski, J-Y. Xue, T. Fister, *J. Am. Chem. Soc.*, **115**, (1993) 6001-6012
- (10) R. S. Givens, P. S. Athey, L. W. Kueper III, B. Matuszewski, J-Y. Xue, *J. Am. Chem. Soc.*, **114**, (1992) 8708-8710
- (11) C. S. Rajesh, R. S. Givens, J. Wirz, *J. Am. Chem. Soc.*, **122** (2000) 611-618
- (12) M. Newcomb, J. H. Horner, P. O. Whitted, D. Crich, X. Huang, Q. Yao, H. Zipse, *J. Am. Chem. Soc.*, **121** (1999) 10685-10694.
- (13) J. M. Peach, A. J. Pratt, J. S. Snaith, *Tetrahedron*, **51**, (1995) 10013-10024
- (14) S. M. Gasper, C. Devadoss, G. B. Schuster, *J. Am. Chem. Soc.* 1995, **117**, 5206-5211.
- (15) M. C. Pirrung, S. W. Shuey, *J. Org. Chem.*, **59**, (1994) 3890-3897
- (16) M. C. Pirrung, J. C. Bradley, *J. Org. Chem.*, **60**, (1995) 1116-1117
- (17) M. C. Pirrung, L. Fallon, D. C. Lever, S. W. Shuey, *J. Org. Chem.*, **61**, (1996) 2129-2136
- (18) J. F. Cameron, C. G. Wilson, J. M. J. Fréchet, *J. Am. Chem. Soc.*, **118**, (1996) 12925-12937
- (19) G. Papageorgiou, J. E. T. Corrie, *Tetrahedron*, **53**, (1998) 3917-3932
- (20) Y. Shi, J. E. T. Corrie, P. Wan, *J. Org. Chem.*, **62**, (1997) 8278-8279
- (21) R. S. Rock, S. I. Chan, *J. Am. Chem. Soc.*, **120**, (1998) 10766-10767
- (22) B. Košmrlj, B. Šket, *unpublished results*

- (23) H. J. Kuhn, S. E. Braslavsky, R. Schmidt, *Pure Appl.Chem.*, **76(12)** (2005) 2105-2146
- (24) G. Gauglitz, S. Hubig, *J. Photochem.*, **30**, (1985) 121-25
- (25) G. Porter, F. Wilkinson, *Proc. Royal Soc.*, 264A (1966)
- (26) S. L. Murov, I. Carmichael, G.L. Hug, *Handbook of photochemistry 2nd edition*, Marcel Dekker, 1993.
- (27) E. Leyva, M.S. Platz, G. Persy, J. Wirz, *J. Am. Chem. Soc.*, **108**, (1986) 3783-3790
- (28) M. Gaplovsky, Ph.D Dissertation, 2004.

7. Summary

Photoremovable protecting groups are used for a broad range of applications in organic synthesis, biophysics and biology. The study of the photorelease mechanisms is key for understanding and controlling their activities and to determine release rates. The benzoin group presents a lot of advantages as a caging compound because it releases the protected group rapidly and in high yields with $\lambda > 300$ nm forming an inert benzofuran by-product.

2-Fluorobenzoin (**1**) and 2-fluoro-3',5'-dimethoxybenzoin (**2**) were studied by steady-state irradiation and laser flash photolysis in order to establish product distributions and to observe transient intermediates. Our investigations show that the two benzoin derivatives have a different photocyclisation mechanism.

Irradiation of **1** in MeCN produces the 2-phenylbenzofuran (within 25 ns) through a fast cyclisation-elimination process involving $^3\mathbf{1}$, observed in the femtosecond experiments. In water or trifluoroethanol heterolytic dissociation of $^3\mathbf{1}$ forms the triplet α -ketocation (570 nm, 400 ns), which reacts with the solvent after intersystem crossing to its singlet state. Photocyclisation of **2** in MeCN, on the other hand, produces the dimethoxyphenylbenzofuran via the singlet state. . We observe a species absorbing at 365 nm, with a lifetime of about 2 ns. This transient, observed during the femtosecond LFP experiments, is tentatively assigned to the biradical **8**, because its decay corresponds to the growth of the cation **3** at 485 nm and gives the rate of F release ($k = (5.05 \pm 0.89) \times 10^8$ in air saturated MeCN). The ultimate intermediate has been assigned (Corrie, Wan)²⁰ to the dimethoxycyclohexadienyl cation (**3**) (485 nm, $\tau = 425$ ns).

8 .Curriculum Vitae

Personal Data

Name	Hassen Boudebous
Date of birth	February 01, 1976
Nationality	French

Education and Research Experience

Jan.2002-Jan.2006	PhD candidate, University of Basel
Oct.-Dec 2002	Laboratory technician – Physical chemistry and bacteriological analysis of milk and cheese. Central dairy of Belfort - 2 months.
2000-2001	Master of Science in Chemistry Physical chemistry, surfaces, interfaces and materials. Ecole Nationale Supérieure de Chimie de Mulhouse
2000-2001	Research assistant in the Laboratory of photochemistry and photopolymerization UMR CNRS 7525 Ecole nationale supérieure de Chimie de Mulhouse 9 months
1994-1996	DUT MESURES PHYSIQUES (Two years university diploma of technology in physical and chemistry measurements) Option materials and physical-chemistry controls Formation in quality insurance management IUT Belfort-Montbéliard
1994	Baccalauréat C, specialized in Mathematics, Physics and Chemistry.
1991-1994	High School, Lycée G.Courbet, Belfort France.
1987-1991	Secondary School, Collège Châteaudun, Belfort, France.
1982-1987	Primary School, Ecole Primaire Raymond Aubert, Belfort, France.

During my studies at the University of Basel I attended lectures by:
H. Huber, J.Wirz, E.Dangel Pelloquin, J.Seelig et al., A.Vedani, M.Lill.

9. Appendix

I've been involved during my PhD study in other projects like the investigations on the mechanism of photorelease of choline from the *N*-methyl-*N*(*o*-nitrophenyl)carbamate derivative, the synthesis of the dihydroxyindane and 1-diazoindan-2-one for a study of their photochemistry. I also participated in the study of the photochemical reaction mechanisms of 2-nitrobenzyl ethers by synthesizing 1-methoxymethyl-6-nitropiperonyl and doing some LFP experiments with this compound. Some caged compounds which release calcium have been also studied (nitr-5, nitr-9, DMNPE, NP-EGTA). Collaboration on the kinetic study of electron transfer through polyprolines gave interesting results and that have been reported in the following publication:

Bernd Giese, Matthias Napp, Olivier Jacques, Hassen Boudebous, Alexander M. Taylor, and Jakob Wirz, "Multistep Electron Transfer in Oligopeptides: Direct Observation of Radical Cation Intermediates", *Angew. Chem. Int. Ed. Engl.* **2005**, *44*, 4073-4075; *Angew. Chem.* **2005**, *117*, 4141-4143.